CHARACTERIZATION OF CERAMIDE SYNTHASES (CERS) IN MAMMALIAN CELLS

A Dissertation
Presented to
The Academic Faculty

by

Hyejung Park

In Partial Fulfillment
of the Requirements for the Degree
Doctor of Philosophy in the
School of Biology

Georgia Institute of Technology
August 2009

CHACTERIZATION OF CERAMIDE SYNTHASES (CERS) IN MAMMALIAN CELLS

Approved by:

Dr. Alfred H. Merrill, Jr, Advisor
School of Biology
Georgia Institute of Technology

Dr. M. Cameron Sullards
School of Chemistry and Biochemistry
Georgia Institute of Technology

Dr. Marion B. Sewer
School of Biology
Georgia Institute of Technology

Dr. Yuhong Fan
School of Biology
Georgia Institute of Technology

Dr. John Cairney
School of Biology
Georgia Institute of Technology

Date Approved: [Mar. 26, 2009]

[This dissertation is dedicated to my husband, Philseok, and my family in Korea for their love and endless support during my Ph. D. study.]

ACKNOWLEDGEMENTS

I would like to express my sincere gratitude to my advisor, Professor Alfred H. Merrill, Jr., for his guidance, encouragement, and endless support and interest provided during the course of this research. He has been my best source of inspiration and support. I am also deeply indebted to Dr. M. Cameron Sullards for the invaluable advice and support he has provided to make this research possible. I would like to thank Professors Marion B. Sewer, John Cairney and Yuhong Fan for serving on my Ph. D. committee and for their discussions and insights.

I would like to thank all other fellow co-workers in Dr. Merrill's group who contributed to this research: Ms. Elaine Wang, Ms. Kacee Sims, Mr. Samuel Kelly, Mr. Christopher Haynes, Ms. Rebecca Shaner, and Mr. Brent Portz.

My collaborators outside Georgia Tech who partially contributed to this research are also acknowledged: Professor Anthony H. Futerman at Weizmann Institute of Science, Israel, Dr. Alison Narin and Professor Kelly Moremen at University of Georgia, Professor Akemi Suzuki at Tokai University, Japan and Dr. Ronald T. Riley at USDA.

This research was financially supported by the NIH grant GM 69338 (Lipid Maps) and the NIH grant RR018502 for the Integrated Technology Resource for Biomedical Glycomics at the University of Georgia.

Finally, I would like to thank my family in Korea and my husband, Philseok, for their continuous support and encouragement. Without them, this dissertation would not be possible.

TABLE OF CONTENTS

LIST OF TABLES

LIST OF FIGURES

LIST OF SYMBOLS AND ABBREVIATIONS

SL	Sphingolipid
GSL	Glycosphingolipid
Cer	Ceramide
CerS	Ceramide Synthase
SPT	Serine Palmitoyltransferase
3-ketoSa	3-Ketosphinganine
Sa	Sphinganine
So	Sphingosine
SaP	Sphinganine 1-Phosphate
SoP	Sphingosine 1-Phosphate
DHCer	Dihydroceramide
SM	Sphingomyelin
DHSM	Dihydrosphingomyelin
GlcCer	Glucosylceramide
DHGlcCer	Dihydroglucosylceramide
GalCer	Galactosylceramide
DHGalCer	Dihydrogalactosylceramide
LacCer	Lactosylceramide
DHLacCer	Dihydrolactosylceramide
ST	Sulfatide
DHST	Dihydrosulfatide
CerP	Ceramide 1-Phosphate
DHCerP	Dihydroceramide 1-Phosphate

SMase	Sphingomyelinase
SMS	Sphingomyelin Synthase
ASAH	Ceramidase
SPHK	Sphingosine Kinase
CerK	Ceramide Kinase
CERT	Ceramide Transporter
DES	Ceramide Desaturase
EP	Ethanolamine Phosphate
C16:0al	Hexadecanal
C16:1al	Hexadecenal
NKT Cells	Natural Killer T Cells
NeuAc	N-Acetyl-neuraminic acid
NeuGc	N-Glycolylneuraminic acid
ER	Endoplasmic Reticulum
Fuc	Fucose
GlcNAc	N-Acetylglucosamine
GalNAc	N-Acetylgalactosamine
Hex A	β-Hexosaminidase A
Chol-1	Cholinergic nerve-specific molecules
MAG	Myelin-Associated Glycoprotein
SSEA	Stage-Specific Embryonic Antigen
iGb_3S	Isoglobotrihexosylceramide Synthase
GlcU	Glucuronic Acid
SGGL	Sulfoglucuronylglycolipid
ES	Embryonic Stem

EC	Embryonic Carcinoma
EGF	Epidermal Growth Factor
VEGF	Vascular Endothelial Growth Factor
CGT	Ceramide Galactosyltransferase
GST	Glucosylceramide Synthase
KEGG	Kyoto Encyclopedia of Genes and Genomes
mESCs	Mouse Embryonic Stem Cells
EBs	Embryoid Bodies
PBS	Phosphate Buffered Saline
LIF	Leukemia Inhibitory Factor
qRT-PCR	quantitative Real Time-Polymerase Chain Reaction
RPL4	Ribosomal Protein L4
GenMAPP	Gene MicroArray Pathway Profiler
LC ESI-MS/MS	Liquid Chromatography Electrospray Ionization-Tandem Mass Spectrometry
IS	Internal Standard
zfp42	Zinc Finger Protein 42
GBX2	Gastrulation Brain Homeobox
Nanog	Nanog Homeobox
Gsc	Goosecoid
Zic1	Zinc Finger Protein of the Celebellum 1
Sox17	SRY-box Containing Gene 17
Afp	Alpha Fetoprotein
Gata6	GATA Binding Protein 6
Elovl	Fatty Acyl-CoA Elongase
CMH	Ceramide Monohexose

DHCMH	Dihydroceramide Monohexose
siRNA	Short Interfering RNA
Hek 293 cells	Human Embryonic Kidney Cells
GAPDH	Glyceraldehyde-3-Phosphate Dehydrogenase
Elovl	Fatty acyl-CoA elongase
MitoTracker	Mitochondria-specific dye
Protein disulfide isomerase	Endoplasmic reticulum marker
FB	Fumonisins
FB_1	Fumonisin B_1
OPA	Ortho-Phthalaldehyde
LC	Liquid Chromatography
1-DeoxySa	1-Deoxysphinganine
1-DesoxyMeSa	1-Desoxymethylsphinganine
1-DeoxyDHCer	1-Deoxydihydroceramide
1-DesoxyMeDHCer	1-Desoxymethyldihydroceramide
d18:0	sphinganine
m18:0	1-Deoxysphinganine
d18:0-P	Sphinganine 1-Phosphate
LLC-PK_1 Cells	Pig Kidney Epithelial Cells
Vero cells	African Green Monkey Kidney Cells
DU-145 Cells	Human Prostate Cancer Cells
MEM	Minimal Essential Medium
DMEM	Dulbecco's Modified Eagle's Medium
UnID	Unidentified Sphingoid Base
HSN1	Human Sensory Neuropathy Type 1

CHO Cells	Chinese Hamster Ovary Cells
PHGDH	3-Phosphoglycerate Dehydrogenase
PSPH	3-Phosphoserine Phosphatase
S.D.	Standard Deviation
WT	Wild Type

SUMMARY

This thesis describes the characterization of ceramide (Cer) biosynthesis by mammalian cells. The possibility that Cer undergo developmental changes was explored using mouse embryonic stem cells versus embryoid bodies by analysis of the Cer subspecies by liquid chromatography, electrospray ionization-tandem mass spectrometry (LC ESI-MS/MS) and of the transcript levels for enzymes involved in Cer biosynthesis by qRT-PCR. Cer of embroid bodies had higher proportions of very-long-chain fatty acids, which correlated with the relative expression of mRNA for the respective Cer synthases (CerS) and fatty acyl-CoA elongases, as well as changes in the fatty acyl-CoA's of the cells. Therefore, it is clear that Cer subspecies change during embryogenesis, possibly for functionally important reasons. One CerS isoform, CerS2, was studied further because it has the broadest tissue distribution and a remarkable fatty acyl-CoA specificity, utilizing longer acyl-chain CoAs (C20–C26) *in vitro*. The fatty acid chain selectivity was refined by analysis of the Cer from livers from CerS2 null mice, which displayed very little Cer with fatty acyl chains with 24 ± 2 carbons. Another interesting structural variation was discovered in studies of cells treated with fumonisin B_1 (FB_1), which inhibits CerS. Under these conditions, cells in culture and animals accumulate substantial amounts of a novel sphingoid base that was identified as 1-deoxysphinganine. This compound arises from utilization of L-alanine instead of L-serine by serine palmitoyltransferase (SPT) based on the inability of LYB cells, which lack SPT, to make 1-deoxysphinganine. In the absence of FB_1, 1-deoxysphinganine is primarily acylated to 1-deoxydihydroceramides. These are an underappreciated category of

bioactive sphingoid bases and "ceramides" that might play important roles in cell regulation and disease. In summary, cells contain a wide variety of Cer subspecies that are determined by changes in expression of CerS, enzymes that produce co-substrates (such as fatty acyl-CoAs), and the types of amino acids utilized by SPT, the initial enzyme of *de novo* sphingolipid biosynthesis. One can envision how these changes might impact membranes structure as well as signaling by this family of highly bioactive compounds.

CHAPTER 1

INTRODUCTION:

TOWARDS CHARACTERIZATION OF THE MOUSE SPHINGOLIPIDOME. A SURVEY OF LITERATURE ON MOUSE SPHINGOLIPID STRUCTURE AND FUNCTION.

This review provides a template to trace the biosynthesis of glycosphingolipids (GSLs) across various murine tissues and organs. The abbreviations and symbols for carbohydrates and lipids follow the recommendations of the IUPAC/IUBMB Commission of Biochemical Nomenclature (1).

Considering its resemblance to human cell behavior, murine systems are one of the most analyzed in sphingolipidomic biology. GSLs mediate crucial aspects of the differentiation, growth and development of mouse tissue beginning at the embryonic stage, and are integral in crucial cellular process that include signaling, trafficking, and cell-cell interactions. As a result, tracing the catabolic pathways of the molecules in their native tissues and describing their functions in the cell would provide an important tool in further analysis. This review provides this tool by survey the known glycosphingolipidomic pathways within a mouse model.

1.1 Classification

GSLs are characterized by a monosaccharide attached directly to a ceramide unit. Each of these units can be extended by the stepwise addition of more monosaccharides.

1.1.1 Ceramide Backbone

Heterogeneity in sphingolipidomic structure can be seen in differences in the acyl chain length of the fatty acid attached to sphingosine (C14 - C24) (2), the degrees of saturation (C4 and C5) (3), hydroxylation (C4 or C6) (4), methyl branches at ω-1 (iso), ω-2 (anti-iso) and other positions (5), and the degrees of unsaturation at other sites along the chain (6). The bases are abbreviated by defining (in order of appearance) the number of hydroxyl groups (d for di- and t for tri-hydroxyl), chain length, and the number of double bonds (7). Ceramide (Cer) as a sphingoid base is an N-acylated fatty acid that is mostly saturated, and is described by either the presence, or the absence of a hydroxyl group at the α, or the ω carbon (8). As mentioned earlier, it contains a glycan as a polar headgroup in GSLs.

1.1.2 Ceramide synthases

Ceramide synthases (*CerS*) are the enzymes that are responsible for the acylation of sphingoid bases through the *de novo* biosynthetic pathway (9,10). Early studies detected *CerS* activity in microsomal fractions, and the enzyme was shown to utilize a variety of fatty acyl-CoAs although some specificity toward certain CoAs was recognized (11). *CerS* activity was later localized to the cytoplasmic leaflet of the endoplasmic reticulum (ER) (12,13). The first evidence for specific functional roles of mammalian *CerS* gene was obtained upon overexpression of *CerS1* (formerly known as *UOG1*), which resulted in a selective increase in C18-ceramide in mammalian cells (14). *CerS4* (*TRH1*) and *CerS5* (*TRH4*) were subsequently shown to selectively utilize C18/20 and C16 acyl-CoAs, respectively (15), *CerS6* to produce shorter acyl chain ceramides (C14

and C16)(16), and *CerS3* to produce C18- and C24-ceramides (17), although the surprisingly high levels of C18-ceramide synthesis are at variance with other analyses. *CerS2* has the broad fatty acyl-CoA specificity (C20-C26) and tissue distribution (18). Verification that mammalian *CerS* proteins are *bona fide* ceramide synthases, rather than regulators of endogenous ceramide synthases, was obtained when purified *CerS* was shown to possess *CerS* activity (19). Together with the *CerS* activity of the purified Lag1-Lac1-Lip1 complex in yeast (20), this supports the concept that *CerS* proteins are genuine *CerS*, with each mammalian protein utilizing a relatively restricted subset of fatty acyl-CoAs. It is assumed that the six known mammalian *CerS* proteins account for the synthesis of all known ceramides, but the possibility cannot be excluded that some other proteins, such as ceramidases (21), might also contribute to the synthesis of (DH)Cer with restricted fatty acid composition.

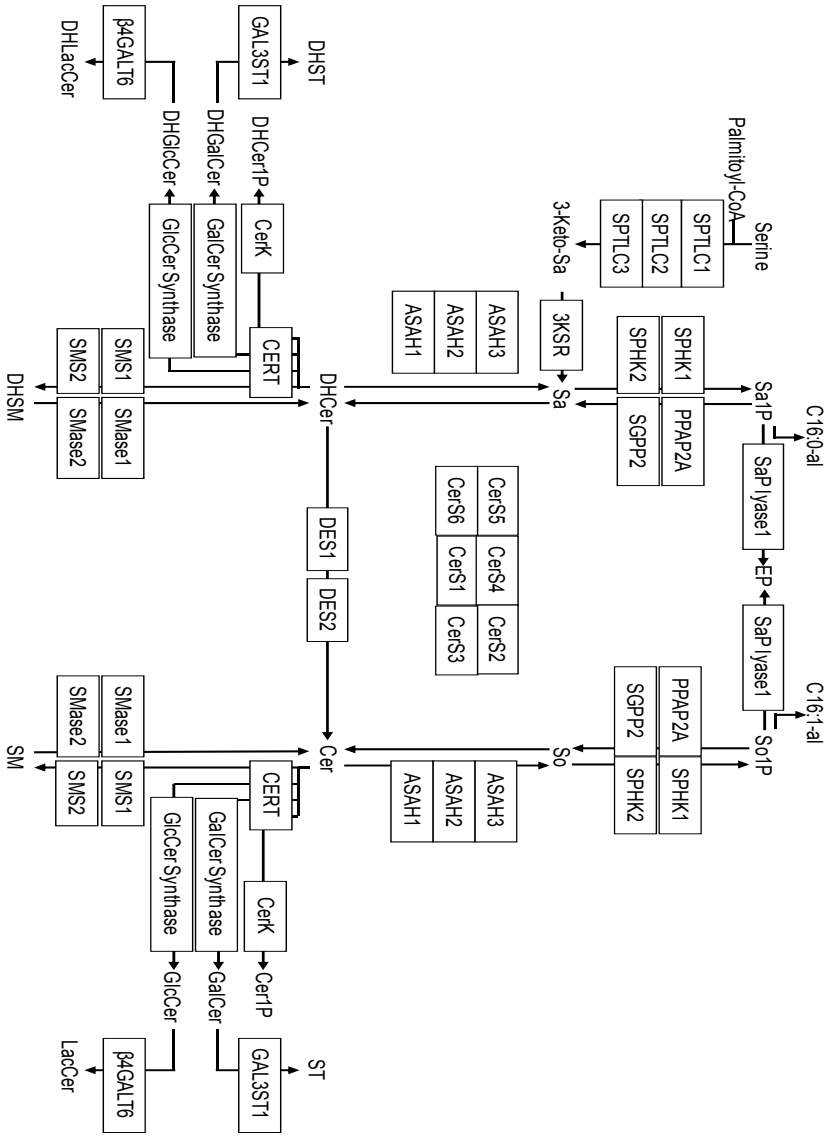

Figure 1.1. *De novo* biosynthesis of sphingolipid metabolism. Illustration of early steps of sphingolipid metabolism using a modified KEGG pathway (www.sphingomap.org). The sphingolipid metabolites and genes (with the gene abbreviations shown in boxes, or enzyme names where gene names are ambiguous) are given for the condensation of serine and palmitoyl-CoA to form 3-ketosphinganine (3-ketoSa) by serine palmitoyltransferase, which is reduced to sphinganine (Sa), acylated to dihydroceramides, DHCer, by (DH)Cer synthases, and incorporated into more complex DH-sphingolipids (the 1-phosphate, DHCerP, sphingomyelins, DHSM, glucosylceramides, DHGlcCer, galactosylceramides, DHGalCer, lactosylceramides, DHLacCer, and sulfatides (DHST), or desaturated to Cer followed by headgroup addition. Also included are a number of the catabolic genes, e.g., sphingomyelinases, *SMases*, ceramidases, *ASAH*, sphingosine kinases, *SphK*, for the formation of sphinganine 1-phosphate (Sa1P) and sphingosine 1-phosphate (So1P), and phosphatases for the reverse reaction and the lyase that cleaves sphingoid base 1-phosphates to ethanolamine phosphate (EP), hexadecanal (C16:0al) and hexadecenal (C16:1al).

1.1.3 Glycan Headgroups

Galactosylceramide (Galβ1-1'Cer, or Gal-Cer), glucosylceramide (Glcβ1-1'Cer, or Glc-Cer), and lactosylceramide (Galβ1-4Glcβ1-1'Cer, or Lac-Cer) are primary in GSL biosynthesis, and serve as branch points for six families as defined by their core structures. While Lac-Cer itself stems off of Glc-Cer and leads to globo-series (Galα1-4Galβ1-4Glcβ1-1'Cer), ganglio-series (NeuAcα2-3Galβ1-4Glcβ1-1'Cer), lacto-series (Galβ1-3GlcNAcβ1-3Galβ1-4Glcβ1-1'Cer), and neolacto-series (Galβ1-4GlcNAcβ1-3Galβ1-4Glcβ1-1'Cer), Gal-Cer leads to the gala-series (Galα1-4Galβ1-1'Cer). GlcCer also forms the sulfoglucuronyl-neolacto series which contains a terminal sulfated glucuronic acid. Either of the molecules in the aforementioned series can also be sulfated and are discussed in a separate section herein. It must be noted that the root molecules are neutral and contain a β-glycosidic linkage to ceramide (7).

These differences in the ceramide and glycan structure are cell-specific and depend on which stage of development the cell is at (22). For instance, the ceramide galactosyltransferase that synthesizes Gal-Cer shows a preference for hydroxy fatty-acid-containing ceramides which are prevalent in the brain. As a result, Gal-Cer is mainly found in neuronal tissues. GSLs contribute to the structure of the outer leaflet of most cell membranes. The molar ratio of these molecules relative to the other major membrane lipids (phospholipids, cholesterol, and glycerolipids) varies from being minor (e.g., <5% in erythrocytes) to being a very major component (e.g., 30% of the total lipids in neuronal plasma membranes) (7,23).

Table 1.1. Functions of GSLs in the mouse

Glycosphingolipids	**Receptors:** Microbial exotoxins and adhesions
	Tumor-associated developmentally regulated antigens
	Allogenic antigens: A_1A_2BH, Lewis, P_1P_2, I/i
	Modulators of: Growth factor/hormone receptor, Function → tyrosine kinase
	Cell adhesion mediators: Lectins (galectins, selectins), Carbohydrates (carbohydrate- carbohydrate interaction)
	Initiators of signal transduction through GSD (GSL signaling domain)

1.2 Distribution

1.2.1 Root Molecules: Precursors to six series in GSL biosynthesis

Galactosylceramide [Galβ1-1'Cer]

Owing to its initial discovery neuronal tissues, galactosylceramide is also called cerebroside. This can be located in the murine adrenal gland (24), and in the erythrocytes of C3H/He and CDF1 inbred mouse strains (25). α-GalCer is involved in the mouse CD1-mediated stimulation of NKT cells, and does not require either antigen processing or endosomal uptake to be presented by mCD1 (26).

Glucosylceramide [Glcβ1-1'Cer]

Like Gal-Cer, this cerebroside can also be found in the adrenal gland (24) in normal mice and in the erythrocytes of C3H/He and CDF1 inbred mouse strains (25). However, Glc-Cer also appears to play a role during development by being present in thymocytes in mice that are 1 to 30 weeks of age. This might account for its presence in murine myelogenous leukemias (27), since molecules that are vital during embryogenesis also account for tumorigenesis. It is also present in the murine lung (28) and uterus (29).

Lactosylceramide [Galβ1-4Glcβ1-1'Cer]

Lac-Cer, or cytolipin H also plays a role in both embryogenesis and tumorigenesis by being present in thymocytes from mice that are 1 to 30 weeks of age and in murine myelogenous leukemias (27). It locates in the mouse lung (28), uterus (29) and adrenal gland (24) in a manner that is similar to its precursor, glucosylceramide. However, this molecule further translocates to muscle tissue in mice (30).

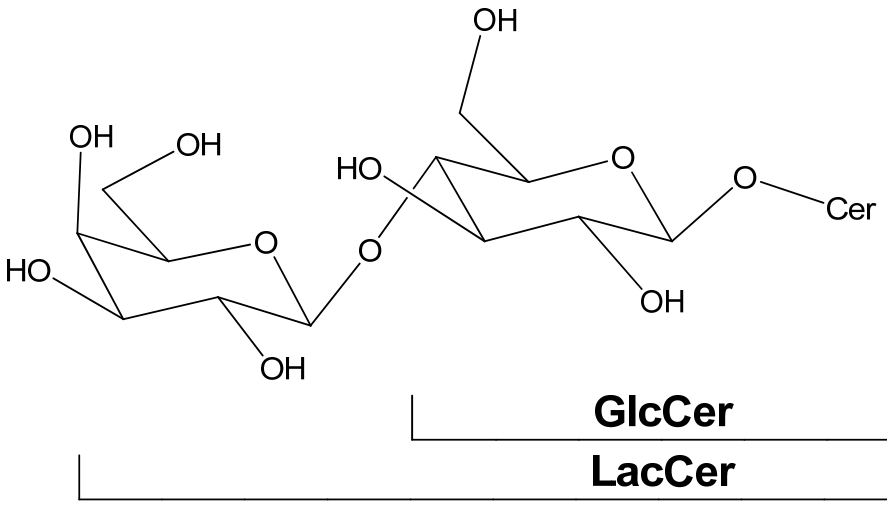

1.2.2 Ganglio-series [NeuAcα2-3Galβ1-4Glcβ1-1'Cer]

First discovered and predominant in nerve ganglions (hence the name), gangliosides are present in all cells in mice. All molecules in this series contain one or more subunits of an acidic monosaccharide called sialic acid, which can have acetyl (N-acetyl-neuraminic acid, NeuAc), or glycolyl (N-glycolylneuraminic acid, NeuGc) groups attached commonly at the C5 position. Sialic acids latch on to the main glycolipid structure via an α2-3, or an α2-6 glycosidic linkage. A chain forms when subsequent acid residues attach to the former via an α2-8 glycosidic linkage.

NeuAc-containing gangliosides are especially present in E-10 and E-11 mouse embryos. These also play major roles in tumorigenesis. Aberrant ganglio-series glycolipids that are neutral can be found in murine myelogenous leukemias (27).

Sialosylcerebroside GM4 [NeuAcα2-3Galβ1-1'Cer]

A departure from the other sialic acid-containing GSLs, sialosylcerebroside contains galactosylceramide as the root structure instead of Glc-Cer. It has immunosuppressive properties and is useful in probing which elements of ganglioside structure are critical to their biological activity (31). Moreover, it has been used to examine the binding specificities of the sialoadhesin family of I-type lectins (32). Besides being predominant in the mouse brain, GM4 is present in the erythrocytes of C3H/He and CDF1 inbred mouse strains (25) alike its precursor Gal-Cer.

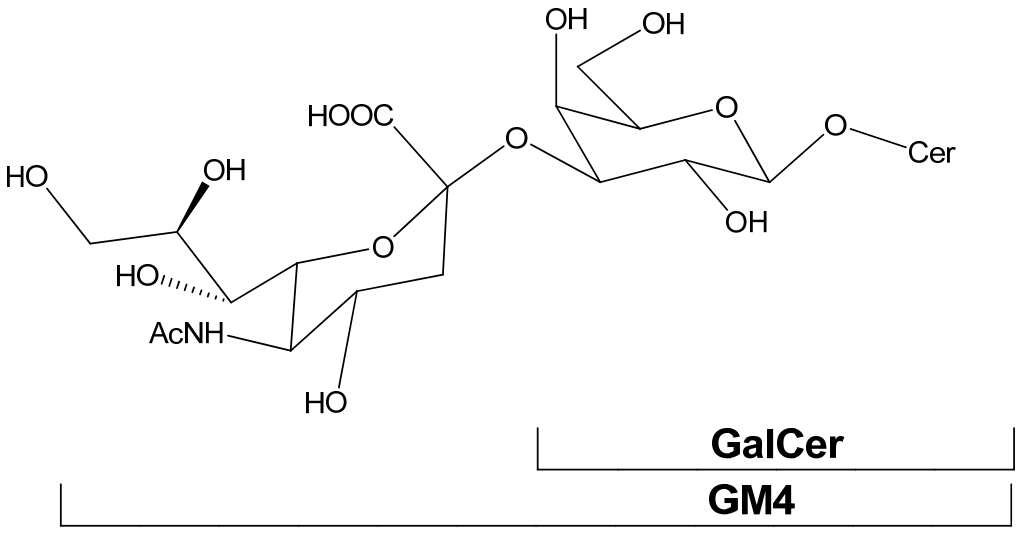

1.2.2.1 o-series

Gangliotriaosylceramide [GalNAcβ1-4Galβ1-4Glcβ1-1'Cer]

Also known as GA2, asialo-GM2, and Gg3-Cer, gangliotriaosylceramide is present in the alveolar epithelium of the murine lung (28) and in low metastatic (Eb)

potential cells (33). It is a tumor-associated antigen and has been shown to be present in murine L5178Y lymphoma (34) and in the murine Lewis lung carcinoma cell line LL2. Moreover, it is also present in the tissue of mice carrying the Tay Sachs' disease (35) and as a result, is termed the Tay-Sachs globoside. This and the subsequent molecule asialo-GM1 are exceptions in that they are part of the ganglio-series, yet contain no sialic acid residues.

Gangliotetraosylceramide [Galβ1-3GalNAcβ1-4Galβ1-4Glcβ1-1'Cer]

Gangliotetraosylceramide, a differentiation antigen in the mouse, is present in myelogenous leukemias (27). In addition to the alveolar epithelium of the murine lung (28) and in low metastatic (Eb) potential cells (33) where it is synthesized from GA2, gangliotetrasylceramide (GA1, Gg_4Cer, asialo-GM1, AM1) is also present in epithelial cells of the small intestine (36), splenic T lymphocytes, uterus (29), thymus, and in peritoneal macrophages.

Monosialoganglioside GM1b [NeuAcα2-3Galβ1-3GalNAcβ1-4Galβ1-4Glcβ1-1'Cer]

GM1b, or cis GM1 is a potent neuronal ligand for myelin-associated glycoproteins (37). It is a tumor ganglioside (38), and is present in low metastatic (Eb) potential cells (33) and peritoneal macrophages like its precursor. However, GM1b is also present in the mouse spleen (39) where it probably translocates to after being synthesized from GA1 in the intestine. Both NeuAc and NeuGc containing GM1b are present in the spleen, myelogenous leukemias (27) and YAC-1 murine lymphoma cells (40). Immature

T cells also contain this molecule. GM1b branches to three other molecules: GalNAc-GM1b, GD1c and GD1α.

Monosialoganglioside GalNAc-GM1b [GalNAcβ1-4(NeuAcα2-3)Galβ1-3GalNAcβ1-4Galβ1-4Glcβ1-1'Cer]

The attachment of a GalNAc via a β1-4 glycosidic linkage to GM1b does not change its location. These remain in the mouse spleen (41), and those containing both NeuGc and NeuAc sialic acids are present in myelogenous leukemias (27) and YAC-1 murine lymphoma cells (40).

Subsequent molecules such as Galβ1-3GalNAcβ1-4(NeuGcα2-3)Galβ1-3GalNAcβ1-4Galβ1-4Glcβ1-1'Cer are also present in the mouse spleen (41).

Monosialoganglioside GD1c [NeuAcα2-8NeuAcα2-3Galβ1-3GalNAcβ1-4Galβ1-4Glcβ1-1'Cer]

GD1c is also responsible for tumors like its precursor, GM1b. It is also present in spontaneous murine thymoma (42) and GD1c (NeuGc-NeuGc) can be found in mouse thymocytes and splenocytes (43).

Monosialoganglioside GD1α [NeuAcα2-3Galβ1-3(NeuAcα2-6)GalNAcβ1-4Galβ1-4Glcβ1-1'Cer]

GD1α is present in low metastatic (Eb) potential cells (33) and in the lactating mammary gland of DDD and ICR mice (39,44). Macrophages also contain this molecule. This can be explained by the existence of its precursor GM1b in immature T cells. GD1α

is also a differentiation-resistant clone of mouse myeloid leukemia cells M1-R1 (45). Present as an accumulated structure in the proximal dendrites and cell bodies of Purkinje cells in murine cerebellum (46).

1.2.2.2 a-series

The a-series of gangliosides are reported as cholinergic nerve-specific molecules (Chol-1) (47,48), or as molecules that bind to myelin-associated glycoproteins *in vitro* (49). Consequently, they play critical roles in the interaction and communication between neuronal cells and their supportive cells (50).

Monosialoganglioside GM3 [NeuAcα2-3Galβ1-4Glcβ1-1'Cer]

Branching from Lac-Cer, GM3 is the defining molecule of the ganglio-series. GD3, the first molecule in the subsequent b-series pathway requires the addition of a sialic acid to the existing structure of GM3. It must be noted that neither GT3, nor the subsequent molecules in the c-series pathway have been shown to exist in the mouse. Like GM4, GM3 has immunosuppressive properties and is useful in probing which elements of ganglioside structure are critical to their biological activity (51). The lymphocyte homing receptor, L-selectin (LECAM-1) binds it at a lower affinity than its corresponding sulfatide (52). It has also been used to examine binding specificities of the sialoadhesin family of I-type lectins (32), and is not the carbohydrate ligand of E-selectin (53). It is weakly recognized by monoclonal antibody AM-3 which was raised against a sialomucin from human colorectal carcinoma (54), and one of the monoclonal antibodies raised against this ganglioside reacts selectively with helper memory T cells (55). GM3

inhibits lung metastases produced by intravenous co-injection of B16-BL-6 melanoma cells (56). And like the gangliosides discussed so far, GM3 also plays a role in mouse embryogenesis by appearing in all tissues during E9 and E11, various neural and non-neural tissues by E13, and centering in the telencephalon, non-neural tissues and liver tissues by E15 (57). A parallel can be drawn in tumorigenesis by studying GM3's appearance in MEB4 murine melanoma cells (58), GRX mouse hepatic stellate cells (59), the murine Lewis lung carcinoma cell line LL2, cultured tumor cells of the VM mouse strain (60), and the lungs of mouse B16 melanoma. It is also present in normal muscle tissue (30), the uterus (29), macrophages, and high metastatic (Eb) potential cells (33). Both NeuAc and NeuGc are present in the ICR mouse spleen (39) and the mouse liver, while only NeuGc remains in the murine adrenal gland (24).

Monosialoganglioside GM2 [GalNAcβ1-4(NeuAcα2-3)Galβ1-4Glcβ1-1'Cer]

Since GM2 is the next step in GM3 anabolism, it is present in most of the tissues that its precursor is in. These include cultured tumor cells of the VM mouse strain (60), GRX mouse hepatic stellate cells (59), the murine Lewis lung carcinoma cell line LL2, lungs of mouse B16 melanoma, high metastatic (Eb) potential cells (33) and macrophages. However, this molecule also appears in the erythrocytes of C3H/He and CDF1 inbred mouse strains (25). Only NeuGc has been shown to be in the mouse liver and the ICR mouse spleen (39). Impaired catabolism of GM2 causes Tay-Sachs disease. The disease can be caused by the resistance of the terminal GalNAc to β-hexosaminidase A (*Hex A*) in the absence of the protein cofactor GM2 activator protein (61) which is

required to assist in the hydrolysis of GM2 (62,63), or from a deficiency of *Hex A* (64-66).

Monosialoganglioside GM1a [Galβ1-3GalNAcβ1-4(NeuAcα2-3)Galβ1-4Glcβ1-1'Cer]

GM1a has been shown to interact with the hormones FSH, LH and HCG, and bind to tetanus toxin (67,68), cholera toxin (69,70), and botulinum toxin (71). It appears in cultured tumor cells of the VM mouse strain (60), GRX mouse hepatic stellate cells (59), the murine Lewis lung carcinoma cell line LL2, and in myelogenous leukemias (27). Normal tissues containing this molecule include muscle (30), brain, the ICR mouse spleen (39) and other high metastatic (Eb) potential cells (33). Unlike GM2, it only appears in peritoneal macrophages and immature T cells. It is also enriched in myelin in sg/sg mice (72). GM1a containing NeuGc is present in the liver.

Disialoganglioside GD1a [NeuAcα2-3Galβ1-3GalNAcβ1-4(NeuAcα2-3)Galβ1-4Glcβ1-1'Cer]

Like its precursor GM1, GD1a is present in cultured tumor cells of the VM mouse strain (60), GRX mouse hepatic stellate cells (59), the murine Lewis lung carcinoma cell line LL2, a differentiation-resistant clone of mouse myeloid leukemia cells, M1-R1 (45), and in normal tissues such as muscle (30), brain, murine macrophages and other high metastatic (Eb) potential cells (33). GD1a (NeuGc, NeuGc) is found in the mouse liver.

Trisialoganglioside GT1a [NeuAcα2-8NeuAcα2-3Galβ1-3GalNAcβ1-4(NeuAcα2-3)Galβ1-4Glcβ1-1'Cer]

GT1a is enriched in Purkinje cells, more concentrated in branchlet spines than in other regions of the Purkinje cell membrane in sg/sg mice (72).

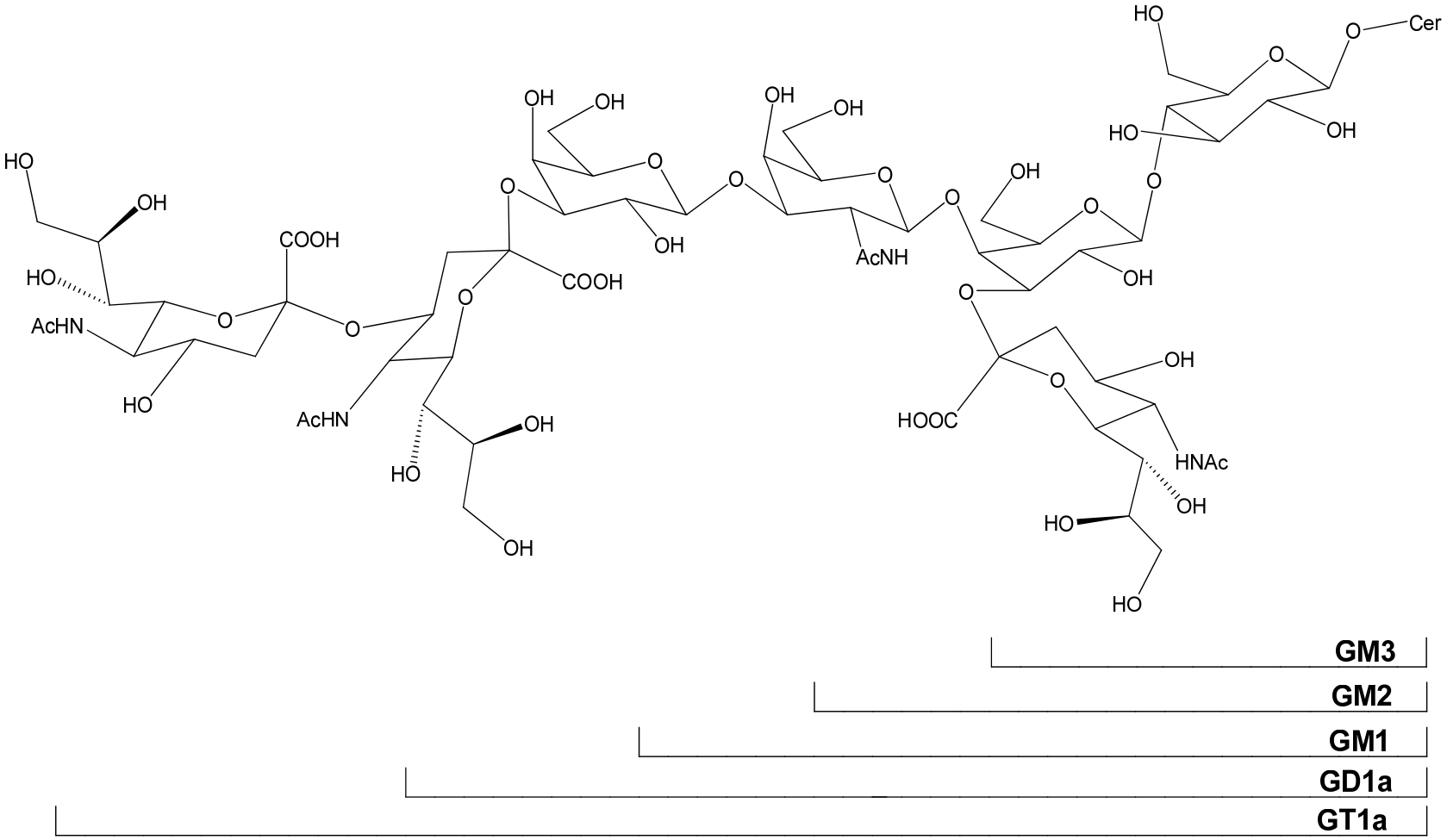
HO
OH
HO
AcHN
HO
COOH
O
O
O
COOH
OH
OH
OH
OH
OH
AcHN
HO
OH
OH
AcNH
O
O
O
O
O
O
OH
OH
HO
O
Cer
OH
HOOC
O
OH
HNAc
OH
HO
HO
GM3
GM2
GM1
GD1a
GT1a

1.2.2.3 b-series

Disialoganglioside GD3 [NeuAcα2-8NeuAcα2-3Galβ1-4Glcβ1-1'Cer]

GD3 appears in murine microglia upon exposure to inflammatory stimuli. GD3 and its acetylated form, 9-O-acetyl GD3 appear in the fetal cortex during development (73). It presents in reactive glia of sg/sg mice at very high levels, accumulates through adulthood (72). While no evidence exists to prove the presence of the subsequent GD2, it may be hypothesized that it is found in mouse tissue by functioning as an intermediate in the pathway from GD3 to GD1b.

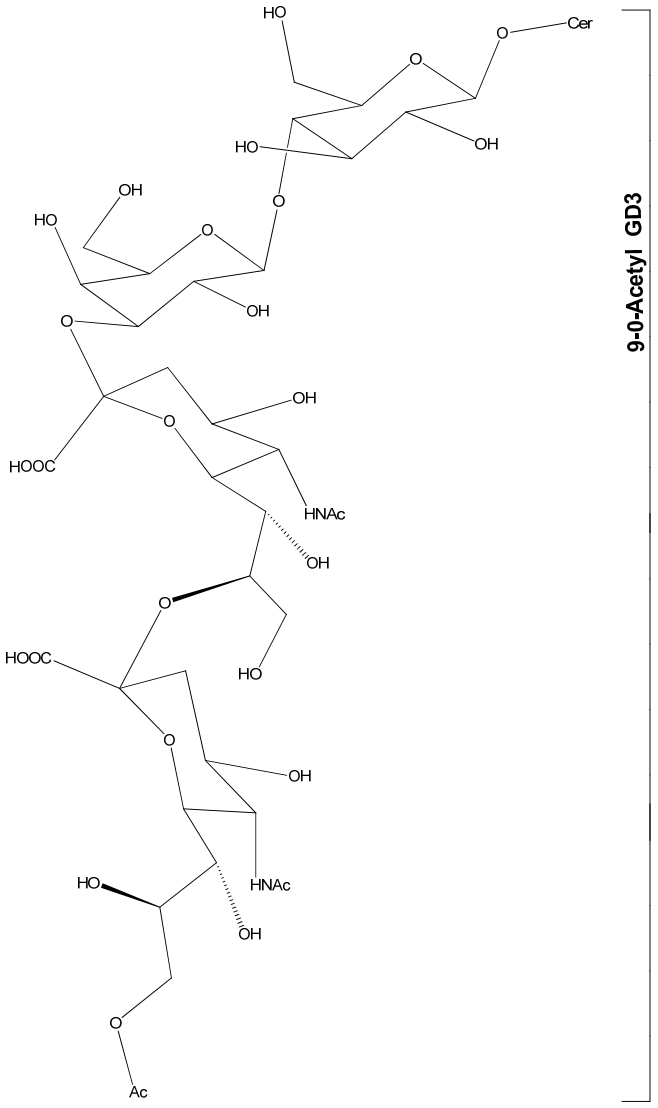

Disialoganglioside GD1b [Galβ1-3GalNAcβ1-4(NeuAcα2-8NeuAcα2-3)Galβ1-4Glcβ1-1'Cer]

GD1b appears in mouse muscle (30), brain and other tissues that include cells with a high metastatic (Eb) potential cells (33). It has a fatty acid composition of d18:1/C18:0 (74), and is also found in the human brain (75).

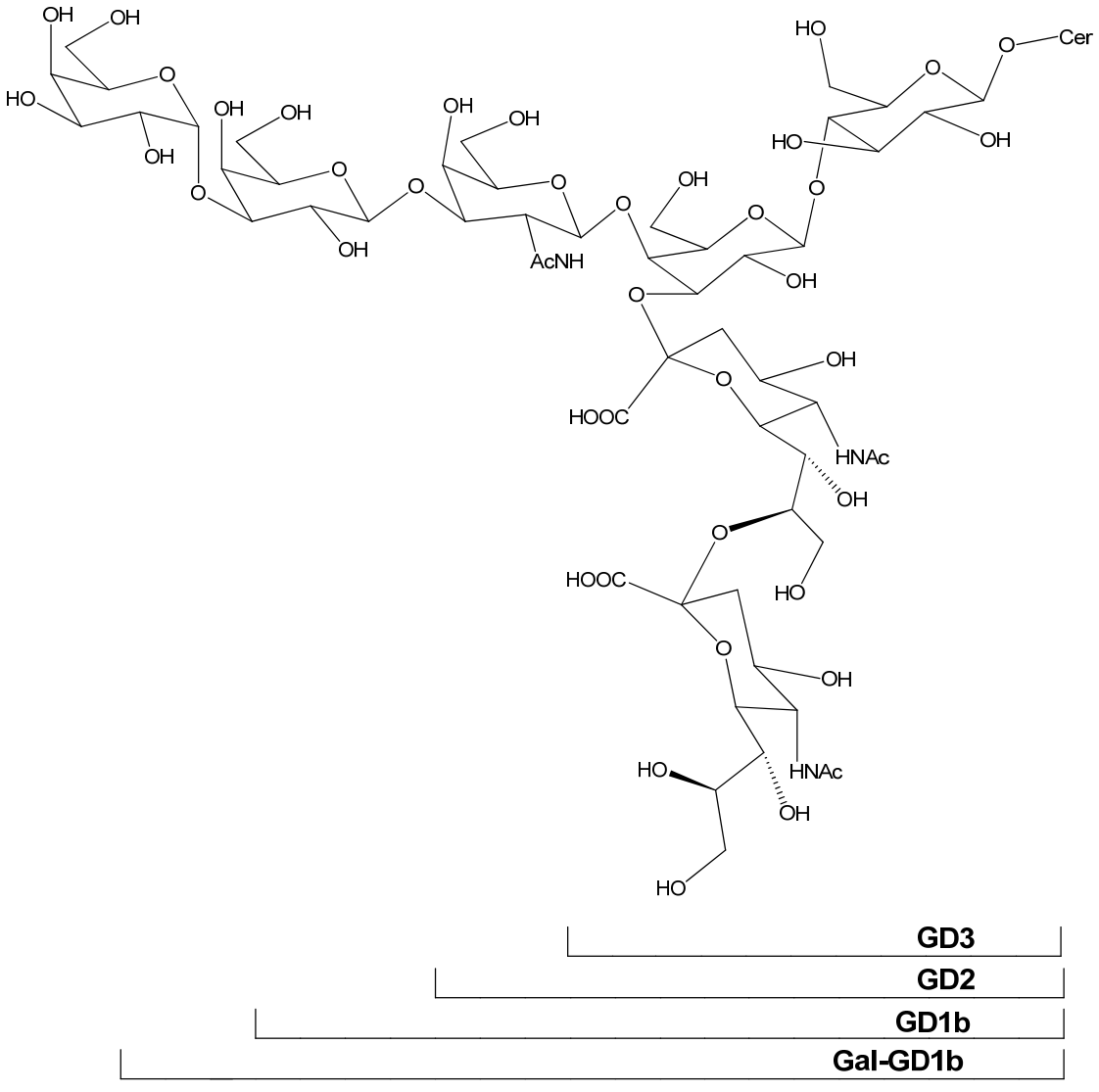

Trisialoganglioside GT1b [NeuAcα2-3Galβ1-3GalNAcβ1-4(NeuAcα2-8NeuAcα2-3)Galβ1-4Glcβ1-1'Cer]

Similar to its precursor GD1b, GT1b (75) exists in mouse muscle (30) and brain tissues. Enriched in both granule cells and Purkinje cells in sg/sg mice (72). A variant of this molecule, GT1bα with the terminal sialic acid residue moved to GalNAc **(**NeuAcα2-6 → GalNAc) is reactive with the anti-cholinergic neuron specific antibody (anti-Chol-1), and has a composition of the ceramides d20:1/C18:0 and d18:1/C18:0 (76).

Tetrasialoganglioside GQ1b [NeuAc2-8NeuAcα2-3Galβ1-3GalNAcβ1-4(NeuAcα2-8NeuAcα2-3)Galβ1-4Glcβ1-1'Cer]

This molecule is mainly present in the mouse brain tissues. The alpha variant of GQ1b (d18:1/C18:0) where the terminal sialic acid has shifted to GalNAc (NeuAcα2-6 → GalNAc) is one of the most potent neuronal ligands for myelin-associated glycoprotein (77), and has been used to examine the binding specificities of the sialoadhesin family of I-type lectins (32).

A novel structure, NeuAcα2-3Galβ1-3GalNAcβ1-4(Ac-O-9NeuAcα2-8NeuAcα2-3)Galβ1-4Glcβ1-1'Cer is also present in the mouse brain (78).

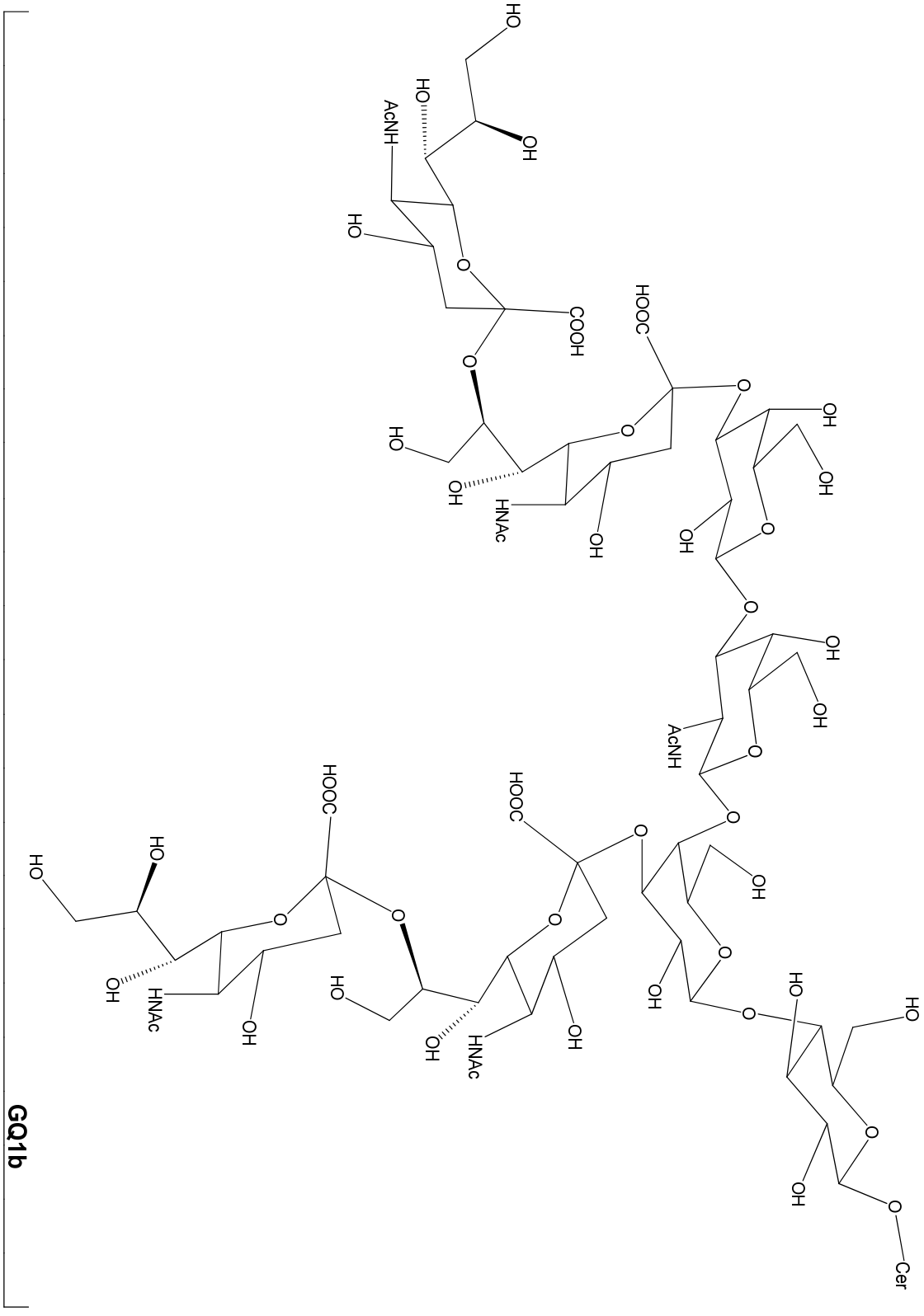
GQ1b
HO
HO
AcNH
OH
HO
O
COOH
HOOC
O
O
OH
OH
HO
OH
HNAc
OH
OH
O
OH
OH
AcNH
O
O
HOOC
HOOC
O
O
OH
HO
OH
O
HO
HO
OH
HNAc
OH
HO
OH
HNAc
OH
O
HO
O
O
Cer

1.2.3 Lacto-series [Galβ1-3GlcNAcβ1-3Galβ1-4Glcβ1-1'Cer]

Type I H antigen (Fucα1-2Galβ1-3GlcNAcβ1-3Galβ1-4Glcβ1-1'Cer)

The H blood group antigen is present in ectoblastic derivatives (ectodermal and neuroectodermal components) of murine teratocarcinoma. The presence of this antigen can be used to presume the existence of its precursors, Lc_3Cer (GlcNAcβ1-3Galβ1-4Glcβ1-1'Cer) and Lc_4Cer (Galβ1-3GlcNAcβ1-3Galβ1-4Glcβ1-1'Cer) in the mouse.

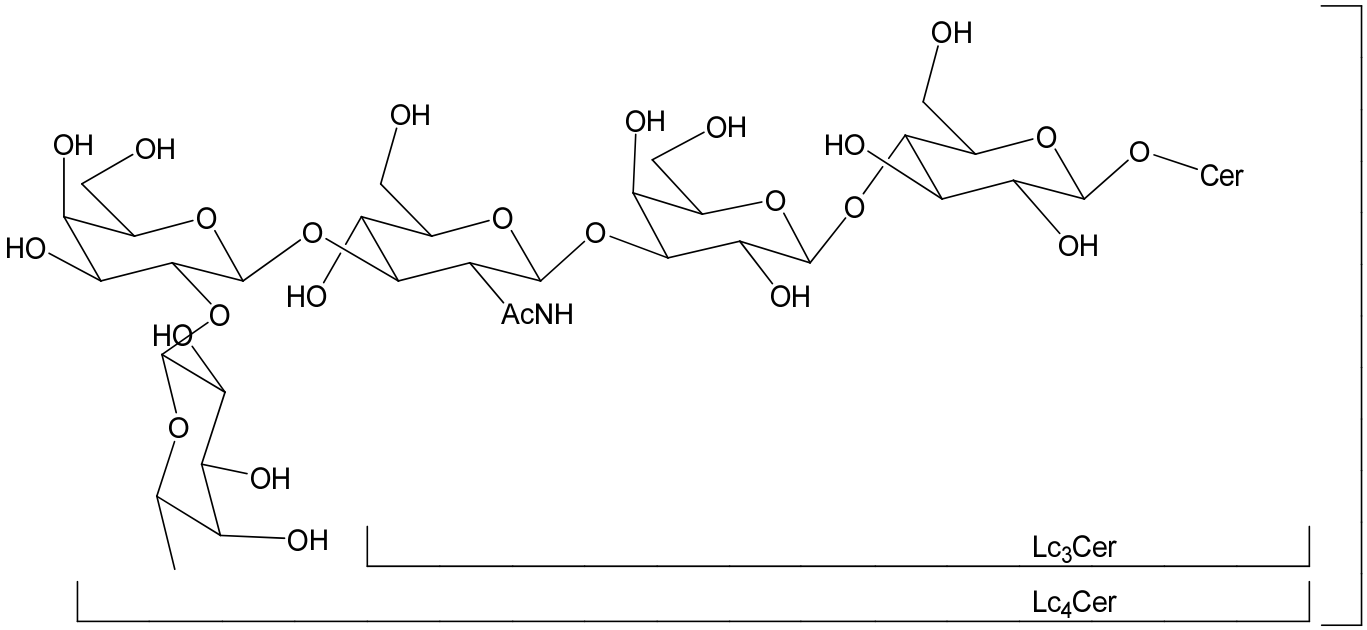

Type I H Antigen

Sialyl Le^a [Galβ1-3GlcNAcβ1-3Galβ1-4Glcβ1-1'Cer]

A product of NeuAcα2-3Galβ1-3GlcNAcβ1-3Galβ1-4Glcβ1-1'Cer which in turn was derived from Lc_4Cer, sialyl Le^a appears in undifferentiated embryonic cells in a pre-implantation embryo from the 8-cell during E14 (79).

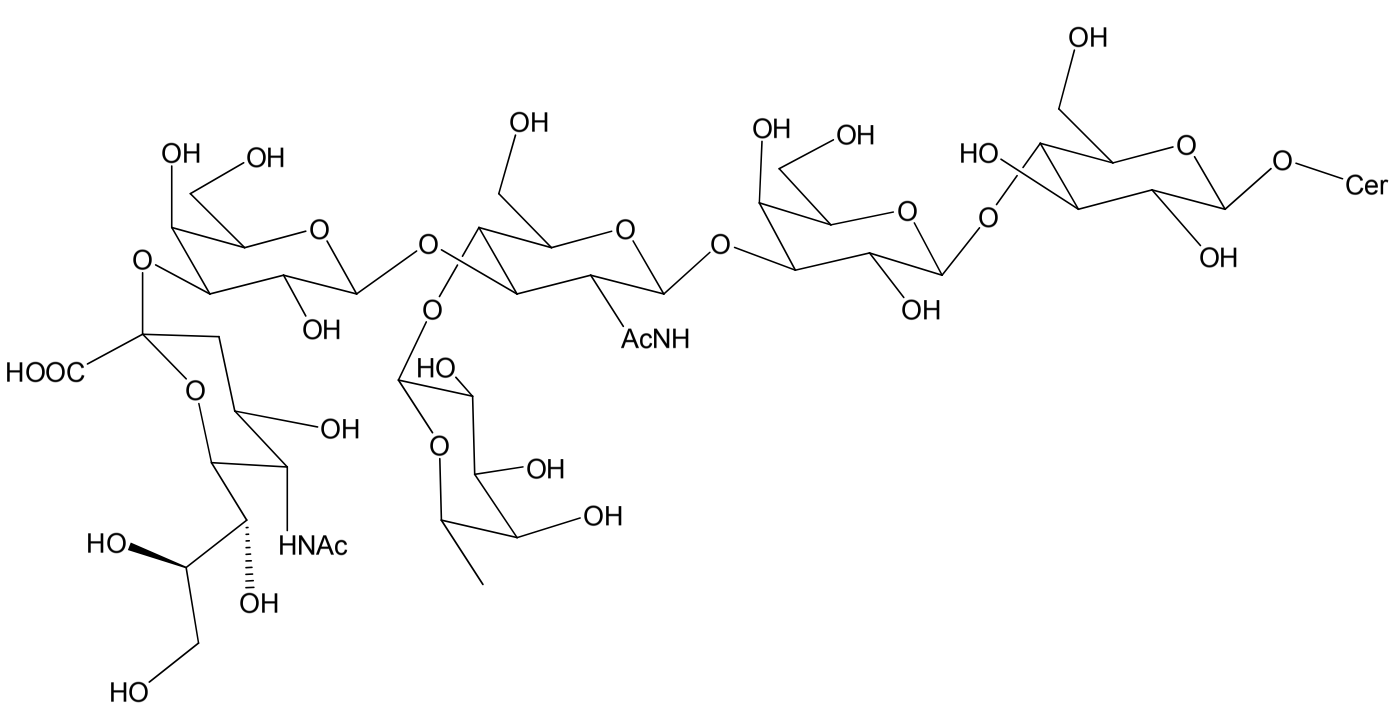
OH
OH
OH
OH
OH
OH
HO
O
O
Cer
OH
O
O
O
O
O
O
O
O
O
O
AcNH
OH
HOOC
O
HO
OH
O
OH
OH
HO
HNAc
OH
HO

Sialyl Le^a

1.2.4 Neolacto-series [Galβ1-4GlcNAcβ1-3Galβ1-4Glcβ1-1'Cer]

A root molecule containing a β-configuration of (1-4) instead of (1-3) in the terminal galactose converts lacto-series into neolacto-series. Molecules such as disialosyl-lacto-N-neotetraosylceramide (LD1) in this family can be found in purkinje cells and the mouse cerebellum (73). The O-acetylated form of LD1 is present in the fetal cortex during embryogenesis, and persists in the adult mouse cerebellum (73).

Paragloboside [Galβ1-4GlcNAcβ1-3Galβ1-4Glcβ1-1'Cer]

Lacto-N-neotetraosylceramide, or nLc_4Cer can be found in the mouse cerebellum, the murine leukemia cell line M1, and in muscle tissue (30).

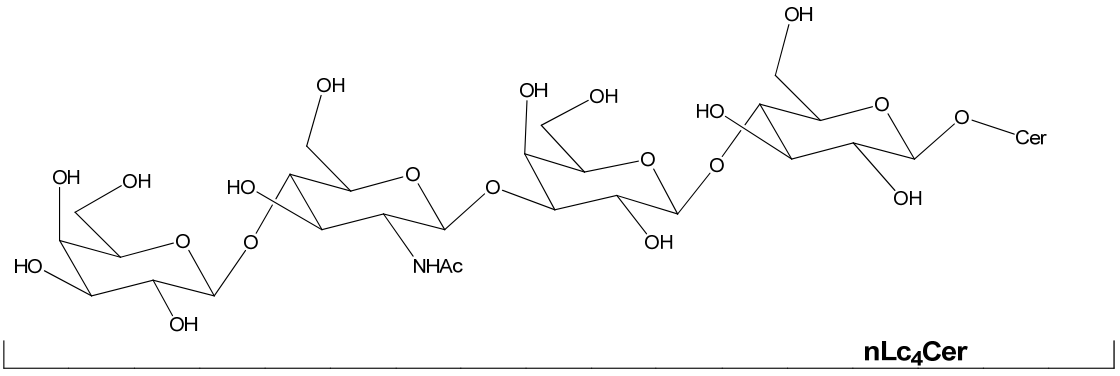

Sialosylparagloboside [NeuAcα2-3Galβ1-4-GlcNAcβ1-3Galβ1-4Glc1-1'Cer]

As its name implies, sialylparagloboside, or sialyl-neolactotetraosylceramide (80) consists of a sialic acid residue attached to the aforementioned nLc_4Cer. It is present in mouse muscle+B187, and the molecule containing NeuGc appears in the ICR mouse spleen (39).

SSEA-1, Le^x [Galβ 1-4(Fucα1-3)GlcNAcβ1-3Gal-β1-4Glcβ1-1'Cer]

This stage-specific embryonic antigen-1 (SSEA-1) is expressed in murine EC cells, more specifically in the inner cell mass. It has been suggested that this molecule mediates the compaction of the mouse embryo (81).

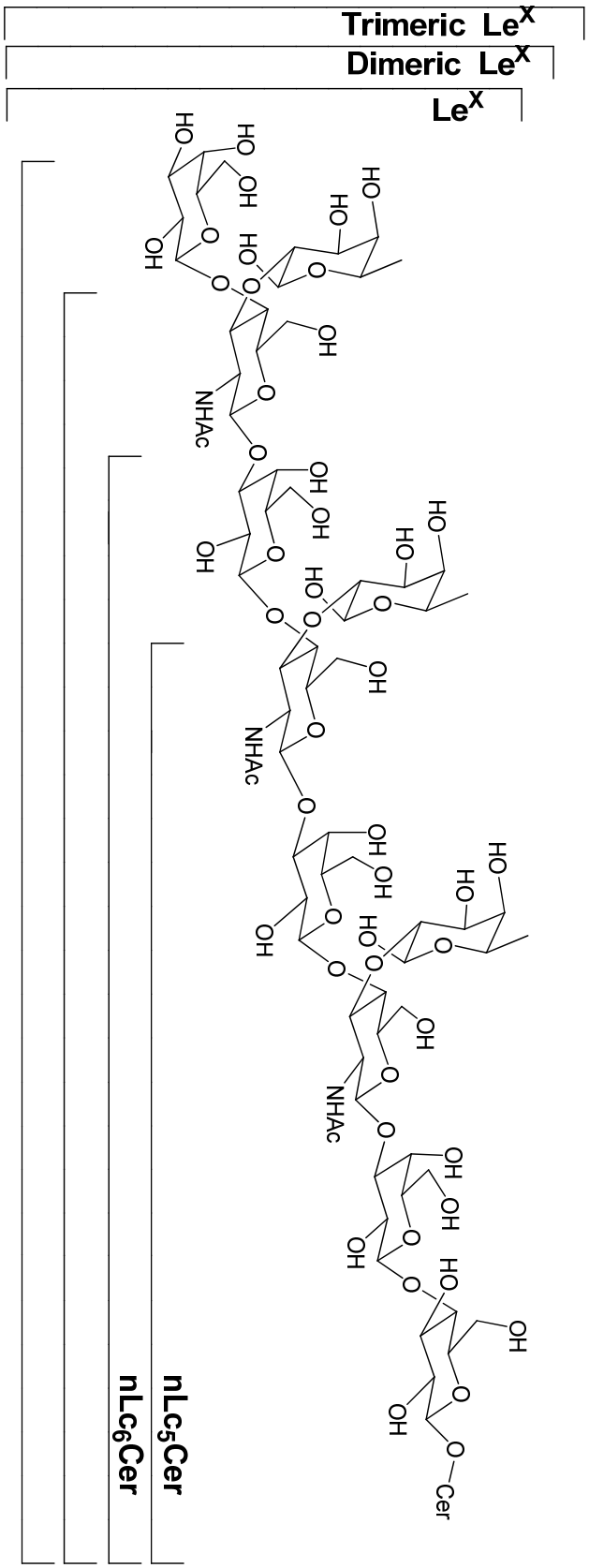
Trimeric Le^X
Dimeric Le^X
Le^X
nLc5Cer
nLc6Cer

Sialyl Le^x [NeuAcα2-3Galβ 1-4(Fucα1-3)GlcNAcβ1-3Gal-β1-4Glcβ1-1'Cer]

Sialyl Le^x is fucosylated sialosylparagloboside, and is recognized by three components of the selectin receptor family that participate in the initial interactions between leukocytes and vascular endothelia (82), although it is not the carbohydrate ligand of E-selectin (53). It appears during E14 in the pre-implantation mouse embryo from the 8-cell stage (79). The lymphocyte homing receptor, L-selectin (LECAM-1) binds it at a lower affinity than its corresponding sulfatide (52). It has also been used to examine binding specificities of the sialoadhesin family of I-type lectins (32). It is weakly recognized by monoclonal antibody AM-3 which was raised against a sialomucin from human colorectal carcinoma (54), and one of the monoclonal antibodies raised against this ganglioside reacts selectively with helper memory T cells (55). Sialyl Le^x inhibits lung metastases produced by intravenous co-injection of B16-BL-6 melanoma cells (56).

Type II H antigen [Fucα1-2Galβ1-4GlcNAcβ1-3Gal-β1-4Glcβ1-1'Cer] and Type III H antigen [Fucα1-2Galβ1-3GalNAcα1-3(Fucα1-2)Galβ1-4GlcNAcβ1-3Gal-β1-4Glcβ1-1'Cer]

Type II H antigen and Type III H antigen are found in the ectodermal and neuroectodermal parts of murine teratocarcinoma (25). The intermediates in the pathway from nLc_4Cer to Type II H antigen (nLc_5Cer and nLc_6Cer) and from Type II H antigen to Type III H antigen have not been found experimentally in the mouse, although can be presumed to exist in minor amounts.

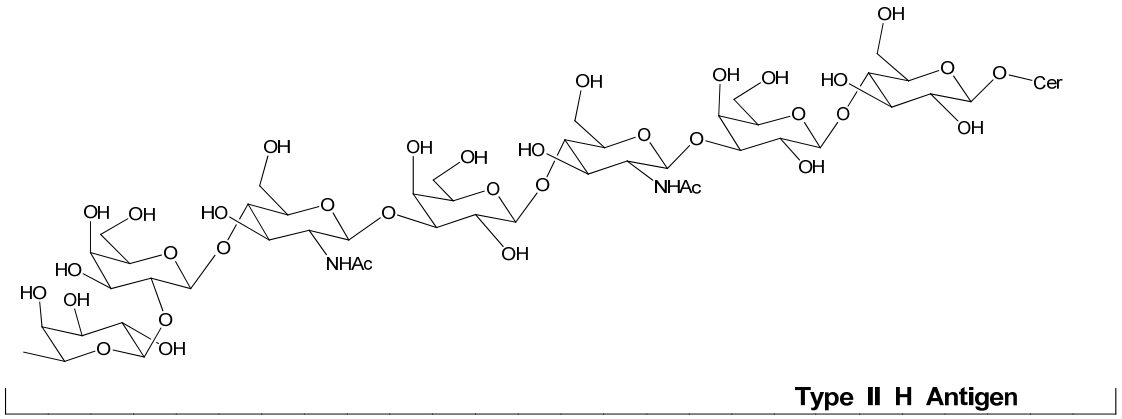

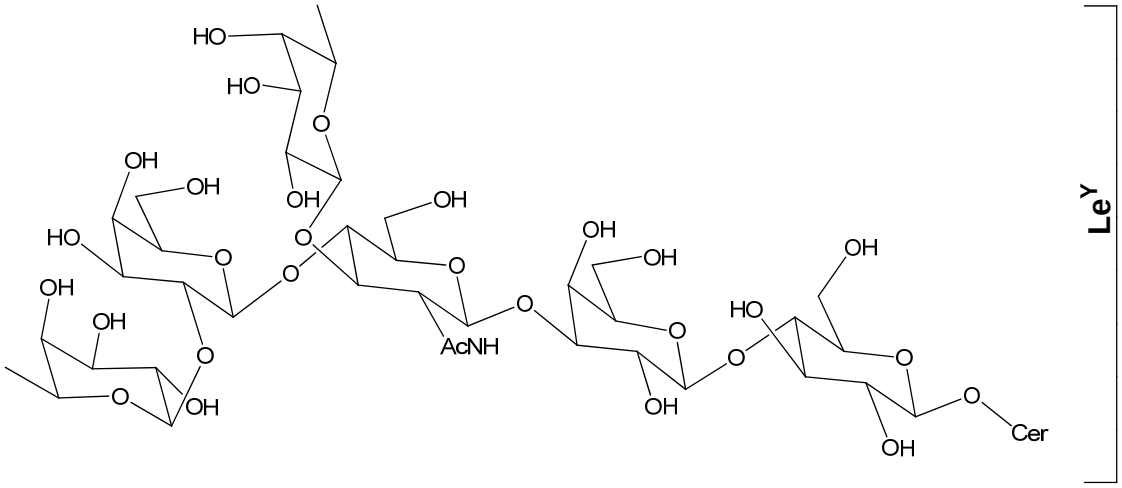

1.2.5 Globo-series [Galα1-4Galβ1-4Glcβ1-1'Cer]

These molecules are more prevalent in the mouse, and play a role in lung (28), muscle (30), kidney (83), uterus (29), and especially embryonic tissues. SSEAs involved with embryogenesis also belong in this family, and have been used to show that a shift of glycolipid synthesis from globo-series to lacto-series glycolipids might occur in pre-implantation mouse embryos (34). These neutral molecules are also present in murine myelogenous leukemias (27).

Globotriaosylceramide Gb_3Cer[Galα1-4Galβ1-4Glcβ1-1'Cer]

The first molecule in the pathway for globo-series, Gb_3Cer is in the murine adrenal gland (24), uterus (29) and myelogenous leukemias (27).

Globotetraosylceramide Gb_4Cer [GalNAcβ1-3Galα1-4Galβ1-4Glcβ1-1'Cer]

Like its precursor Gb_3Cer, Gb_4Cer is present in the murine adrenal gland (24), uterus (29) and myelogenous leukemias (27). However, it moves to mouse muscle (30) and is also present in the murine Lewis lung carcinoma cell line LL2, F9 cells (84), WHT/Ht mouse thymoma and thymocytes (85) and in embryonic and extra-embryonic tissues (84). Minor amounts of it are present in NF-1 cells (84).

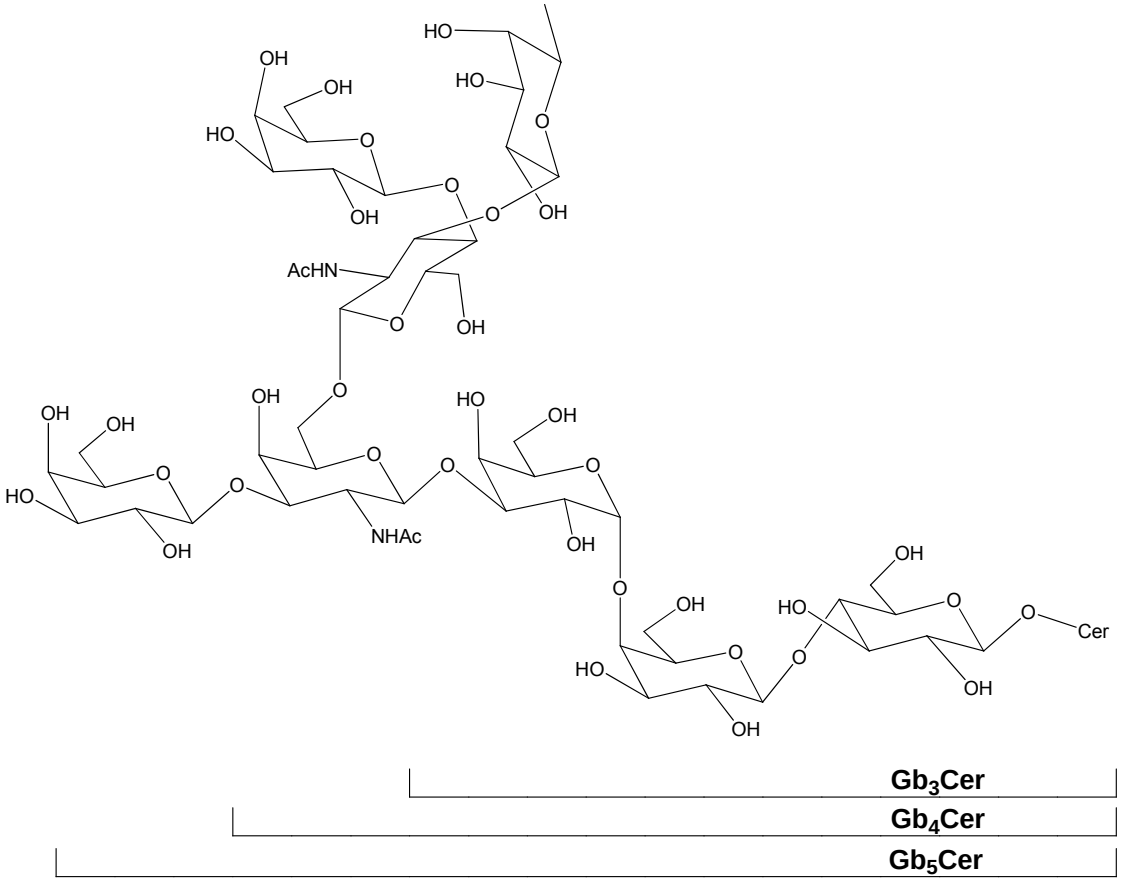

SSEA-3, Globopentaosylceramide Gb_5Cer[Galβ1-3GalNAcβ1-3Galα1-4Galβ1-4Glcβ1-1'Cer]

SSEA-3, a stage-specific embryonic antigen is present in the visceral yolk sac and placenta (84). It has been detected on surfaces resembling the primitive endoderm and trophectoderm in murine teratocarcinoma-derived cell lines (84). Gb_5Cer can also be located in the mouse adrenal gland (24) and kidney (83).

SSEA-4 antigen [NeuAcα1-3Galβ1-3GalNAcβ1-3Galα1-4Galβ1-4Glcβ1-1'Cer]

The molecule subsequent to SSEA-3, SSEA-4, or GL7 is also a stage-specific embryonic antigen, and commonly occurs in the visceral yolk sac and placenta in the developing mouse embryo (84).

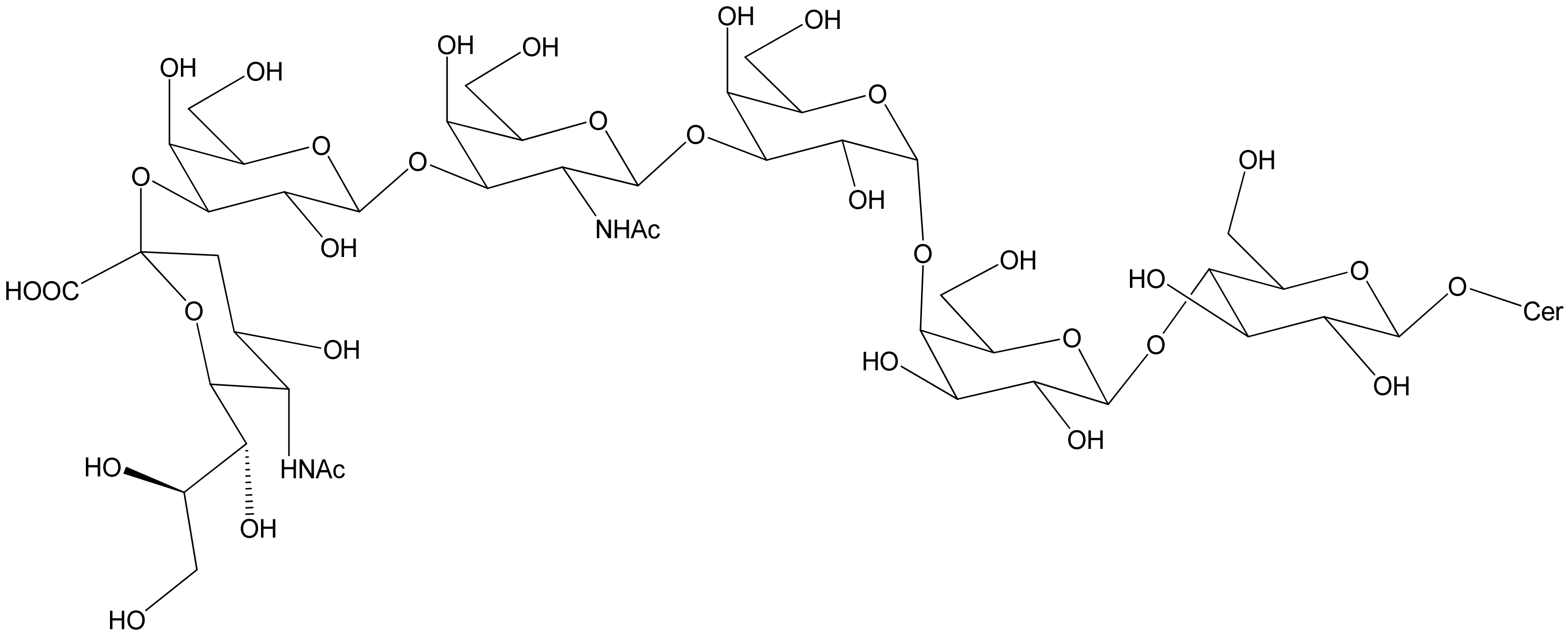

SSEA-4

Forssman antigen [GalNAcα1-3GalNAcβ1-3Galα1-4Galβ1-4Glcβ1-1'Cer]

Forssman antigen is also present in embryonic and extra-embryonic tissues, specifically in the visceral yolk sac and placenta (84). It shows no Lewis activity in the mouse small intestine (86), although is present in muscle tissue (30), F9 cells (84), and murine myelogenous leukemias (27).

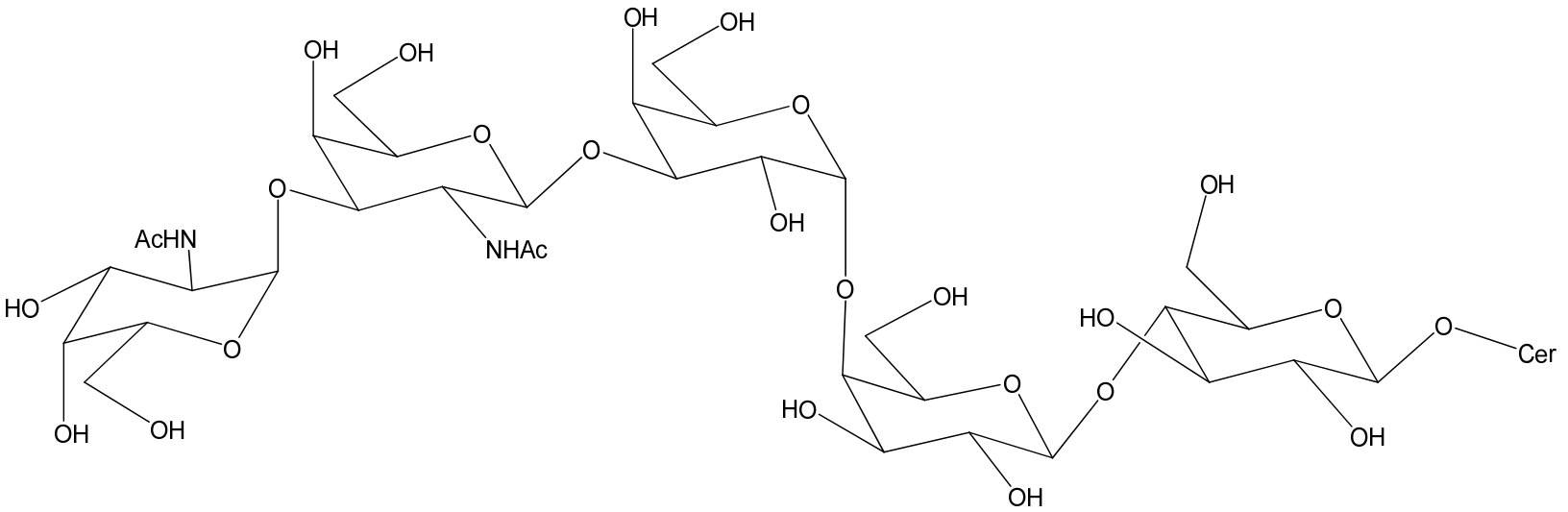

Forssman Antigen

Globo-Lex-9 [Galβ1-4(Fucα1-3)GlcNAcβ1-6(Galβ1-3)GalNAcβ1-3Galα1-4Galβ1-4Glcβ1-1'Cer]

Globo-Lex-9 and its precursor [Galβ1-3(GlcNAcβ1-6)GalNAcβ1-3Galα1-4Galβ1-4Glcβ1-1'Cer] appear in the mouse kidney (83).

Type IV H antigen [Fucα1-2Galβ1-3GalNAcβ1-3Galα1-4Galβ1-4Glcβ1-1'Cer]

Similar to the H blood group antigens in the neolacto-series, Type IV H antigen has also been detected on the ectodermal and neuroectodermal parts of murine teratocarcinoma (25).

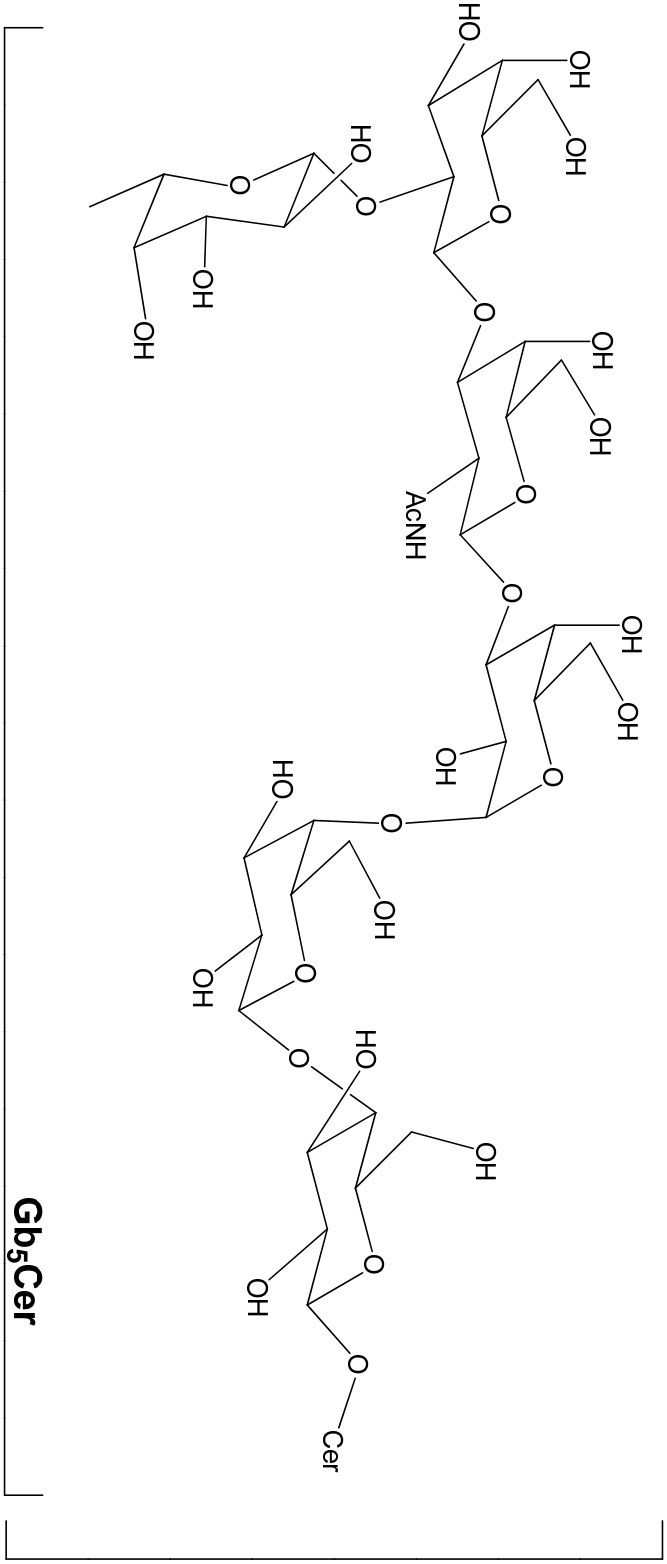

Type IV H Antigen

1.2.6 Isoglobo series GSLs [Galα1-3Galβ1-4Glcβ1-1'Cer]

The isoglobo series of GSLs are derived from a relatively minor GSL biosynthesis pathway catalyzed by iGb_3 synthase (iGb_3S) (87).

Isoglobotrihexosylceramide, iGb_3Cer [Galα1-3Galβ1-4Glcβ1-1'Cer]

iGb_3Cer was detected solely in the dorsal root ganglion in wild type mice (87) and is likely to be a natural invariant natural killer T cell-selecting ligand in the thymus of mouse (87).

Isoglobotetrahexosylceramide, iGb_4Cer [GalNAcβ1-3Galα1-3Galβ1-4Glcβ1-1'Cer]

It has been reported that mouse kidney lacks iGb_4Cer (88).

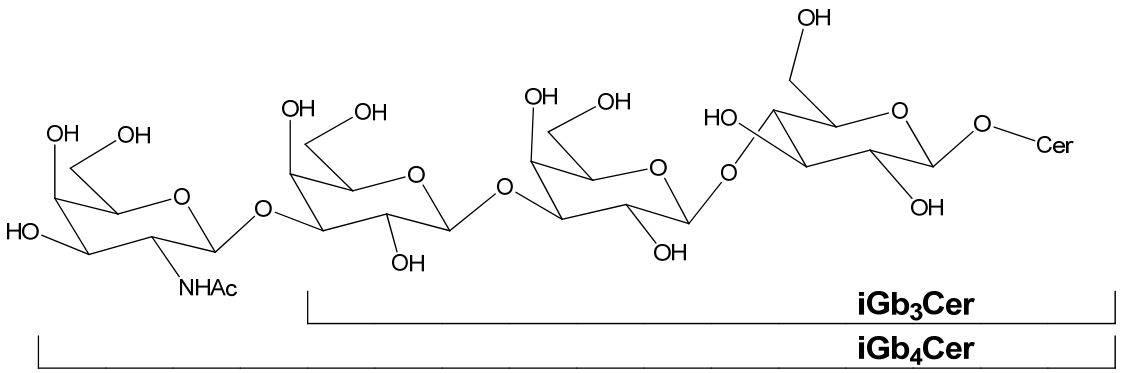

1.2.7 Sulfated GSLs

The sulfate group generally attaches to the terminal end of the growing monosaccharide chain at C3. Usually, these molecules are ligands for L-selectin, the lymphocyte homing receptor (52). In the mouse, both sulfated and bis-sulfated GSLs are abundant in the kidney. Such molecules include lactosylsulfatide [SM3, HSO_3 -3Galα1-

4Glcβ1-1'Cer], bis-sulfo-gangliotetraosylceramide [SB1a, HSO_3 -3Galβ1-3GalNAcβ1-4(HSO_3)Galβ1-4Glcβ1-1'Cer] and gangliotriaosylceramide sulfate [SM2a, GalNAcβ1-4(HSO_3-3)Galβ1-4Glcβ1-1'Cer] (89,90). Sulfogangliotetraosylceramide [SM1b, HSO_3-3Galβ1-3GalNAcβ1-4Galβ1-4Glcβ1-1'Cer] stands as an exception and is present in the mouse intestine (91,92).

Galactosylsulfatide [HSO_3-3Galβ1-1'Cer]

Galactosylceramide 3-sulfate (SM4s) plays a role in the stimulation of the evolution of oxygen radicals in polymorphonuclear leukocytes (93). Moreover, it interacts with the GM2 activator protein (94), and cannot be hydrolyzed by glucosulfatase (95). In addition to the murine kidney (90,96), it is present in myelin components (97,98), specifically the myelin sheath in the mouse brain.

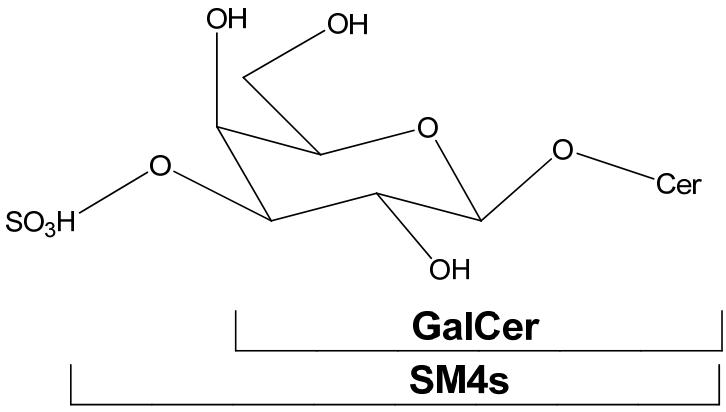

1.2.8 Gala-series [Galα1-4Galβ1-1'Cer]

Only one molecule from this series, galabiosylceramide (Galα1-4Galβ1-1Cer) has been found in the kidney of BALB/c, A, and C57/BL mouse strains (99). It plays a role in

the modulation of the affinity of alpha-interferon for its membrane protein receptors in human cells (100). Its level fluctuates in the mouse on account of sex hormones (101).

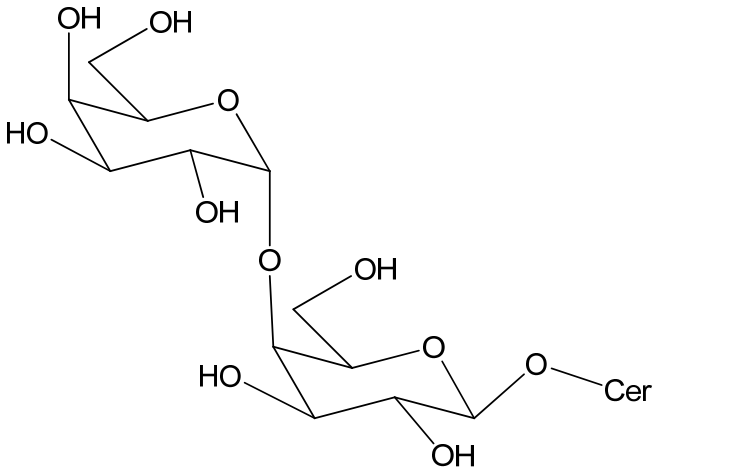

Galabiosylceramide

1.2.9 Sulfoglucuronyl-neolacto series [HSO3-3GlcUβ1-3Galβ1-4GlcNAcβ1-3Galβ1-4Glcβ1-1'Cer] and [HSO3-3GlcUβ1-3Galβ1-4GlcNAcβ1-3Galβ1-4GlcNAcβ1-3Galβ1-4Glcβ1-1'Cer]

This family of GSLs is unique in that it includes the monosaccharide glucuronic acid (GlcU) on the carbohydrate moiety of sulfated glycolipids in the neolacto-series. Also known as sulfoglucuronylglycolipids (SGGLs), or HNK-1 antibody glycolipids on account of detection via a reaction with HNK-1, these are primarily adhesion molecules of neurons (102), and are present in mouse purkinje cells (103), peripheral nerves (104,105), and the cerebellum (103,106). On comparing the fatty acid composition of all molecules of SMUnLc4Cer, 13% are C16:0, 16% are C18:1, 11% are C18:0, 13% are C24:1, and 15% are C24:0 (107).

1.2.10 Psychosine, galactosylsphingosine

Globoid cell leukodystrophy or Krabbe disease is an antosomal recessive inherited neurological disorder caused by the deficiency of the lysosomal enzyme β-galactobrosidase (108,109). The twitcher mouse is an authentic murine model of Krabbe disease (110,111) and shows a remarkable accumulation of psychosine in the brain, spinal cord and peripheral nerves (108,109,111-113).

1.3. Roles in development

A remarkable change of expression of carbohydrate markers has been reported in early embryo, embryonic stem (ES) and embryonic carcinoma (EC) cells (114). During mouse embryogenesis *in vitro*, the globo-series GSLs (SSEA-3 and SSEA-4) express highly at earlier stage (2-to-4-cell stage) of embryo. As SSEA-3 and SSES-4 decrease and disappear, the neolacto-series GSL (SSEA-1) first appears at late 8-cell stage and express highly at 16-to-32-cell stage. And another globo-series GSL, forssman antigen, begins to be expressed on late morulae in mouse development (115). SSEA-3 disappears faster than SSEA-4 (114). After differentiation, these antigens are down-regulated (116). SSEA-1 is greatly expressed in mouse EC cells, but disappears after most cells are differentiated completely *in vitro* (117). These data suggest that glycolipid core structural changes regulated by a few key glycosyl transferases may be critical during cell differentiation in embryogenesis and during oncogenesis (114).

Although the expression of SSEAs is strictly controlled during embryogenesis, SSEA-1 has been suggested that mediate compaction, a tight adhesion of the blastomeres,

in mouse embryos, and a function of SSEA-3 and SSEA-4 may be related to the P-blood-group system (114,116,118,119).

GSLs have also important roles in mouse brain developments. Gangliosides (GM2, GM1, GD3, GD1a, GD2, GD1b, GT1b, GQ1b, GT3, GQ1c, GT1aα and GQ1bα) and different categories of GSLs (Glc-Cer, Gal-Cer, Sulfatide and Le^x) have developmental changes of their expression patterns in developing mouse brains. GD3 is the most abundant expressed ganglioside at E12 to E14 (120). As GD3 and GM3 decrease, GD1a increases after E16 (120). Glc-Cer, SSEA-1 and GT3 are also expressed in embryonic mouse brains (120). Therefore, SSEAs may be useful to identify, isolate, or specifically target EC cells (121,122) and the dramatic changes in GSL pattern and content can serve as important markers in developmental biology.

Day	**0**	**0.5**	**1**	**1.5**	**2**	**2.5**	**3.5**	**7**
SSEA-1 (Le^x)	-	-	-	++	+++	+	+	-
(Le^y)	-	-	-	-	-	-	++	-
SSEA-3/4		++	+++	+	+	-	-	
Gb_4			+	++	+++	-	**?**	
Ganglio-Series		-	-	-	-	-	-	+/++

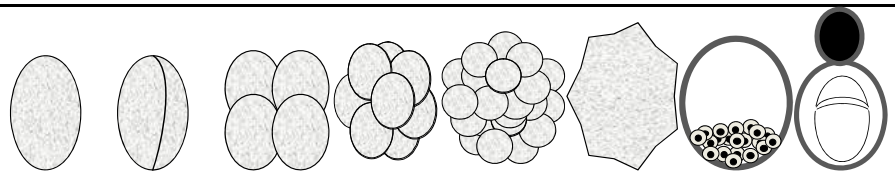

Figure 1.2. Glycosphingolipidomic role in defining tumor potency (Hakomori 2002). SSEA-1 (Le^x) is not expressed until morula stage, declines after compaction, and is restricted to inner cell mass of blastocyst. SSEA-3 and -4 are expressed highly at four-cell stage and decline later. Globoside (Gb_4) is expressed maximally at morula stage. Ganglio-series epitopes are not expressed during the preimplantation stage, but appear only upon further differentiation (neural crest formation).

Table 1.2. Functions of GSLs in tumors (Hakomori 2000)

Tumor associated GSLs	Binding to E-selecting on activated EC
	Platelet activation to release factors that activate EC
	Gal- or sialic acid-binding lectins expressed on target cells
	Promotion or inhibition of angiogenesis
	Multiple drug resistance associated with ceramide: glycosylation
	Binding to carbohydrates expressed on EC (carbohydrate-carbohydrate interaction)

1.4. Roles in tumorigenesis

Little is known about the mechanisms through which specific GSLs induce invasive and metastatic phenotypes of tumor cells. However, high expression of some GSLs promotes invasion and metastasis of tumor cells. Sialyl-Le^x, sialyl-Le^a, Le^y, GM2, GD3, and sialyl-Gb_5 promote invasion and metastasis of cancer (123). On the other hand, expression of some other GSLs suppresses tumor progression, for examples, 4GlcNAc competitive with 6GlcNAc; histo-blood group A and B competitive with sialylated structures including sialyl-Le^x and sialyl-Le^a; Gb_5 competitive with sialyl-Gb_5 (61,123).

Lac-Cer was claimed to inhibit apoptosis, mainly through increased *Bcl*-2 and decreased caspase expression (123,124). Apoptosis was previously found to be associated with Le^y expressed in various types of cancer (125) and continuous expression of GM3 in Chinese hamster ovary mutant ldlD, associated with CD9 and CD82, induces apoptosis, because GM3 inhibits cell motility and invasiveness when complexed with CD9 or CD82 (126). However, a different ganglioside monosialo-Gb5, complexed with CD9 in breast cancer MCF7 cells, strongly enhances motility and invasiveness (127). Similar considerations may apply to the inhibitory effect of GM3 on epidermal growth factor

(EGF) receptor tyrosine kinase (128). GM3 in mouse ependymoblastoma tumor cell line EPEN inhibits tumor growth and angiogenesis, whereas induction of GM2, GM1, and GD1a synthesis through β4GalNAc-T transfection leads to higher vascularization and enhanced endothelial growth factor (VEGF) production (129). GD3 may promote tumor cell motility and growth, possibly through angiogenesis and vascular VEGF production, as evidenced by antisense approach using GD3 synthase gene (130).

SLe^x and SLe^a have been identified as tumor-associated antigens and as E-selectin epitopes, and may promote adhesion of tumor cells to endothelial cells. Clinically, expression of SLe^x (131) and SLe^a (132) is inversely correlated with postoperative survival rate of patients. Therefore, GSLs involved in tumor cell metastasis are targets for cancer therapy, such as antitumor vaccines.

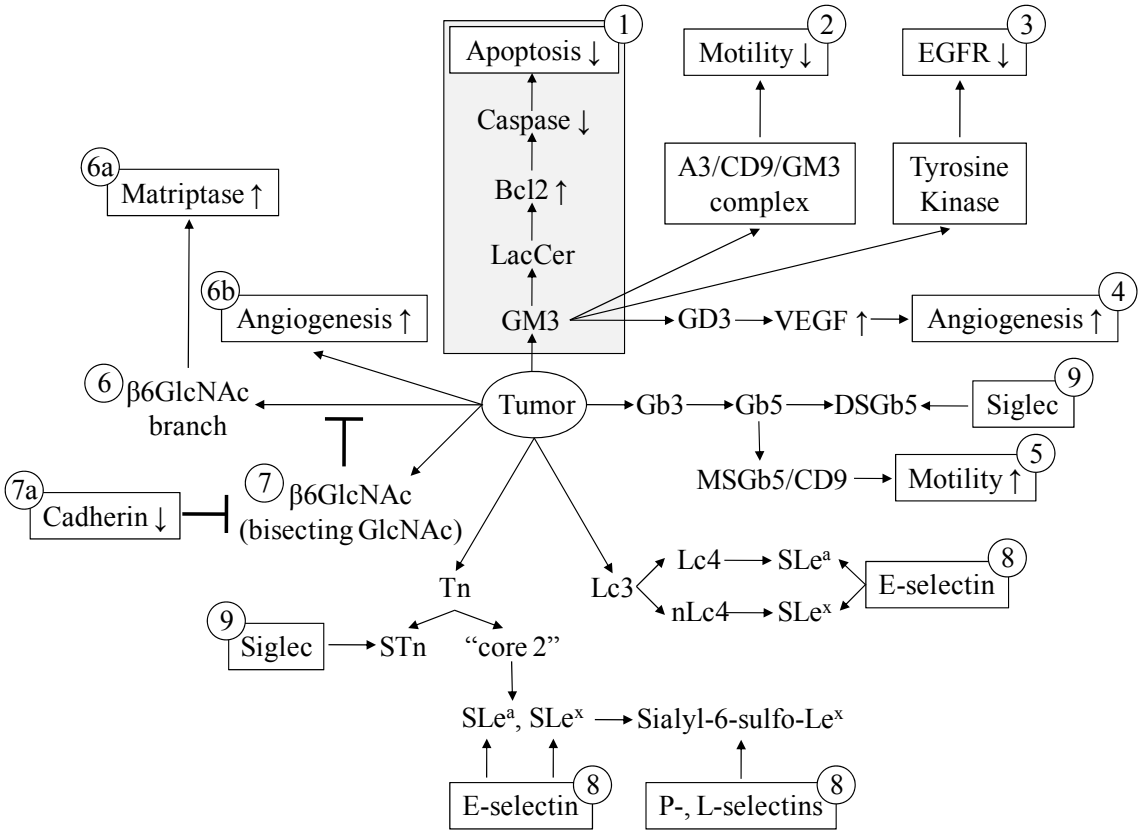

Figure 1.3. Glycosphingolipidomic role in defining tumor potency (Hakomori 2002). Tumor cell malignancy is defined by several key phenotypes: apoptosis (route 1), motility (routes 2 and 5), EGF receptor tyrosine kinase (route 3), angiogenesis (routes 4 and 6b), matriptase (matrix-destroying enzyme) activity (route 6a), self-adhesion (through cadherin) (route 7a), adhesion to ECM (through integrin), adhesion to ECs and platelets (through E- or P- selectin) (route 8), adhesion to blood cells and other parenchymatous cells (through siglecs) (route 9). Each phenotype is up- or down-regulated (↑, ↓) by different status of glycosylation as indicated in the figure. Phenotypes with (↑, ↓) and routes 2, 3, and 7a, and inhibit tumor invasiveness. Those with (↑, ↓) and routes 1, 4, 5, 6a, 6b, and 8 promote tumor invasiveness. Glycosyl epitopes capable of binding to specific ligands promote invasiveness. Some ligands (α3/CD9/GM3 complex, tyrosine kinase and siglec) have variable or unclear effect on invasiveness. A given phenotype is produced by different glycosylations, and a given glycosylation produces different phenotypes. Phenotypic changes have cooperative effects on malignancy. For instance, GM3 inhibits motility through α3/CD9 complex, and also inhibits EGF receptor tyrosine kinase (routes 2 and 3). Reduction of GM3 inhibits apoptosis (route 1), but also promotes motility and proliferation (negative route 2 and 3 effect). All glycosylation pathways catalyzed by multiple glycosyltransferases and their genes are well established, although the mechanism by which each type of glycosylation affects the various phenotypes remains to be studied.

1.5 Mouse models

The deficiency of degradation of GSLs may cause serious physiological problems because of the importance of the balance between synthesis and degradation. Gal-Cer synthase (ceramide galactosyltransferase, CGT) knockout mice generate severe generalized tremor, mild ataxia and conduction deficits and male sterility (133). The severe dysmyelinosis leads to the death of the null mice at the end of the myelination period, because Gal-Cer and/or sulfatides play important roles in myelin function and its stability (133). The knockout mice of sulfatides synthase lead to similar neurological abnormalities and disrupt spermatogenesis to Gla-Cer knockout mice (134).

The knockout mice of Glc-Cer synthase (GST) resulted in a complete loss of GlcCer and die at 7.5 embryonic day (135). This suggests that GSL synthesis is important for embryogenesis. Although embryogenesis proceeded into the primitive germ layers in case of the *Ugcg-/-* embryos, the overall embryonic structure was halted by a massive apoptotic process (134).

The GD3 synthase knockout mice resulted in the increase of all a-series gangliosides and the loss of all b-series gangliosides (136,137). Although there is no remarkable morphological changes in these null mice, the regenerative activity were reduced in the hypoglossal nerve resection system (137). The mice lacking GM2/GD2 synthase showed complete loss of gangliosides such as GM1, GD1a, GD1b, GT1b, GQ1b, GM2, GD2, and asialo-series gangliosides (138). The GM2/GD2 synthase null mice induced a mild damage of nerve system (138) and a severe disruption of male fertility (139). Double knockout mice of the GD3 synthase and GM2/GD2 synthase had only GM3 ganglioside and were born and grew up almost normally at a glance (140). However, they started to

die suddenly at 12 weeks after birth or later by unknown reason and had refractory skin lesions (140). There is another report that this genetic disruption caused an audiogenic seizure and consequent sudden death by noise (137).

These knockout studies in mice have shown that GSLs are critical in development and differentiation.

1.6 Future directions

Knowledge about existing GSLs in murine tissues is in tandem with the development and discoveries regarding new structures are constantly underway. These molecules are structurally very diverse, and uncovering each nuance of the glycan and lipid structure will require analysis via methods such as mass spectrometry and an understanding of their metabolic pathways in murine tissues. On the other hand, knowing the functional role of GSLs in signal transduction, membrane leaflets, embryogenesis and tumorigenesis will also help predict structures.

1.7 References

1. Chester, M. A. (1998) *Eur J Biochem* **257**, 293-298
2. Thudichum, J. L. W. (1884) A Treatise on the Chemical Constitution of Brain. (Bailliere, T., and Cox ed., London
3. Hakomori, S. I. (1983) Chemistry of Glycosphingolipids. in *Sphingolipid Biochemistry* (Kanfer, J. N., Hakomori, S. ed.), Plenum, New York. pp 1-64
4. Schuette, C. G., Doering, T., Kolter, T. and Sandhoff, K. (1999) *Biol. Chem.* **380**, 759 - 766
5. Brown, D. A., and London, E. (2000) *J. Biol. Chem.* **27**, 17221 - 17224
6. Merrill, A. H., Jr., Sullards, M. C., Wang, E., Voss, K. A., and Riley, R. T. (2001) *Environ Health Perspect* **109 Suppl 2**, 283-289
7. Merrill, A. H., Jr., and Sandhoff, K. (2002) Sphingolipids: metabolism and cell signaling. in *Biochemistry of Lipids, Lipiproteins and Membranes.* (Devaje, V. ed.), Elsevier Science B. V. pp 373-407
8. Zheng, W., Kollmeyer, J., Symolon, H., Momin, A., Munter, E., Wang, E., Kelly, S., Allegood, J. C., Liu, Y., Peng, Q., Ramaraju, H., Sullards, M. C., Cabot, M., and Merrill, A. H., Jr. (2006) *Biochim Biophys Acta* **1758**, 1864-1884
9. Pewzner-Jung, Y., Ben-Dor, S., and Futerman, A. H. (2006) *J Biol Chem* **281**, 25001-25005
10. Lahiri, S., Lee, H., Mesicek, J., Fuks, Z., Haimovitz-Friedman, A., Kolesnick, R. N., and Futerman, A. H. (2007) *FEBS Lett* **581**, 5289-5294
11. Morell, P., and Radin, N. S. (1970) *J Biol Chem* **245**, 342-350
12. Mandon, E. C., Ehses, I., Rother, J., van Echten, G., and Sandhoff, K. (1992) *J Biol Chem* **267**, 11144-11148
13. Hirschberg, K., Rodger, J., and Futerman, A. H. (1993) *Biochem J* **290 (Pt 3)**, 751-757
14. Venkataraman, K., Riebeling, C., Bodennec, J., Riezman, H., Allegood, J. C., Sullards, M. C., Merrill, A. H., Jr., and Futerman, A. H. (2002) *J Biol Chem* **277**, 35642-35649
15. Riebeling, C., Allegood, J. C., Wang, E., Merrill, A. H., Jr., and Futerman, A. H. (2003) *J Biol Chem* **278**, 43452-43459
16. Mizutani, Y., Kihara, A., and Igarashi, Y. (2005) *Biochem J* **390**, 263-271
17. Mizutani, Y., Kihara, A., and Igarashi, Y. (2006) *Biochem J* **398**, 531-538
18. Laviad, E. L., Albee, L., Pankova-Kholmyansky, I., Epstein, S., Park, H., Merrill, A. H., Jr., and Futerman, A. H. (2008) *J Biol Chem* **283**, 5677-5684
19. Lahiri, S., and Futerman, A. H. (2005) *J Biol Chem* **280**, 33735-33738
20. Vallee, B., and Riezman, H. (2005) *Embo J* **24**, 730-741
21. El Bawab, S., Birbes, H., Roddy, P., Szulc, Z. M., Bielawska, A., and Hannun, Y. A. (2001) *J Biol Chem* **276**, 16758-16766
22. Hakomori, S.-i. (2000) *Glycoconjugate Journal* **17**, 627-647
23. Gagneux, P., and Varki, A. (1999) *Glycobiology* **9**, 747-755
24. Sekine M, A. T., Miyatake T, Kase R, Suzuki A, Yamakawa T. (1985) *J Biochem (Tokyo).* **97**, 1219-1227
25. Hansson GC. (1988) *Adv Exp Med Biol.* **228**, 465-494
26. Burdin, N., Brossay, L., Koezuka, Y., Smiley, S. T., Grusby, M. J., Gui, M., Taniguchi, M., Hayakawa, K., and Kronenberg, M. (1998) *J Immunol.* **161**

27. Ariga T, Y. K., Nemoto K, Seki M, Miyatani N, Yu RK. (1991) *Biochemistry. 1991 Aug 13;30(32):7953-61.* **30**, 7953-7961
28. Momoeda K, H. K., Utsuki T, Tsuchida Y, Hanaoka K, Iwamori M. (1996) *J Biochem (Tokyo)* **119**, 1189-1195
29. Mikami M. (1991) *Keio J Med.* **40**, 82-89
30. Muthing J, M. U., Sostaric K, Neumann U, Brandt H, Duvar S, Peter-Katalinic J, Weber-Schurholz S. (1994) *J Biochem (Tokyo)* **115**, 248-256
31. Ladisch, S., Hasegawa, A., Li, R., and Kiso, M. (1995) *Biochemistry.* **34**, 1197-1202
32. Collins, B. E., Kiso, M., Hasegawa, A., Tropak, M. B., Roder, J. C., Crocker, P. R., and Schnaar, R. L. (1997) *The Journal of Biological Chemistry* **272**, 16889 - 16895
33. Murayama K, L. S., Schirrmacher V, Hakomori S. (1986) *Cancer Res.* **46**, 1395-1402
34. Kannagi R, C. N., Ishigami F, Hakomori S, Andrews PW, Knowles BB, Solter D. (1983) *EMBO J.* **2**, 2355-2361
35. Bertoni C, L. Y., Li SC. (1999) *J Biol Chem.* **274**, 28612-28618
36. Hansson GC, K. K., Leffler H, Stromberg N. (1982) *FEBS Lett.* **139**, 291-294
37. Furuya, S., Hashikawa, T., Irie, F., Hasegawa, A., Nakao, T., and Hirabayashi, Y. (1995) *Neurosci Res* **22**, 411-421
38. Hirabayashi, Y., Taki, T., and Matsumoto, M. (1979) *FEBS Lett* **100**, 253-257
39. Nakamura K, H. Y., Suzuki M, Suzuki A, Yamakawa T. (1984) *J Biochem (Tokyo).* **96**, 949-957
40. Li R, G. D., Ladisch S. (1993) *Biochim Biophys Acta.* **1170**, 282-290
41. Nakamura K, S. M., Inagaki F, Yamakawa T, Suzuki A. (1987) *J Biochem (Tokyo).* **101**, 825-835
42. Bartoszewicz, Z., Koscielak, J., and Pacuszka, T. . (1986) *Carbohydrate Research* **151**, 77-88
43. Nakamura K, S. H., Hirabayashi Y, Suzuki A. (1995) *J Biol Chem. 1995 Feb 24;270(8):3876-81.* **270**, 3876-3881
44. Momoeda M, M. K., Takamizawa K, Matsuzawa A, , and Hanaoka K, T. Y., Iwamori M. (1995) *Biochim Biophys Acta.* **1256**, 151-156
45. Taki T, M. H., Arai K, Matsumoto M, Kon K, Ando S. (1988) *Cell Struct Funct.* **13**, 61-72
46. Furuya, S., Irie, F., Hashikawa, T., Nakazawa, K., Kozakai, A., Hasegawa, A., Sudo, K., and Hirabayashi, Y. (1994) *J. Biol. Chem.* **269**, 32418 - 32425
47. Ando, S., Hirabayashi, Y., Kon, K., Inagaki, F., Tate, S., and Whittaker, V. P. (1992) *J. Biochem. (Tokyo).* **111**, 287-290
48. Hirabayashi, Y., Nakao, T., Irie, F., Whittaker, V. P., Kon, K., and Ando, S. (1992) *J. Biol. Chem.* **267**, 12973 - 12978
49. Collins, B. E., Yang, L. J., Mukhopadhyay, G., Filbin, M. T., Kiso, M., Hasegawa, A., and Schnaar, R. L. (1997) *J. Biol. Chem.* **272**, 1248 - 1255
50. Okajima, T., Chen, H. H., Ito, H., Kiso, M., Tai, T., Furukawa, K., Urano, T., Furukawa, K. (2000) *J Biol Chem.* **275**, 6717-6723
51. Krishnaraj, R., Lengle, E. E., and Kemp, R. G. (1982) *Eur J Cancer Clin Oncol* **18**, 89-98

52. Suzuki, Y., Toda, Y., Tamatani, T., Watanabe, T., Suzuki, T., Nakao, T., Murase, K., Kiso, M., Hasegawa, A., Tadano-Aritomi, K., et al. (1993) *Biochemical and biophysical research communications* **190**, 426 - 434
53. Tyrrell, D., James, P., Rao, N., Foxall, C., Abbas, S., Dasgupta, F., Nashed, M., Hasegawa, A., Kiso, M., Asa, D., et al. (1991) *Proceedings of the National Academy of Sciences of the United States of America* **88**, 10372 - 10376
54. Hanisch, F. G., Hanski, C., and Hasegawa, A. (1992) *Cancer Research* **52**, 3138 - 3144
55. Ohmori, K., Takada, A., Ohwaki, I., Takahashi, N., Furukawa, Y., Maeda, M., Kiso, M., Hasegawa, A., Kannagi, M., and Kannagi, R. (1993) *Blood* **82**, 2797 - 2805
56. Saiki, I., Koike, C., Obata, A., Fujii, H., Murata, J., Kiso, M., Hasegawa, A., Komazawa, H., Tsukada, H., Azuma, I., Okada, S., and Oku, N. (1996) *International Journal of Cancer* **65**, 833 - 839
57. Ji MY, L. Y., Do S 2nd, Nam SY, Jung KY, Kim HM, Park , and LK, C. Y. (2000) *Arch Pharm Res.* **23**, 525-530
58. Deng W, L. R., Guerrera M, Liu Y, Ladisch S. (2002) *Glycobiology.* **12**, 145-152
59. Andrade CM, T. V., Cardoso CC, Ziulkoski AL, , and Trugo LC, G. R., Borojevic R, Guma FC. (2003) *J Cell Biochem.* **88**, 533-544
60. El-Abbadi M, S. T., Yates AJ, Orosz C, Lee MC. (2001) *Br J Cancer.* **85**, 285-292
61. Li YT, L. S., Hasegawa A, Ishida H, Kiso M, Bernardi A, Brocca P, Raimondi L, Sonnino S. (1999) *J Biol Chem.* **274**, 10014 - 10018
62. Conzelmann E, S. K. (1979) *Hoppe Seylers Z Physiol Chem.* **360**, 1837 - 1849
63. Li, S. C., Hirabayashi, Y., and Li, Y. T. (1981) *J. Biol. Chem.* **256**, 6234 - 6240
64. Hultberg, B. (1969) *Lancet* **2**, 1195
65. Okada, S., and O'Brien, J. S. (1969) *Science* **165**, 698 - 700
66. Sandhoff, K. (1969) *FEBS Lett.* **4**, 351-354
67. van Heyningen, S. (1976) *FEBS Lett* **68**, 5-7
68. Chen, C., Baldwin, M. R., and Barbieri, J. T. (2008) *Biochemistry* **47**, 7179-7186
69. Noguchi, M., Suping, Z., Taguchi, J., Hirano, T., Hashimoto, H., Hirose, S., Iwamori, M., and Okumura, K. (1994) *Cell Immunol* **156**, 402-413
70. Wiegandt, H., Ziegler, W., Staerk, J., Kranz, T., Ronneberger, H. J., Zilg, H., Karlsson, K. A., and Samuelsson, B. E. (1976) *Hoppe Seylers Z Physiol Chem* **357**, 1637-1646
71. Simpson, L. L., and Rapport, M. M. (1971) *J Neurochem* **18**, 1751-1759
72. Seyfried, T. N., Bernard, D. J., Yu, R. K. (1984) *J Neurochem.* **43**, 1152-1162.
73. Chou DK, F. S., Jungalwala FB. (1990) *J Neurochem.* **54**, 1598-1607
74. Ishida, H. K., Ishida, H., Kiso, M., and Hasegawa, A. (1994) *Tetrahedron: Asymmetry* **5**, 2493 - 2515
75. Kuhn. (1963) *Z Naturforsch* **18**, 541 - 543
76. Irie, F., Kurono, S., Li, Y.- T., Seyama, Y., and Hirabayashi, Y. (1996) *Glycoconj. J.* **13**, 177 - 186
77. Yang, L. J., Zeller, C. B., Shaper, N. L., Kiso, M., Hasegawa, A., Shapiro, R. E., and Schnaar, R. L. (1996) *Proc Natl Acad Sci U S A* **93**, 814-818
78. Seyfried, T. N., Miyazawa, N., and Yu, R. K. (1983) *J Neurochem* **41**, 491-505

79. Kimber SJ, B. D., Pahlsson P, Nilsson B. (1993) *Histochem J.* **25**, 628-641
80. Wiegandt. (1968) *Z Naturforsch* **24**, 945 - 946
81. Andrews, P. W. (2002) *Phil. Trans. R. Soc. Lond. B* **357**, 405 - 417
82. Foxall, C., Watson, S. R., Dowbenko, D., Fennie, C., Lasky, L. A., Kiso, M., Hasegawa, A., Asa, D., and Brandley, B. K. (1992) *J Cell Biol* **117**, 895-902
83. Sekine M., S. M., Inagaki F., Suzuki A., and Yamakawa, T. (1987) *J. Biochem. (Tokyo).* **101**, 553-562
84. Krupnick JG, D. I., Damjanov A, Zhu ZM, Fenderson BA. (1994) *Int J Cancer.* **59**, 692-698
85. Nakamura K, S. M., Taya C, Inagaki F, Yamakawa T, , and A., S. (1991) *J Biochem (Tokyo).* **110**, 832-841
86. Breimer ME, H. G., Karlsson KA, Leffler H. (1981) *J Biochem (Tokyo).* **90**, 589-609
87. Speak, A. O., Salio, M., Neville, D. C., Fontaine, J., Priestman, D. A., Platt, N., Heare, T., Butters, T. D., Dwek, R. A., Trottein, F., Exley, M. A., Cerundolo, V., and Platt, F. M. (2007) *Proc Natl Acad Sci U S A* **104**, 5971-5976
88. Siddiqui, B., Kawanami, J., Li, Y. T., and Hakomori, S. (1972) *J Lipid Res* **13**, 657-662
89. Ishizuka Ineo. (1997) *Prog. Lipid Res.* **36**, 245-319
90. Tadano-Aritomi, K. a. I., Ineo. (2003) *Trends in Glycoscience and Glycotechnology* **15**, 15-27
91. Breimer, M. E., Hansson, G. C., Karlsson, K. A., and Leffler, H. (1983) *J Biochem* **93**, 1473-1485
92. Leffler, H., Hansson, G. C., and Stromberg, N. (1986) *J Biol Chem* **261**, 1440-1444
93. Kakinuma, K., Yamaguchi,T.,Suzuki,H., and Nagai,Y. (1982) *Febs Lett.* **145**, 16-20
94. Hama, Y., Li, Y.-T., and Li, S.-C. (1997) *J. Biol. Chem.* **272**, 2828-2833
95. Hatanaka, H., Ogawa, Y., and Egami, F. (1976) *The Biochemical Journal* **159**, 445-448
96. Ishizuka, I. (1997) *Progress in Lipid Research* **36**, 245-319
97. Burkart, T., Caimi,L.,Siegrist,H.P.,Herschkowitz,N.N., and Wiesmann,U.N. (1982) *J. Biol. Chem.* **257**, 3151-3156
98. Farooqui, A. A., Rebel,G., and Mandel, P. (1977) *Life Sci.* **20**, 569-583
99. Adams EP, G. G. (1968) *Chem Phys Lipids.* **2**, 147-155
100. Cohen, A., Hannigan, G. E., Williams, B. R., and Lingwood, C. A. (1987) *J. Biol. Chem.* **262**, 17088-17091
101. Shayman, J. A., Radin, N. S. (1991) *Am J Physiol.* **260**, F291-302
102. Jungalwala, F. B. (1994) *Neurochem. Res.* **19**, 945 - 957
103. Chou DK, F. S., Jungalwala FB. (1990) *J Neurochem.* **54**, 1589-1597
104. Chou DK, S. G., Evans JE, Jungalwala FB. (1987) *J Neurochem.* **49**, 865-873
105. Ilyas AA, D. M., Brady RO, Quarles RH. (1986) *Brain Res.* **385**, 1-9
106. Nair SM, P. N., Tobet SA, Jungalwala FB. (1993) *J Comp Neurol.* **332**, 282-292
107. Chou, D. K. H., Ilyas,A.A.,Evans,J.E.,Costello,C.,Quarles,R.H., and Jungalawala,F.D. (1986) *J. Biol. Chem.* **261**, 11717-11725

108. Whitfield, P. D., Sharp, P. C., Taylor, R., and Meikle, P. (2001) *J Lipid Res* **42**, 2092-2095
109. Wenger, D. A. (2000) *Mol Med Today* **6**, 449-451
110. Duchen, L. W., Eicher, E. M., Jacobs, J. M., Scaravilli, F., and Teixeira, F. (1980) *Brain* **103**, 695-710
111. Kobayashi, T., Yamanaka, T., Jacobs, J. M., Teixeira, F., and Suzuki, K. (1980) *Brain Res* **202**, 479-483
112. Kobayashi, T., Shinoda, H., Goto, I., Yamanaka, T., and Suzuki, Y. (1987) *Biochem Biophys Res Commun* **144**, 41-46
113. Shinoda, H., Kobayashi, T., Katayama, M., Goto, I., and Nagara, H. (1987) *J Neurochem* **49**, 92-99
114. Andrews, P. W. (1987) *J Cell Biochem* **35**, 321-332
115. Solter, D., and Knowles, B. B. (1978) *Proc Natl Acad Sci U S A* **75**, 5565-5569
116. Draper, J. S., Pigott, C., Thomson, J. A., and Andrews, P. W. (2002) *Journal of Anatomy* **200**, 249-258
117. Muramatsu, T. (1988) *Journal of Cellular Biochemistry* **36**, 1-14
118. Hakomori, S.-i. (1991) *Pure & Appl. Chem.* **63**, 473-482
119. Muramatsu, T., and Muramatsu, H. (2004) *Glycoconj J* **21**, 41-45
120. Ngamukote, S., Yanagisawa, M., Ariga, T., Ando, S., and Yu, R. K. (2007) *J Neurochem* **103**, 2327-2341
121. Cui, L., Johkura, K., Yue, F., Ogiwara, N., Okouchi, Y., Asanuma, K., and Sasaki, K. (2004) *Journal of Histochemistry & Cytochemistry* **52**, 1147-1457
122. Bieberich, E. (2004) *Glycoconj J* **21**, 315-327
123. Hakomori, S. I. (2002) *Proceedings of the National Academy of Sciences of the United States of America* **99**, 10231-10233
124. Kakugawa, Y., Wada, T., Yamaguchi, K., Yamanami, H., Ouchi, K., Sato, I., and Miyagi, T. (2002) *Proc Natl Acad Sci U S A* **99**, 10718-10723
125. Hiraishi, K., Suzuki, K., Hakomori, S., and Adachi, M. (1993) *Glycobiology* **3**, 381-390
126. Ono, M., Handa, K., Withers, D. A., and Hakomori, S. (1999) *Cancer Res* **59**, 2335-2339
127. Steelant, W. F., Kawakami, Y., Ito, A., Handa, K., Bruyneel, E. A., Mareel, M., and Hakomori, S. (2002) *FEBS Lett* **531**, 93-98
128. Bremer, E. G., Schlessinger, J., and Hakomori, S. (1986) *J Biol Chem* **261**, 2434-2440
129. Manfredi, M. G., Lim, S., Claffey, K. P., and Seyfried, T. N. (1999) *Cancer Res* **59**, 5392-5397
130. Zeng, G., Gao, L., Suetake, K., Joshi, R. M., and Yu, R. K. (2002) *Cancer Lett* **178**, 91-98
131. Nakamori, S., Kameyama, M., Imaoka, S., Furukawa, H., Ishikawa, O., Sasaki, Y., Kabuto, T., Iwanaga, T., Matsushita, Y., and Irimura, T. (1993) *Cancer Res* **53**, 3632-3637
132. Kannagi, R. (1997) *Glycoconj J* **14**, 577-584
133. Coetzee, T., Fujita, N., Dupree, J., Shi, R., Blight, A., Suzuki, K., and Popko, B. (1996) *Cell* **86**, 209-219

134. Honke, K., Hirahara, Y., Dupree, J., Suzuki, K., Popko, B., Fukushima, K., Fukushima, J., Nagasawa, T., Yoshida, N., Wada, Y., and Taniguchi, N. (2002) *Proc Natl Acad Sci U S A* **99**, 4227-4232
135. Yamashita, T., Wada, R., Sasaki, T., Deng, C., Bierfreund, U., Sandhoff, K. & Proia, R. L. (1999) *Proc. Natl Acad. Sci. U S A.* **96**, 9142-9147
136. Okada, M., Itoh Mi, M., Haraguchi, M., Okajima, T., Inoue, M., Oishi, H., Matsuda, Y., Iwamoto, T., Kawano, T., Fukumoto, S., Miyazaki, H., Furukawa, K., and Aizawa, S. (2002) *J Biol Chem* **277**, 1633-1636
137. Kawai, H., Allende, M. L., Wada, R., Kono, M., Sango, K., Deng, C., Miyakawa, T., Crawley, J. N., Werth, N., Bierfreund, U., Sandhoff, K., and Proia, R. L. (2001) *J Biol Chem* **276**, 6885-6888
138. Takamiya, K., Yamamoto, A., Furukawa, K., Yamashiro, S., Shin, M., Okada, O., Fukumoto, S., Haraguchi, M., Takeda, N., Fujimura, K., Sakae, M., Kishikawa, M., Shiku, H., Furukawa, K. & Aizawa, S. (1996) *Proc. Natl Acad. Sci. U S A.* **93**, 10662-10667
139. Takamiya, K., Yamamoto, A., Furukawa, K., Zhao, J., Fukumoto, S., Yamashiro, S., Okada, M., Haraguchi, M., Shin, M., Kishikawa, M., Shiku, H., and Aizawa, S. (1998) *Proc Natl Acad Sci U S A* **95**, 12147-12152
140. Inoue, M., Fujii, Y., Furukawa, K., Okada, M., Okumura, K., Hayakawa, T., and Sugiura, Y. (2002) *J Biol Chem* **277**, 29881-29888
141. Miyazaki, M., and Ntambi, J. M. (2008) Fatty acid desaturation and chain elongation in mammals. in *Biochemistry of Lipids, Lipoproteins and Membranes.* (Vance, D. E., and Vance, J. E. eds.), 5th Ed., Elsevier, Amsterdam. pp 191-212
142. Matsuzaka, T., Shimano, H., Yahagi, N., Yoshikawa, T., Amemiya-Kudo, M., Hasty, A. H., Okazaki, H., Tamura, Y., Iizuka, Y., Ohashi, K., Osuga, J., Takahashi, A., Yato, S., Sone, H., Ishibashi, S., and Yamada, N. (2002) *J Lipid Res* **43**, 911-920

CHAPTER 2

TRANSCRIPT PROFILING AND METABOLOMIC ANALYSIS OF CERAMIDE BIOSYNTHESIS IN MOUSE EMBRYONIC STEM CELLS AND EMBRYOID BODIES

2.1 Introduction

Sphingolipids (SL), including glycosphingolipids (GSL), are ubiquitous components of all eukaryotic organisms (1) and participate in cell-type specific recognition, cell-cell interaction, cell-substratum adhesion, cell signaling and other events in embryogenesis (2-4). The lipid backbones of SL are sphingoid bases and N- acyl sphingoid bases (termed ceramides, Cer), which are known to change in amount during embryogenesis (2-6) and to be important in developmental signaling (4, 7-10).

Ceramides are biosynthesized by *de novo* (1, 11) and recycling (12) pathways that have been well characterized with respect to the genes for most of the early steps of the pathway (i.e., production of ceramide, Cer, and its initial metabolites) (1, 11, 13, 14). As depicted in Figure 2.1A,[1] a modified KEGG pathway (Kyoto Encyclopedia of Genes and Genomes, http://www.genome.ad.jp/kegg/pathway/ map/map00600.html) (15), the *de novo* biosynthetic pathway starts with condensation of serine and palmitoyl-CoA by serine palmitoyltransferase (*SPT*) (16) to form 3-ketosphinganine (3-Keto-Sa) which is reduced to sphinganine (Sa) then acylated to dihydroceramides (DHCer) by a family of

[1] Fig. 2.1 displays only mammalian genes and includes genes that have not yet been added to the online KEGG pathway for sphingolipids; for more information, see www.sphingomap.org.

ceramide synthases, *CerS*, that differ in fatty acyl-CoA selectivity as shown in Fig. 2.1B (17-20). DHCer can be incorporated into more complex SL, as shown in the lower left corner of Fig. 2.1A, or converted to Cer by addition of a 4-*trans*-double bond to the sphingoid base backbone (21), then incorporated into more complex SL (in some tissues, the lipid backbones are also hydroxylated on the sphingoid base (22) and/or fatty acid (23)).

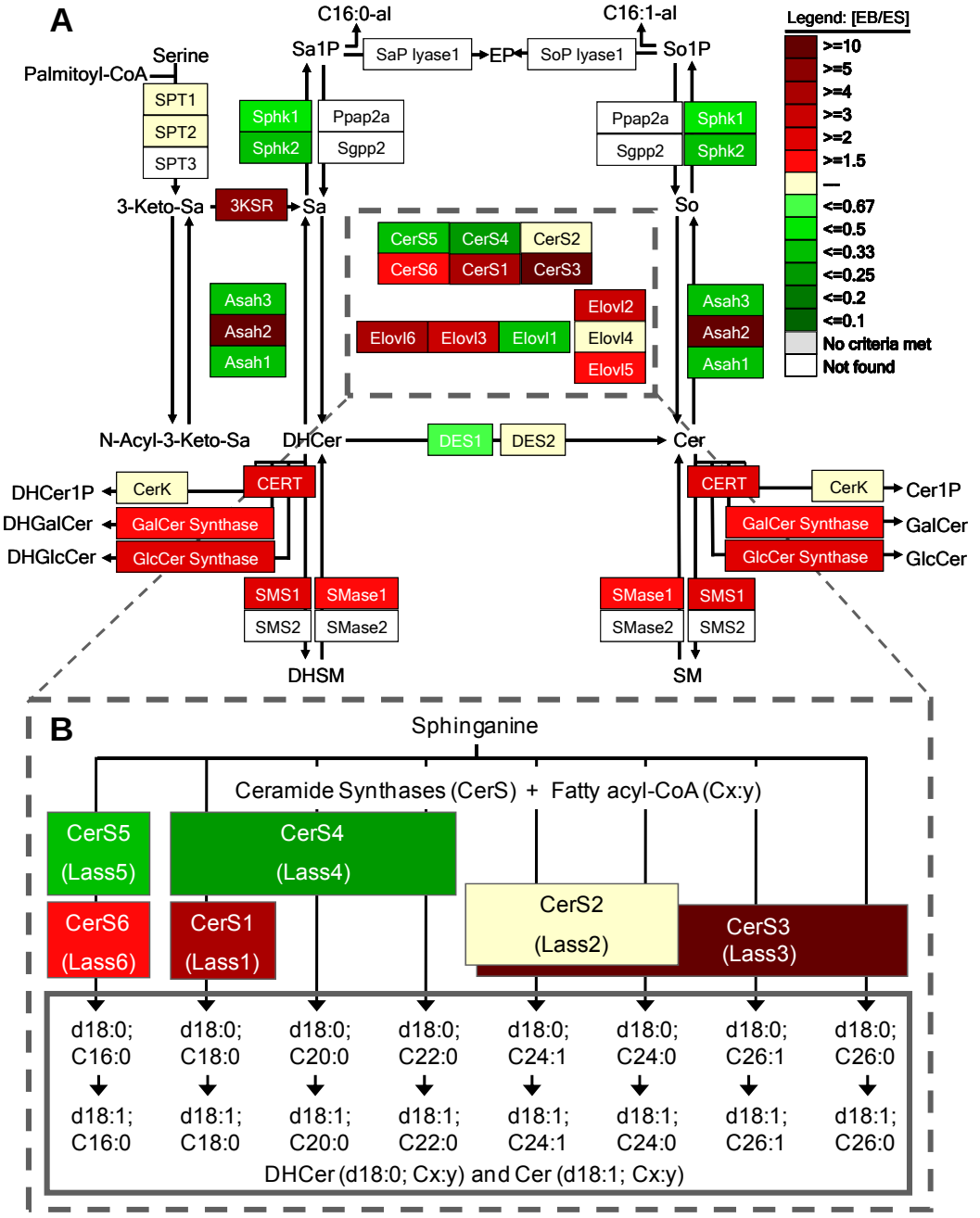

Figure 2.1 Depiction of the early steps of sphingolipid biosynthesis using a modified KEGG pathway scheme (Sphingo-GenMAPP) to facilitate visualization of differences in gene expression in by R1 mESCs and EBs. (A) Sphingolipid *de novo* biosynthesis (B) Expansion of the pathway to depict the individual molecular species made by different *CerS* isoforms (formerly named *Lass*), with abbreviation of the sphingoid base as d18:0 for sphinganine (citing the number of hydroxyl groups, d for dihydroxyl), d18:1 for sphingosine, and the N-acyl chain length and number of double bonds as Cx:y, respectively. As described in the text, the "heat" scale depicts the relative amounts of mRNA for each of these genes for R1 EBs versus mESCs as measured by qRT-PCR.

None of the previous studies of sphingolipids in embryogenesis have explored whether there are developmental changes in the backbone Cer subspecies. Therefore, this investigation has analyzed expression of the *CerS* genes (17, 19, 24) and the amounts and types of Cer subspecies in mouse ESCs (mESCs) compared to embryoid bodies (EBs) as part of an investigation of all of the known genes for sphingolipid biosynthesis (25). Also analyzed were the co-substrate fatty acyl-CoAs and expression of the mRNA for fatty acid elongases and desaturases. These studies found that there were shifts in the expression of many of the genes of this pathway as well as in the associated metabolites in EBs versus ESCs.

2.2 Experimental Procedures

2.2.1 Growth and Characterization of mESCs and EBs

The R1 and D3 mESCs (26,27) (ATCC, Manassas, VA) were cultured in the absence of feeder cells on tissue-culture-grade plastic ware pre-coated with 0.1% gelatin-phosphate buffered saline (PBS), as described previously (28). The mESC culture medium consisted of Dulbecco's Modified Eagle Medium (DMEM, Gibco BRL) supplemented with 10% fetal calf serum (GIBCO BRL), 1 mM L-glutamine, 0.1 mM 2-mercaptoethanol, 100 U/ml penicillin, 100 U/ml streptomycin and 1000 U/ml recombinant human LIF (Leukemia inhibitory factor; ESGRO, Chemicon International) at 37°C under 10 % CO_2.

Differentiation of mESCs into EBs was carried out as described previously (29). mESCs were harvested by trypsinization to convert suspensions of single ESCs into aggregates that were seeded into 10-cm bacteriological dishes at a density of 1×10^5 cells/ml, in 10 ml mESC-medium lacking LIF. EBs were harvested daily, the medium was changed every 2 days and cultures were split one into two at day 4. Cell populations of mESCs and EBs were characterized by flow cytometry using the lineage specific marker CD9 and by transcript analysis using qRT-PCR.

2.2.2 Measurement of Gene Expression Levels Using quantitative RT-PCR (qRT-PCR*)*

Primer Design and Validation

Primer pairs for sphingolipid synthesis genes and control genes were designed within a single exon using conditions described in Nairn *et al* (25). Primer sequences and accession numbers for genes in this study are presented in Nairn *et al.* (30). Individual qRT-PCR reactions were also checked for efficiency 100 ± 5% using reaction raw fluorescence data in the LinReg PCR program (31).

Total RNA Isolation and cDNA Synthesis

mESCs and EBs (day 6) cell pellets were harvested and flash frozen in liquid nitrogen and stored at -80ºC until use. Cell pellets were homogenized followed by RNA isolation and cDNA synthesis which was performed as previously described (30).

qRT-PCR reactions and Calculation of Relative Gene Expression Levels

Triplicate reactions (20 µl each) containing 5 µl of diluted cDNA or genomic DNA template (primer validation reactions), 5 µl of primer pair mix (125 µM final concentration) and 10 µl of iQ™ SYBR Green Supermix (BioRad, Hercules, CA) were assembled in 96-well microtitre plates. Amplification reactions and the calculation of relative gene expression levels was carried out as previously described (30). The control gene, Ribosomal Protein L4 (RPL4, NM_024212) was included on each plate to control for run variation and to normalize individual gene expression.

2.2.3 Integration of Gene Expression Data with Sphingo-GenMAPP pathway

GenMAPP (Gene MicroArray Pathway Profiler; http://www.genmapp.org/) v2.1 (32) is a tool to visualize global gene-expression profiles in the context of cell signaling pathways or KEGG metabolic pathways (http://www.genome.jp/kegg/). In the context of the present study, the mRNA expression data for R1 mESCs and EBs from the qRT-PCR analysis was imported into a GenMAPP pathway for sphingolipid metabolism that had been modified (33) based on the current literature (34) (Fig. 2.1).

2.2.4 Liquid Chromatography Electrospray Ionization Tandem Mass Spectrometry (LC ESI-MS/MS)

Sphingolipids

The SL were extracted from cells using published methods (35-37). Briefly, approximate 1 to 10 x 10^6 cells were scraped from culture dishes in a small volume of PBS, then centrifuged to remove excess PBS for a final volume of 0.05-0.1 ml. The cells were suspended in 0.5 ml of CH_3OH and 0.25 ml of $CHCl_3$, spiked with internal standards for each species being monitored (see details below), disrupted using a bath-type sonicator at room temperature, and incubated overnight in a heating block at 48°C. After cooling the tubes to room temperature, 75 µl of 1 M KOH in CH_3OH was added and the mixture was sonicated for 30 sec, then incubated for 2 hr at 37°C. The solution was neutralized with several µl of glacial acetic acid, 1 ml of $CHCl_3$ was added followed by 2 ml of H_2O, and sonicated. After centrifugation, the upper phase was carefully removed and discarded. The lower phase was dried using a SpeedVac and redissolved in 0.3 ml of 98% of 97:2:1 $CH_3CN/CH_3OH/CH_3COOH$ (v/v/v) (mobile-phase A) and 2% of

64:15:20 $CH_3OH/H_2O/CH_3(CH_2)_3OH/CH_3COOH$ (v/v/v/v) (mobile-phase B); both contained 5 mM ammonium acetate.

The methods used for LC ESI-MS/MS analysis of sphingolipid metabolites have been reported in detail (36,37). SL data was collected using a Perkin Elmer Series 200 MicroPump system (Perkin-Elmer, Norwalk, CT) coupled to a PE Sciex API 3000 triple quadrupole mass spectrometer equipped with a turbo ion-spray source (Applied Biosystems, Foster City, CA). Complex SLs, such as Cer, CMH (ceramide monohexoses, the sum of glucosylceramide and galactosylceramide), and SM are separated by normal-phase LC using 2.1 mm x 5 cm Supelco NH_2 column (Supelco, Bellefonte, PA) at a flow rate of 1.5 ml/min. The elution protocol was: 0.5 min of pre-equilibration of the column with 98:2 A/B (v/v), sample injection, elution with 98:2 A/B (v/v) for 1.1 min followed by a linear gradient to 82:18 A/B (v/v) in 0.2 min, elution at this composition for 0.4 min, then a linear gradient to 100% B over 0.8 min. Afterwards, the column was reequilibrated by a 0.5-min linear gradient to 98:2 A/B (v/v) and a wash of the column with 98:2 A/B (v/v) for 0.3 min.

Quantitation was performed by comparison of the unknowns with the spiked internal standards (IS), which were uncommon chain length homologs of each SL class: C12-ceramide, C12-sphingomyelin, and C12-glucosylceramide (for CMH), all of which were obtained from Avanti Polar Lipids (Alabaster, AL). The IS were added as 10 µl of a 50 µM of stock for a total of 500 pmol of each IS molecular species per sample (see above). Student's t-test was used for statistical analyses.

Fatty Acyl-CoAs

The fatty acyl-CoAs were extracted from cells using published method (38). The medium from cells cultured in 100-mm dishes was aspirated, and cells were gently washed twice with 5 ml of 4°C PBS, ~1 ml of ice-cold PBS was added, and the cells were scraped from the dishes using a rubber policeman and transferred to chilled 13 x 100 mm screw-cap borosilicate tubes with Teflon-lined caps (Kimble Chase, Vineland, NJ). An additional ~1 ml of PBS was used to recover the remaining cells by this same procedure, and these were added to the first. After centrifugation (1500 rpm, 3 min), the PBS was removed by aspiration and 0.5 ml of CH_3OH containing 1 mM EDTA was added together with 10 μl of an IS mixture that contained 100 pmol each of C17:0- and C25:0-CoA, which were prepared in $CH_3OH/CHCl_3$ (2:1 v/v) containing 30 mM triethylammonium acetate. After sonication (3 times at ~0.5 min each), 0.25 ml of $CHCl_3$ was added, followed by another brief sonication.

The single-phase extraction mixture was incubated in a 50°C heating block for 30 min. After cooling to room temperature, $CHCl_3$ and water (0.25 ml each) were added with mixing by vortexing after each addition. After brief centrifugation using a table-top centrifuge, the fatty acyl-CoAs were in the upper phase and interface and most of the other lipids (which would interfere with the subsequent reverse-phase LC) were in the lower phase. The upper phase was removed with a Pasteur pipette and transferred into a clean screw-cap glass tube. The upper layer was adjusted with 5% CH_3OH (v/v), 5% butanol (v/v), and 5% $CHCl_3$ (v/v). These organic additives improved the stability of the very-long-chain acyl-CoAs for at least 24 hr at room temperature in the autosampler.

HPLC separations used a Shimadzu SCL-10A VP system controller, two LC-10AD VP pumps, a DGU-14A degassing unit, a Perkin-Elmer series 200 autosampler, a Phenomenex (Torrance, CA) Gemini C18 column (2 mm ID x 150 mm with 3 μm particles, 110 Angstrom pores) and a 2 x 4 mm guard column with the same packing material. A Metatherm column oven (Torrance, CA) was used to maintain the column temperature at 40°C.

The flow rate was 0.2 ml/min in binary gradient mode with the following elution program: the column was equilibrated with mobile phase C [H_2O/ CH_3CN (85:15, v/v), containing 0.05% triethylamine], the sample was injected, and mobile phase C was continued for 5 min, followed by a 13 min gradient to 48% mobile phase C and 52% mobile phase D (CH_3CN containing 0.05% triethylamine) during which the long-chain and very-long-chain fatty acyl-CoAs eluted. Afterward, the column was washed by a 1-min gradient to 100% D and a 5 min hold at 100% D, followed by reequilibration of the column by a 1 min gradient to 100% C and a 5 min hold at 100% C before injection of the next sample.

Tandem mass spectrometry of fatty acyl-CoAs in positive ion mode was performed on a 4000 QTrap triple quadrupole linear ion trap mass spectrometer (Applied Biosystems, Foster City, CA) as recently described (38).

2.3 Results

2.3.1 Characterization of R1 mESCs and EBs

The R1 mESCs and EBs were examined for gross morphological changes and transcript abundances as markers for these cells. The mESC's expressed Zinc finger

protein 42 (*zfp42/Rex1*), Gastrulation brain homeobox (*GBX2*), and Nanog homeobox (*Nanog*) as pluripotent markers, and the qRT-PCR transcript profiles for Goosecoid (*Gsc*), Zinc finger protein of the celebellum 1 (*Zic1*), SRY-box containing gene 17 (*Sox17*), Alpha fetoprotein (*Afp*) and GATA binding protein 6 (*Gata6*) were typical for the transition from mESCs to EBs (25).

2.3.2 Differences in the expression of sphingolipid metabolism genes in R1 mESCs and EBs using Sphingo-GenMAPP

The relative transcript expression levels of R1 EBs versus mESCs are depicted in the pathway diagram (Fig. 2.1) and with the fold differences shown by the "heat" scale defined on the right side of the figure. There were no differences in the transcript levels for serine palmitoyltransferases (*SPT1* and *SPT2*), the first enzymes of the pathway, but EBs had higher expression of transcripts for 3-ketosphinganine reductase and some of the CerS isoenzymes (*CerS1*, *3* and *6*), as is also shown by bar graphs in Fig. 2.2 (upper panel). The transcripts were also higher in EBs for enzymes that utilize Cer for biosynthesis of more complex sphingolipids, i.e., both of the SM synthases and the glycosyltransferases that produce GlcCer and GalCer (Fig. 2.1). EBs had lower transcript abundances for the major desaturase that synthesizes Cer from DHCer (dihydroCer desaturase, *DES1*) and transcripts for the other desaturase (*DES2*, which makes phytoceramides) (22) were barely detectable in both mESCs and EBs.

Since the *CerS* enzymes utilize very-long-chain fatty acyl-CoA's that are made by elongation of palmitoyl- and stearoyl-CoA's, the transcripts for the pertinent fatty acyl-CoA elongases were also analyzed by qRT-PCR. As shown in Fig. 2.1 and 2.2B, the

transcript level for *Elovl6*, a fatty acyl-CoA elongase that catalyzes the elongation of saturated and monosaturated acyl-CoAs with 12-16 carbons (39,40), was 4-fold higher for EBs than mESCs. A fatty acyl-CoA elongase that extends C16:0-CoA to C24:0-CoA, *Elovl3* (39,41,42) showed 3-fold higher transcript levels for EBs than mESCs, although lower transcript levels were observed for *Elovl1,* which is also responsible for elongating very-long-chain saturated fatty acyl-CoAs (39,43). EBs also had ~3.5-fold higher *Elovl2* (39,44) transcript levels, no evident change in *Elovl4* (39,45) transcripts, and slightly higher *Elovl5*(39,44) transcript abundance (which are all elongases for polyunsaturated fatty acids).

These differences in gene expression imply that the sphingolipid backbones of EBs might differ from mESCs by having: *i*) higher proportions of subspecies with longer acyl chains (i.e., >C16) since EBs have a higher transcript abundance of *CerS1*, which is relatively specific for stearoyl-CoA (C18:0) (46), and *CerS3*, which is selective for very-long-chain fatty acyl-CoA's (>C20) (47); *ii*) higher, lower or unchanged C16-Cer since an elevation in *CerS6*(18), one of the CerS responsible for biosynthesis of C16-Cer, may be offset by a decrease in the transcripts encoding a *CerS* that utilizes C16-fatty acyl-CoA, *CerS5*(48); *iii*) increases in DHSL since *DES1* is lower and *DES2* unchanged; and *iv*) possibly lower amounts of (DH)Cer because the transcripts encoding most of the enzymes that metabolize (DH)Cer were elevated (including the transcripts for one of the ceramidases, *Asah2*). The gene expression data also suggest that the EBs have the capacity to elongate fatty acyl-CoA's to produce the co-substrates that are utilized to make these Cer subspecies. To test these hypotheses, the Cer subspecies (and fatty acyl-CoA's) were analyzed by LC ESI-MS/MS.

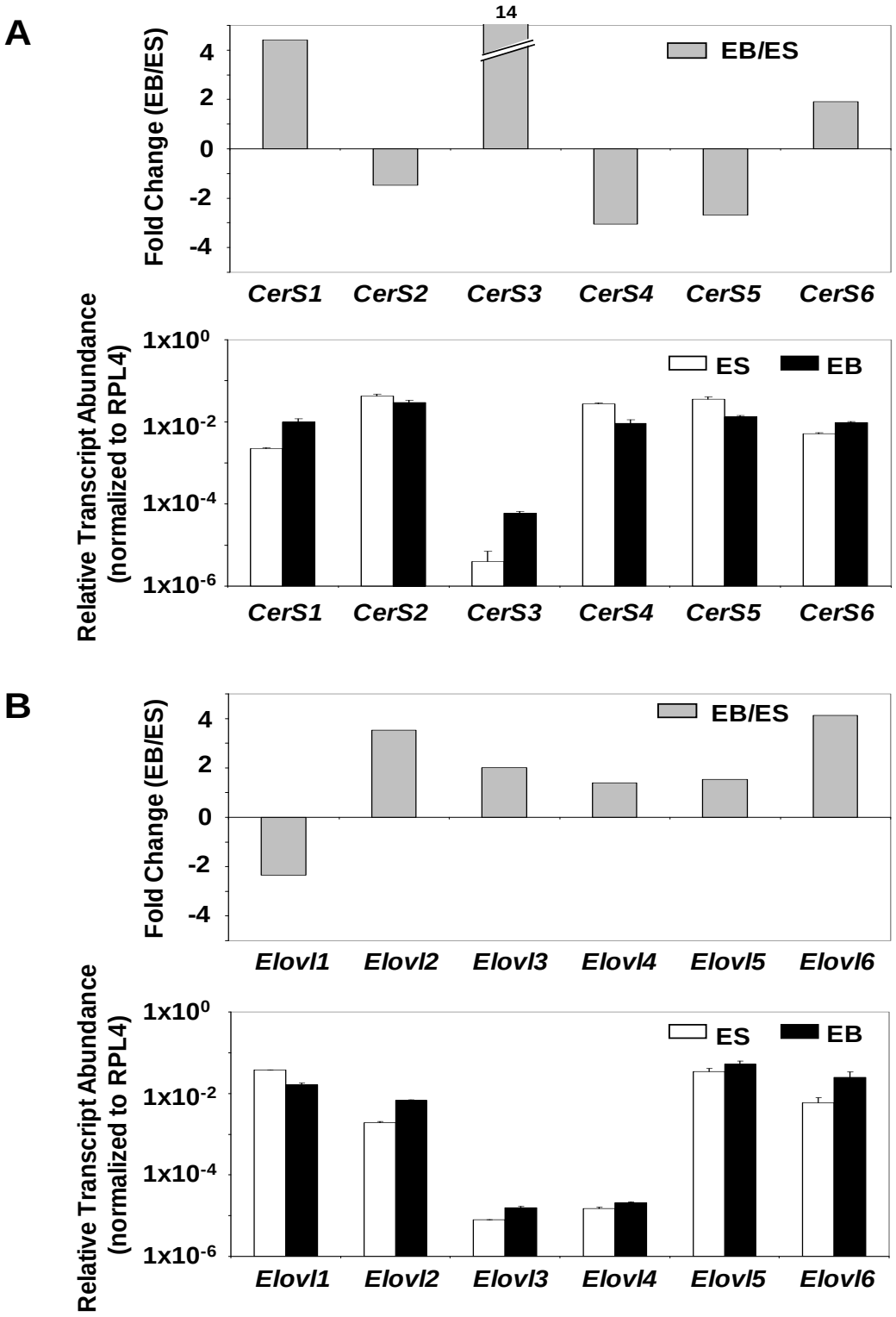

Figure 2.2. Relative transcript abundance of *CerS* (*Lass*) genes (A) and fatty acyl-CoA elongase (*Elovl*) genes (B) by qRT-PCR for R1 mouse embryonic stem cells and day 6 EBs.

2.3.3 Characterization of the Cer backbone subspecies of R1 mESCs and EBs

Fig. 2.3A shows the relative proportions of the Cer subspecies in R1 mESCs (day 0) and EBs on days 4 and 6 as "donut" charts[2]. The rationale for the latter depiction is that *CerS*'s have approximately the same K_m for the sphingoid base substrate (49), therefore, as a first approximation, one would predict that the relative amounts of the different subspecies would correlate with the relative abundances of the respective *CerS* transcripts, which have been re-graphed in Fig. 2.3B to show the differences between mESCs and EBs. The order of the *CerS* genes has been arranged so they correspond to the respective types of Cer that are made, i.e., C16-Cer (*CerS6* and *CerS5*), C18-Cer (*CerS1*), C20 $\pm$ 2 Cer (*CerS4*), C24-Cer (*CerS2*), and C26-Cer (*CerS3*) (c.f. Fig. 2.1).

Comparison of Fig. 2.3A and B reveals a close correspondence between the differences in transcript abundances for *CerS* in mESC versus EBs and the Cer subspecies distribution: a lower *CerS6* + *CerS5* for EBs vs mESC corresponding to a decrease in C16-Cer; higher *CerS1* in EBs corresponding to an increase in C18-Cer; and higher *CerS2* corresponding to a small increase in C24-Cer. Lower *CerS4* transcripts in EBs did not translate into a decrease in the sum of C18 + C20 + C22-Cer, however, this might be due to the large increase in *CerS1* transcripts.

---

[2] Bar graphs with the amounts of each subspecies of (DH)Cer, (DH)CMH and (DH)SM for R1 and D3 mESCs and EBs are available as Fig. 2.6 and 2.7.

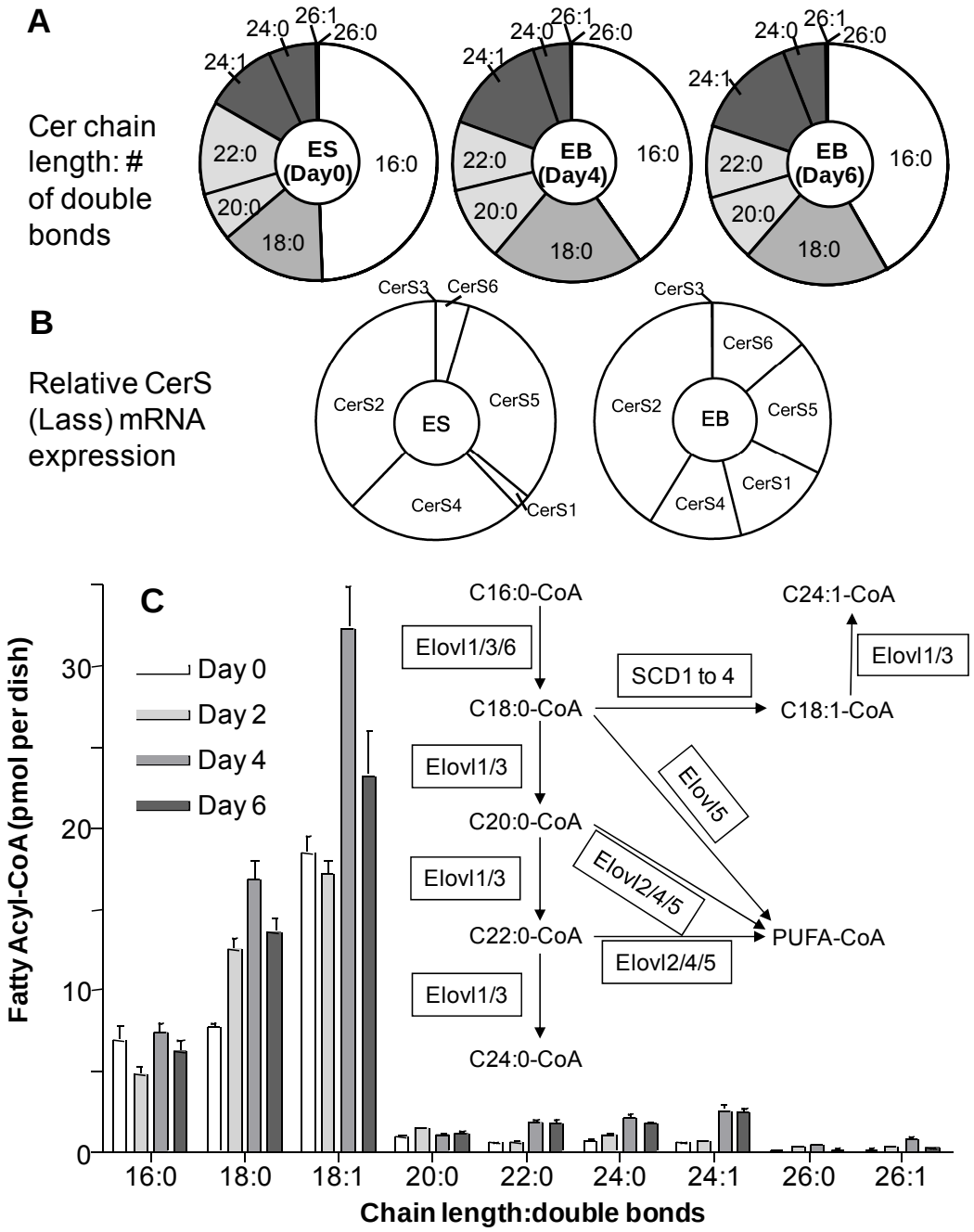

Figure 2.3. Ceramide and fatty acyl-CoA composition of R1 mouse embryonic stem cells at different timepoints during EB formation. (A) Cer subspecies distribution with the chain length and number of double bonds depicted by x:y, respectively, for mESCs and EBs after days 4 and 6. The Cer subspecies were analyzed by LC ESI-MS/MS as described in references 35-37. (B) Representation of relative changes in *CerS* transcript abundance of mESCs versus day 6 EBs arranged with the approximate order of the fatty acyl-CoA selectivities of the *CerS* to match the acyl-chain lengths of the Cer in panel A. (C) Fatty acyl-CoA subspecies of mESCs and EBs for days 2, 4, and 6.

2.3.4 Analysis of the fatty acyl-CoA species in R1 mESCs and EBs

The amounts of the fatty acyl-CoAs in R1 mESCs and EBs are shown in Fig. 2.3C. During the time course for conversion of mESCs to EBs, C18:0- and C18:1-fatty acyl-CoAs increased by ca 2 fold, as did many of the very-long-chain (C22:0-, C24:0- and C24:1-) fatty acyl-CoAs. In contrast, palmitoyl-CoA derivatives (C16:0-) were approximately the same in mESCs and EBs. Thus, these results are consistent with the observed changes in the higher amounts of C18:1-, C22:0-, C24:0-, and C24:1-fatty acyl-CoAs in EBs versus mESCs. These results additionally indicate that the CerS that would utilize these fatty acyl-CoAs to produce the pertinent Cer subspecies are not hampered by a lack of co-substrate availability during EB development.

2.3.5 Characterization of the DHCer and Cer backbone subspecies of (DH)SL in R1 mESCs and EBs

The DHCer of mESCs and day 6 EBs also exhibited shifts in fatty acyl-chain length (Fig. 2.4A) that correlated with the differences in *CerS* expression that were similar to the changes in Cer (c.f., Fig. 2.4A and Fig. 2.4D), namely lower proportions of C16-DHCer and more C18-and C24/24:1 DHCer, which the greatest increase in C24:1-Cer. Since DHCer is the first N-acylated intermediate of *de novo* sphingolipid biosynthesis (Fig. 2.1) versus Cer, which is formed next and during the turnover of more complex sphingolipids, perhaps this accounts for the closer resemblance between the chain length subspecies of DHCer and the mRNA abundance of the *CerS* isoforms (c.f., Fig. 2.3A and 2.4).

The (DH)CMH (Fig. 2.4B and E) and SM (Fig. 2.4F) of EBs displayed higher proportions of the C24/C24:1 backbones, however, most of the other subspecies differences that were seen in Cer and DHCer were not evident in these downstream metabolites.

There were also differences in the proportion of DHCer versus Cer backbones in EBs versus mESCs (which are not evident in Fig. 2.3 or 2.4 since the data are shown only as proportions within each category). When summed across all chain lengths and categories, the total amount of these sphingolipids did not differ between mESCs and day 6 EBs (i.e., 780 vs 740 pmol/mg protein, respectively), but the DHSL percentage increased from approximately 8% for mESCs to 19% for EBs. This finding was consistent with the lower *DES1* expression in EBs versus mESCs (Fig. 2.1).

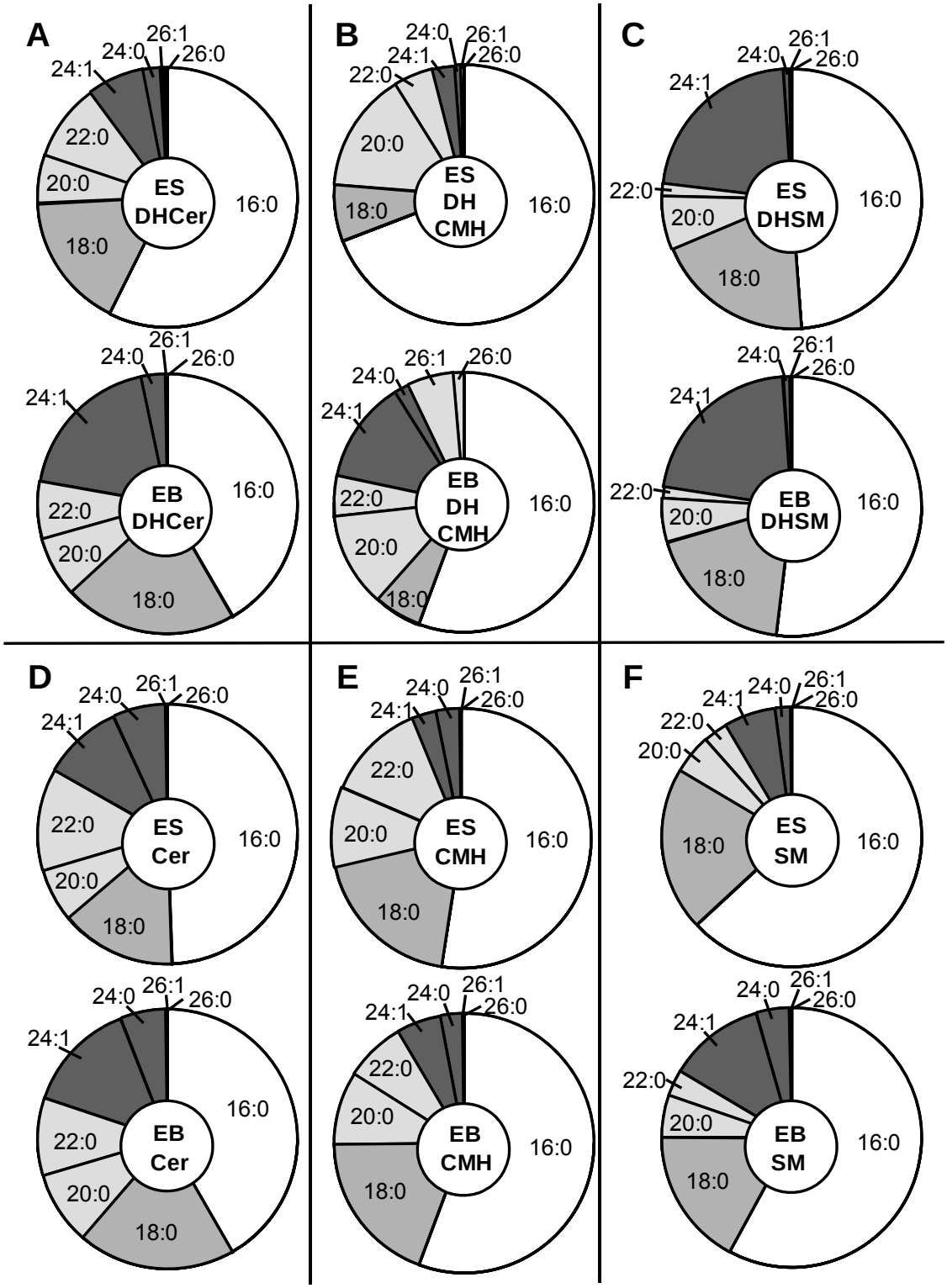

Figure 2.4. Subspecies distributions of (dihydro)ceramides, (dihydro)ceramide monohexoses and (dihydro)sphingomyelins of R1 mouse embryonic stem cells and day 6 embryoid bodies.

2.3.6 Characterization of the DHCer and Cer backbone subspecies of (DH)SL in D3 mESCs and EBs

To determine if these compositional changes were unique to the R1 cells, the lipids of another frequently studied mESCs, D3 cells (28), were analyzed by LC ESI-MS/MS. The two similarities were decreases in the proportion of C16-(DH)Cer and increases in C24/C24:1 (DH)Cer in D3 EBs versus mESCs, Fig. 2.5A and D). Furthermore, these differences were also more prevalent in the downstream metabolites (Fig. 2.5B, C, E and F). Based on these similarities, it is possible that the phenomena that these shifts in (DH)Cer subspecies are common in this developmental transition.

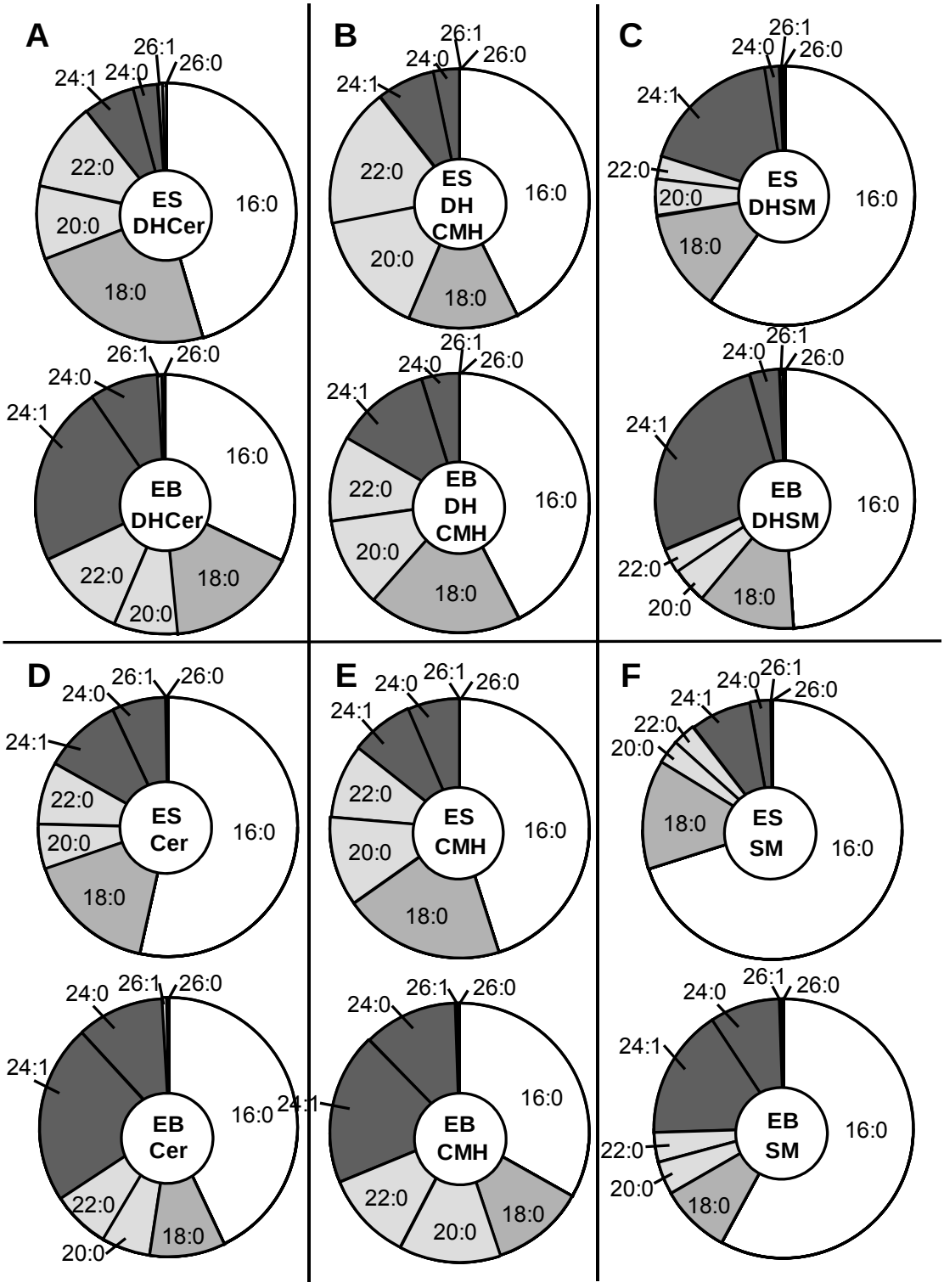

Figure 2.5. Subspecies distributions of (dihydro)ceramides, (dihydro)ceramide monohexoses and (dihydro)sphingomyelins of D3 mouse embryonic stem cells and day 6 embryoid bodies.

2.4 Discussion

The goal of these studies was to explore whether mESCs undergo changes in expression of genes for the early steps of *de novo* sphingolipid biosynthesis upon conversion to EBs. There were changes in transcript levels for many of the early enzymes of sphingolipid biosynthesis (Fig. 2.1), including increases in some of the *CerS* subspecies and downstream synthases for sphingomyelins and glycosphingolipids and decreases in some of the *CerS*, sphingosine kinases, and some of the ceramidases. While all of these are worthy of further investigation, this study focused on analysis of (dihydro)ceramide backbones of mESCs and EBs using LC ESI-MS/MS to determine how well the changes in gene expression predicted changes in these important compounds.

For all of the mESCs and EBs sphingolipids investigated in this study, the prevalent fatty acid of the (DH)Cer backbone was C16:0 (palmitate), which is biosynthesized by *CerS5* and *CerS6*. Consistent with this, the transcript abundance of *CerS5* plus *CerS6* is higher than that for most of the other *CerSs* (1, 3 and 4) except *CerS2* (Fig. 2.2). We do not know if *CerS2* enzymatic activity is also relatively high (since transcript abundance is not necessarily equivalent to protein amount or enzymatic activity), but even if it is, the low amounts of the corresponding C24-fatty acyl-CoA's might be rate limiting (Fig. 2.3C). Consistent with this point of view, EBs had lower percentages of C16-(DH)Cer and higher (DH)Cer with C18- and very-long-chain fatty acids (Fig. 2.3A), which corresponded not only to changes in the relative abundance of the respective transcripts (Fig. 2.3B) but also to shifts in the amounts of isolated fatty

acyl-CoAs (Fig. 2.3C). The D3 EBs showed even greater increases in the very-long-chain (DH)Cer (Fig. 2.5 and 2.6).

The functional significance of these differences in (DH)Cer subspecies is not known. However, synthesis of C16-Cer by *CerS5*, is elevated during apoptosis (50-52); in some cell types, C18-Cer is associated with cell growth control (53); and differences in the time course of changes in C16- versus C24-Cer have been associated with different phases of apoptosis (52, 54). Therefore, changes in the types of Cer backbones may play important roles in membrane structure and signaling during development.

In addition to these shifts in (DH)Cer types, there were also higher total amounts of these compounds in R1 EBs vs mESCs (Fig. 2.7), which might participate in the regulation of primitive ectoderm cell polarity and/or Cer-induced apoptosis in embryonic development (8, 55). In contrast, the Cer monohexoses (CMH) of R1 and D3 EB were much lower than for mESCs, despite increases in the mRNA's for the synthases for GlcCer and GalCer (Fig. 2.1), which might reflect that these intermediates are being utilized for the biosynthesis of more complex glycosphingolipids that are important during development (3, 56, 57). This would be an interesting direction for future studies.

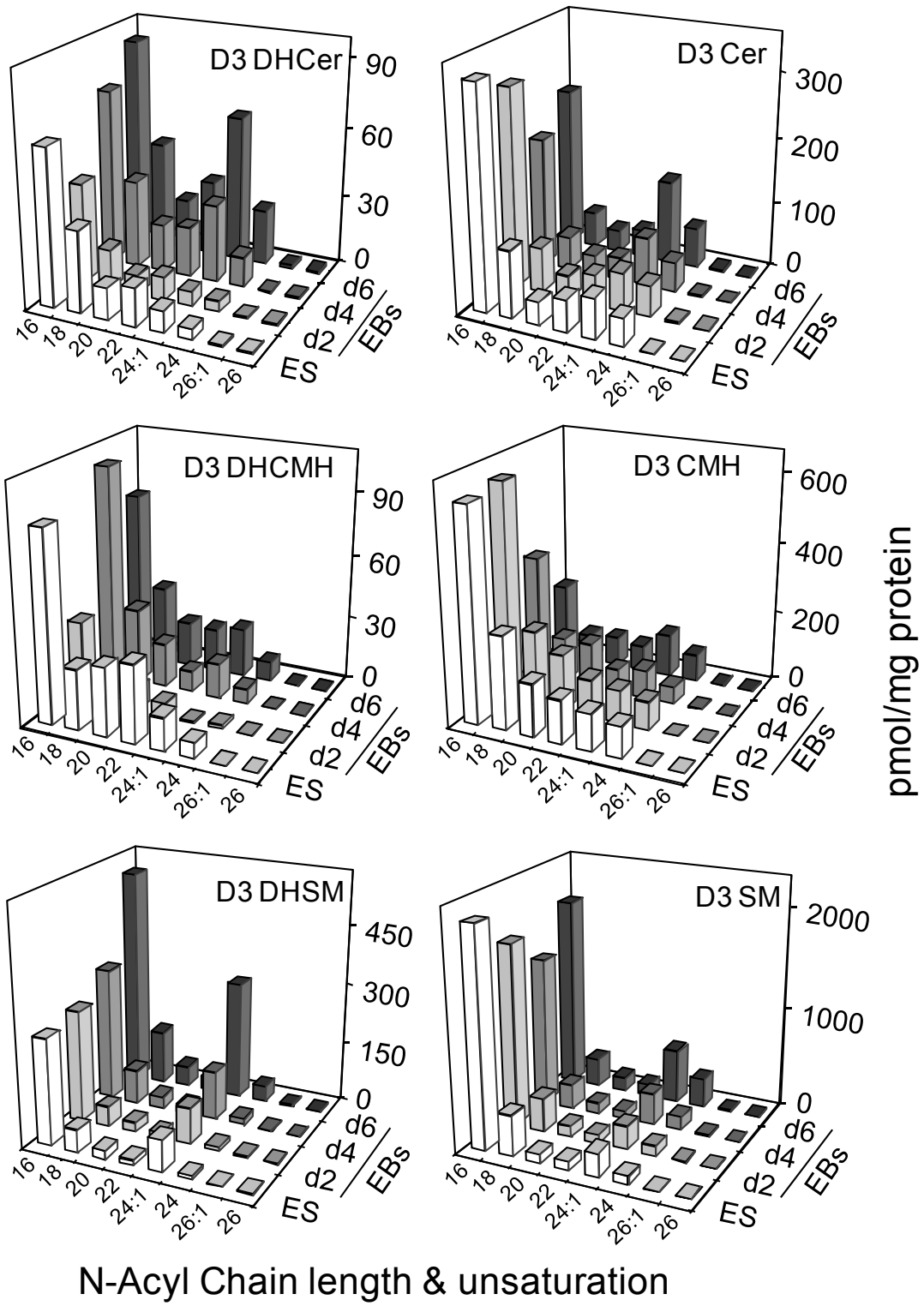

Figure 2.6. Sphingolipid subspecies composition of D3 mouse embryonic stem cells at different timepoints during ES formation.

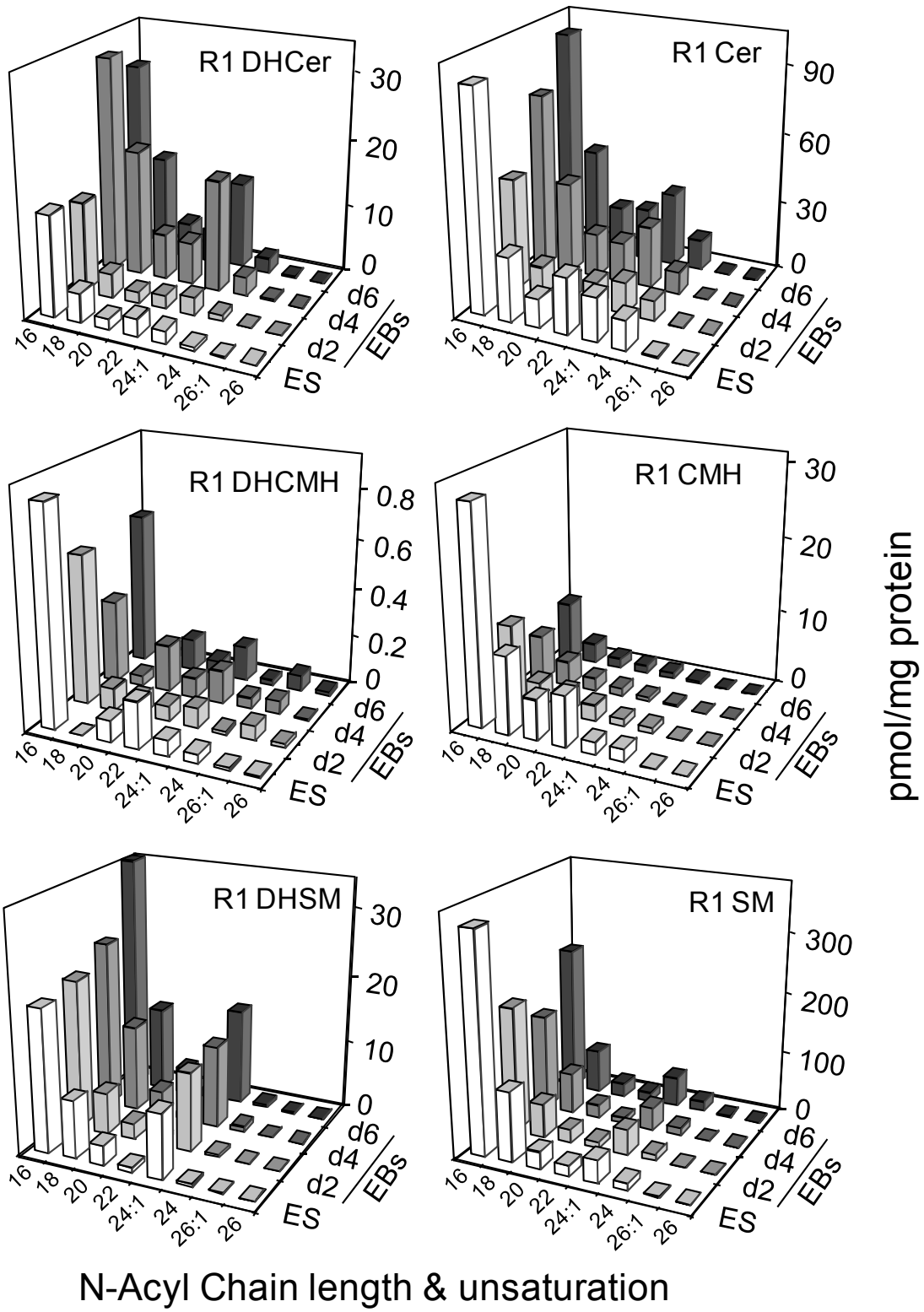

Figure 2.7. Sphingolipid subspecies composition of R1 mouse embryonic stem cells at different timepoints during ES formation.

Transcript profiling is used widely in characterization of gene expression during development (58-60), however, prior to this study, the *CerS* gene family has not been included because it was only recently characterized (17). Furthermore, no previous study of this pathway has combined genomic analysis with measurement of the related downstream metabolites. Therefore, it is hoped that this approach may be useful in understanding both the developmental regulation of sphingolipid metabolism and the roles of Cer in stem cell biology and embryonic development (61, 62).

2.5 References

1. Merrill, A. H., Jr., Wang, M. D., Park, M., and Sullards, M. C. (2007) *Trends Biochem Sci* **32**, 457-468
2. Fenderson, B. A., Eddy, E. M., and Hakomori, S. (1990) *Bioessays* **12**, 173-179
3. Muramatsu, T. (2000) *J Biochem (Tokyo)* **127**, 171-176
4. Bieberich, E. (2004) *Glycoconj J* **21**, 315-327
5. Regina Todeschini, A., and Hakomori, S. I. (2008) *Biochim Biophys Acta* **1780**, 421-433
6. Ngamukote, S., Yanagisawa, M., Ariga, T., Ando, S., and Yu, R. K. (2007) *J Neurochem* **103**, 2327-2341
7. Bieberich, E., MacKinnon, S., Silva, J., Noggle, S., and Condie, B. G. (2003) *J Cell Biol* **162**, 469-479
8. Krishnamurthy, K., Wang, G., Silva, J., Condie, B., and E, B. (2007) *J. Biol. Chem.* **282**, 3379-3390
9. Bieberich, E., Silva, J., Wang, G., Krishnamurthy, K., and Condie, B. G. (2004) *J Cell Biol* **167**, 723-734
10. Bieberich, E., MacKinnon, S., Silva, J., and Yu, R. K. (2001) *J Biol Chem* **276**, 44396-44404
11. Lahiri, S., and Futerman, A. H. (2007) *Cell Mol Life Sci* **64**, 2270-2284
12. Tettamanti, G. (2004) *Glycoconj J* **20**, 301-317
13. Sabourdy, F., Kedjouar, B., Sorli, S. C., Colie, S., Milhas, D., Salma, Y., and Levade, T. (2008) *Biochim Biophys Acta* **1781**, 145-183
14. Bartke, N., and Hannun, Y. A. (2008) *J Lipid Res*
15. Merrill, A. H., Jr., Stokes, T. H., Momin, A., Park, H., Portz, B. J., Kelly, S., Wang, E., Sullards, M. C., and Wang, M. D. (2008) *J Lipid Res*
16. Wei, J., Tokumbo, Y., Liepelt, M., Momin, A., Wang, E., Hanada, K., and Merrill, A. (2006) Serine Palmitoyltransferase. in *Sphingolipid Biology* (Hirabayashi, Y., Igarashi, Y., and Merrill, A. eds.), Springer, Tokyo. pp 25-47
17. Pewzner-Jung, Y., Ben-Dor, S., and Futerman, A. H. (2006) *J Biol Chem* **281**, 25001-25005
18. Mizutani, Y., Kihara, A., and Igarashi, Y. (2005) *Biochem J* **390**, 263-271
19. Pewzner-Jung, Y., Ben-Dor, S., and Futerman, A. (2006) *J Biol Chem* **281**, 25001-25005
20. Laviad, E. L., Albee, L., Pankova-Kholmyansky, I., Epstein, S., Park, H., Merrill, A. H., Jr., and Futerman, A. H. (2008) *J Biol Chem* **283**, 5677-5684
21. Ternes, P., Franke, S., Zahringer, U., Sperling, P., and Heinz, E. (2002) *J Biol Chem* **277**, 25512-25518
22. Omae, F., Miyazaki, M., Enomoto, A., Suzuki, M., Suzuki, Y., and Suzuki, A. (2004) *Biochem J* **379**, 687-695
23. Uchida, Y., and Holleran, W. M. (2008) *J Dermatol Sci* **51**, 77-87
24. Futerman, A., and Riezman, H. (2005) *Trends Cell Biol* **15**, 312-318
25. Nairn, A. V., York, W. S., Harris, K., Hall, E. M., Pierce, J. M., and Moremen, K. W. (2008) *J Biol Chem* **283**, 17298-17313
26. Doetschman, T., Eistetter, H., Katz, M., Schmidt, W., and Kemler, R. (1985) *J Embryol Exp Morphol* **87**, 27-45

27. Hadjantonakis, A., Gertsenstein, M., Ikawa, M., Okabe, M., and Nagy, A. (1998) *Mech Dev* **76**, 79-90
28. Rathjen, J., Lake, J., Bettess, M., Washington, J., Chapman, G., and Rathjen, P. (1999) *J Cell Sci* **112**, 601-612
29. Lake, J., Rathjen, J., Remiszewski, J., and Rathjen, P. (2000) *J Cell Sci.* **113**, 555-566
30. Nairn, A. V., Kinoshita-Toyoda, A., Toyoda, H., Xie, J., Harris, K., Dalton, S., Kulik, M., Pierce, J. M., Toida, T., Moremen, K. W., and Linhardt, R. J. (2007) *J Proteome Res* **6**, 4374-4387
31. Ramakers, C., Ruijter, J. M., Deprez, R. H., and Moorman, A. F. (2003) *Neurosci Lett* **339**, 62-66
32. Salomonis, N., Hanspers, K., Zambon, A. C., Vranizan, K., Lawlor, S. C., Dahlquist, K. D., Doniger, S. W., Stuart, J., Conklin, B. R., and Pico, A. R. (2007) *BMC Bioinformatics* **8**, 217
33. Merrill, A. H. J., Stokes, T. H., Momin, A., Park, H., Portz, B. J., Kelly, S., Wang, E., Sullards, M. C., and Wang, M. D. (2009) *J Lipid Res* **(in press)**
34. Taniguchi, N., Honke, K., and Fukuda, M. (eds). (2002) *Handbook of Glycosyltransferases and Related Genes*, Springer-Verlag, Tokyo
35. Sullards, M. C., and Merrill, A. H., Jr. (2001) *Sci STKE* **2001**, PL1
36. Merrill, A. H., Jr., Sullards, M. C., Allegood, J. C., Kelly, S., and Wang, E. (2005) *Methods* **36**, 207-224
37. Shaner, R. L., Allegood, J. C., Park, H., Wang, E., Kelly, S., Haynes, C. A., Sullards, M. C., and Merrill, A. H., Jr. (2008) *J Lipid Res* **(in press)**
38. Haynes, C. A., Allegood, J. C., Sims, K., Wang, E. W., Sullards, M. C., and Merrill, A. H., Jr. (2008) *J Lipid Res* **49**, 1113-1125
39. Miyazaki, M., and Ntambi, J. M. (2008) Fatty acid desaturation and chain elongation in mammals. in *Biochemistry of Lipids, Lipoproteins and Membranes.* (Vance, D. E., and Vance, J. E. eds.), 5th Ed., Elsevier, Amsterdam. pp 191-212
40. Matsuzaka, T., Shimano, H., Yahagi, N., Yoshikawa, T., Amemiya-Kudo, M., Hasty, A. H., Okazaki, H., Tamura, Y., Iizuka, Y., Ohashi, K., Osuga, J., Takahashi, A., Yato, S., Sone, H., Ishibashi, S., and Yamada, N. (2002) *J Lipid Res* **43**, 911-920
41. Westerberg, R., Mansson, J. E., Golozoubova, V., Shabalina, I. G., Backlund, E. C., Tvrdik, P., Retterstol, K., Capecchi, M. R., and Jacobsson, A. (2006) *J Biol Chem* **281**, 4958-4968
42. Westerberg, R., Tvrdik, P., Unden, A. B., Mansson, J. E., Norlen, L., Jakobsson, A., Holleran, W. H., Elias, P. M., Asadi, A., Flodby, P., Toftgard, R., Capecchi, M. R., and Jacobsson, A. (2004) *J Biol Chem* **279**, 5621-5629
43. Tvrdik, P., Westerberg, R., Silve, S., Asadi, A., Jakobsson, A., Cannon, B., Loison, G., and Jacobsson, A. (2000) *J Cell Biol* **149**, 707-718
44. Leonard, A. E., Kelder, B., Bobik, E. G., Chuang, L. T., Lewis, C. J., Kopchick, J. J., Mukerji, P., and Huang, Y. S. (2002) *Lipids* **37**, 733-740
45. Zhang, K., Kniazeva, M., Han, M., Li, W., Yu, Z., Yang, Z., Li, Y., Metzker, M. L., Allikmets, R., Zack, D. J., Kakuk, L. E., Lagali, P. S., Wong, P. W., MacDonald, I. M., Sieving, P. A., Figueroa, D. J., Austin, C. P., Gould, R. J., Ayyagari, R., and Petrukhin, K. (2001) *Nat Genet* **27**, 89-93

46. Venkataraman, K., Riebeling, C., Bodennec, J., Riezman, H., Allegood, J. C., Sullards, M. C., Merrill, A. H., Jr., and Futerman, A. H. (2002) *J Biol Chem* **277**, 35642-35649
47. Mizutani, Y., Kihara, A., and Igarashi, Y. (2006) *Biochem J* **398**, 531-538
48. Riebeling, C., Allegood, J. C., Wang, E., Merrill, A. H., Jr., and Futerman, A. H. (2003) *J Biol Chem* **278**, 43452-43459
49. Lahiri, S., Lee, H., Mesicek, J., Fuks, Z., Haimovitz-Friedman, A., Kolesnick, R. N., and Futerman, A. H. (2007) *FEBS Lett* **581**, 5289-5294
50. Thomas, R. L., Jr., Matsko, C. M., Lotze, M. T., and Amoscato, A. A. (1999) *J Biol Chem* **274**, 30580-30588
51. Eto, M., Bennouna, J., Hunter, O. C., Hershberger, P. A., Kanto, T., Johnson, C. S., Lotze, M. T., and Amoscato, A. A. (2003) *Prostate* **57**, 66-79
52. Eto, M., Bennouna, J., Hunter, O., Lotze, M., and Amoscato, A. (2006) *Int J Urol* **13**, 148-156
53. Koybasi, S., Senkal, C. E., Sundararaj, K., Spassieva, S., Bielawski, J., Osta, W., Day, T. A., Jiang, J. C., Jazwinski, S. M., Hannun, Y. A., Obeid, L. M., and Ogretmen, B. (2004) *J Biol Chem* **279**, 44311-44319
54. Kroesen, B. J., Jacobs, S., Pettus, B. J., Sietsma, H., Kok, J. W., Hannun, Y. A., and de Leij, L. F. (2003) *J Biol Chem* **278**, 14723-14731
55. Hoekstra, D., Maier, O., van der Wouden, J. M., Slimane, T. A., and van, I. S. C. (2003) *J Lipid Res* **44**, 869-877
56. Muramatsu, T., and Muramatsu, H. (2004) *Glycoconj J* **21**, 41-45
57. Yamashita, T., Wada, R., Sasaki, T., Deng, C., Bierfreund, U., Sandhoff, K., and Proia, R. L. (1999) *Proc Natl Acad Sci U S A* **96**, 9142-9147
58. Palmqvist, L., Glover, C. H., Hsu, L., Lu, M., Bossen, B., Piret, J. M., Humphries, R. K., and Helgason, C. D. (2005) *Stem Cells* **23**, 663-680
59. zur Nieden, N. I., Price, F. D., Davis, L. A., Everitt, R. E., and Rancourt, D. E. (2007) *Mol Endocrinol* **21**, 674-685
60. Hailesellasse Sene, K., Porter, C. J., Palidwor, G., Perez-Iratxeta, C., Muro, E. M., Campbell, P. A., Rudnicki, M. A., and Andrade-Navarro, M. A. (2007) *BMC Genomics* **8**, 85
61. Marasas, W. F., Riley, R. T., Hendricks, K. A., Stevens, V. L., Sadler, T. W., Gelineau-van Waes, J., Missmer, S. A., Cabrera, J., Torres, O., Gelderblom, W. C., Allegood, J., Martinez, C., Maddox, J., Miller, J. D., Starr, L., Sullards, M. C., Roman, A. V., Voss, K. A., Wang, E., and Merrill, A. H., Jr. (2004) *J Nutr* **134**, 711-716
62. Gelineau-van Waes, J., Starr, L., Maddox, J., Aleman, F., Voss, K. A., Wilberding, J., and Riley, R. T. (2005) *Birth Defects Res A Clin Mol Teratol* **73**, 487-497

CHAPTER 3

CHARACTERIZATION OF CERAMIDE SYNTHASE 2: TISSUE DISTRIBUTION, SUBSTRATE SPECIFICITY AND CERS2 KNOCKOUT MICE

3.1 Introduction

The past decade has seen an upsurge of interest in sphingolipids (SLs), due largely to the extraordinary number of complex species that have been found in eukaryotes (1), as well as the involvement of the lipid backbones in signaling pathways as both first and second messengers (2–4). Indeed, ceramide (3) and sphingosine 1-phosphate (S1P) (5) appear to play opposing roles in cell proliferation, migration, and survival, which underscores how the balance of the levels of these two lipids has ramifications for diverse pathological and pathophysiological processes (6–8).

In mammals, ceramide is synthesized by a family of six enzymes, ceramide synthases (*CerS*) 1–6 (9), each of which uses a relatively restricted subset of fatty acyl-CoAs for N-acylation (10–12) of the sphingoid long chain base. Thus, *CerS1* and *CerS5*, which are the best characterized *CerS* proteins, synthesize C18- and C16-ceramide, respectively (10,11,13,14), whereas *CerS2* and *-3* appear to have a broader specificity (15). The existence of these six *CerS* genes in mammals implies an important and largely unexplored role for ceramides containing specific fatty acids in cell physiology (9). One possibility is that different tissues contain ceramides with defined fatty acids, necessitating the presence of specific *CerS* in specific tissues for their synthesis. However,

with the exception of an early study by semi-quantitative reverse transcription-PCR (11), little is known about *CerS* tissue distribution.

This study describes the characterization of *CerS2*, which has received relatively little attention. We demonstrate that *CerS2* mRNA occurs at much higher levels than most other *CerS*, has the broadest tissue distribution, and —in studies of cells in culture— synthesizes ceramides containing mainly C20–C26 fatty acids, with little or no synthesis of C16- and C18-ceramides. However, studies with a *CerS2* null mouse that has been generated by our collaborators, Dr. Tony Futerman and associates, our analyses suggest that *CerS2* is responsible for a somewhat more narrow number of Cer subspecies—those with C24 $\pm$ 2 carbon atoms.

3.2 Experimental Procedures

My role on these studies was to analyze the sphingolipids that are made by these cells in culture and animal models. For these analyzes, I used the same methods as described in Chapter 2, with minor modifications as described in figure legends and text. To show how these were critical for the entire study, I have included the procedures and results from these analyses as well as the others that were reported in the published paper from the cell studies (42); the data for the knockout mouse are now being prepared for publication.

3.2.1 Materials

D-*erythro*-[4,5-3H]Sphinganine was synthesized as described (16). S1P was from Sigma-Aldrich or from Avanti Polar Lipids (Alabaster, AL); fatty acyl-CoAs and the internal standards for liquid chromatography electrospray ionization tandem mass spectrometry (LC ESI-MS/MS) were also from Avanti. An anti-protein disulfide isomerase antibody was from Stressgen (Victoria, BC, Canada), and an anti-hemagglutinin (HA) antibody was from Santa Cruz Biotechnology (Santa Cruz, CA). Horseradish peroxidase was from Jackson Laboratories (Bar Harbor, MA). *Pfu* polymerase was from Promega (Madison, WI) or from Stratagene (La Jolla, CA). TaqManTM was from Applied Biosystems (Foster City, CA). A PerfectPure RNA Kit was from 5Prime (Gaithersburg, MD). A Reverse-iT first strand synthesis kit was from Thermo Scientific (Epsom, UK). All solvents were of analytical grade and were purchased from Biolab (Jerusalem, Israel).

3.2.2 Real-time qPCR

Tissues were harvested from 6- to 8-weekold mice; females were used for all tissues except prostate and testis. RNA was isolated using a PerfectPure RNA kit according to manufacturer's instructions, which included a DNase step. cDNA synthesis was performed using a Reverse-iT first strand synthesis kit using random decamers with 30-min incubation at 42 °C and then at 47 °C. cDNA generation demonstrated equivalent efficiency of synthesis with input RNA ranging from 15 to 500 ng per reaction (Fig. 3.1).

100 ng of total RNA was used to determine expression levels of mouse *CerS* mRNA, using TaqManTM analysis and a 7300 Sequence Detection System (Applied Biosystems). Relative CerS expression levels were determined in all tissues as compared with brain; quantitative analysis was assessed in brain by comparison to a standard curve generated via dilution of expression plasmids for each gene. To control for variability of RNA input, all PCR reactions were normalized to the amount of hypoxanthine guanine phosphoribosyltransferase 1 mRNA. Primer/probe sets for *CerS1* (Mm00433562_m1), *CerS2* (Mm00504086_m1), *CerS4* (Mm01212479_m1), *CerS5* (Mm00510996_g1), and *CerS6* (Mm00556165_m1), and for hypoxanthine guanine phosphoribosyltransferase 1 (Mm00446968_m1) were pre-validated sets obtained from Applied Biosystems. *CerS3* was custom ordered from Applied Biosystems and designed to span exon 2 and exon 3 (Locus DQ646881). Oligonucleotides used for generation of qPCR templates are given in Table 3.1.

3.2.3 Short Interfering RNA (siRNA)

siRNAs were subcloned into the pSUPER vector according to the manufacturer's instructions (OligoEngine, Seattle, WA). Two siRNA targets were chosen for *CerS2*: siCerS2i, 5'-AAGCAGGTGGAAGTAGAGCTTTT-3', and siCerS2ii, 5'-AAGCCAGCTGGAGATTCACATTT-3'. The sequences were chosen because they recognize all known *CerS2* isoforms (9) and do not recognize other *CerS* genes. *CerS2* knockdown was accomplished by transfecting Hek cells with the pSUPER vector using the calcium phosphate method. After various times of incubation, total RNA was

extracted using the RNeasy Mini Kit (Qiagen). Reverse transcription was performed using the EZ-First strand cDNA synthesis kit (Biological Industries, Beit Haemek, Israel), and PCR was performed using the primers listed in Table 3.1.

Table 3.1. Primers used in the current study

Gene	Sequence	Tm [°C]	Cycles
Oligonucleotides used for generation of qPCR templates[a]			
CerS1	Sense-ACAGCCAAGCCCTGCAAA Anti-sense-TCCACCACCATGTCTTCGTA	60	35
CerS2	Sense-GGCGCTAGAAGTGGGAAAC Anti-sense-TCGAATGACGAGAAAGAGCA	60	35
CerS3	Sense-GCTACACCTCTAGCAAATGCAC Anti-sense-ATCTTTCAACCTGGCGCTCT	60	30
CerS6	Sense-TTAATCATCCACGGAACAAGGACCAGTG Anti-sense-TTAATCATCCACGGAACAAGGACCAGTG	55	30
Primers used to clone CerS2 and for site-directed mutagenesis of CerS2[b]			
CerS2-HA	Primer A, CCCAAGCTTATGCTCCAGACCTTGTAT (Hind3) Primer B, CCGGAATTCTCATCAAGCGTAATCTGGAACATC GTATGGGTAGTCATTCTTACGATGGTT (EcorI)	48	30
CerS2 R230A	Primer C, CAATTACATCGCAGCTGGGACTCTAATCATGGC Primer D, AGTCCCAGCTGCGATGTAATTGGCAAACCAG	54/62	5/30
CerS2 R325A	Primer E, TCATTTTGGCCATGGCCCACAAGTTCATAA Primer F, GCCATGGCCAAAATGAGGTAGGCCCAG	54/62	5/30
Primers used for mRNA expression analysis after siRNA treatment			
CerS2	5'GCTGGAGATTCACATTTTAC 5'-GAAGACGATGAAGATGTTGT	50	25
GADPH	5'-TTAGCACCCCTGGCCAAGG 5'-CTTACTCCTTGGAGGCCATG	50	25

[a] Oligonucleotides were used to generate templates for calibration of the qPCR reactions (see Fig. 3.1).

[b] Primers A and D were used for amplification of the N terminus of the R230 construct and primers B and C for the C terminus. Primers A and F were used for amplification of the N terminus of the R325 construct and primers B and E for the C terminus. In the second step, the two fragments were annealed using an additional touch-up PCR step. Annealing temperatures of 54 °C were used for the first 5 cycles, and a temperature of 62 °C for the next 30 cycles.

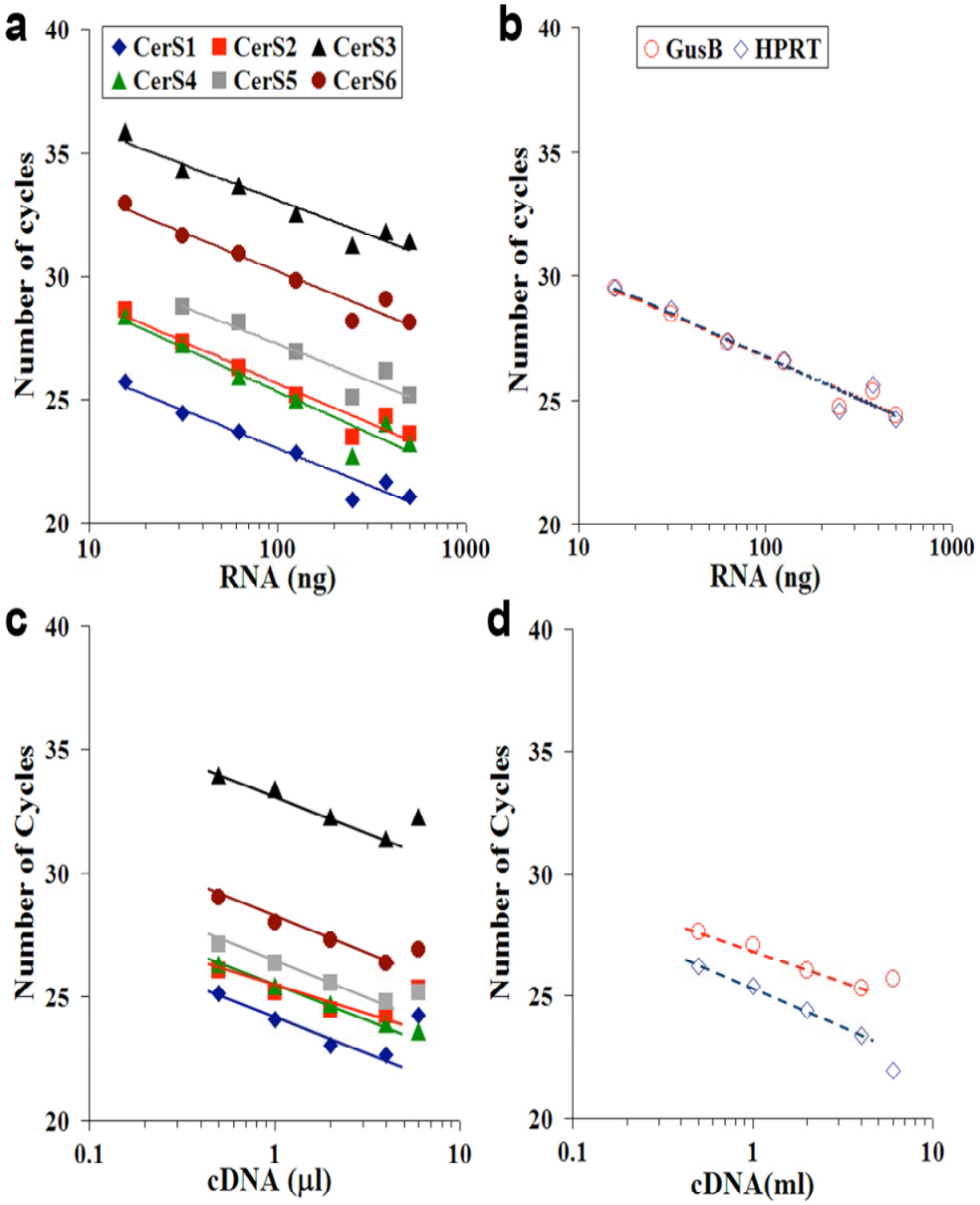

Figure 3.1. qPCR assays are linear over a wide range of RNA and cDNA concentrations. a-b) To validate real time PCR assays, a first step is to determine the amount of total RNA used in the cDNA synthesis reactions that is linear with respect to conditions for each primer and probe set. Taqman assays for the *CerS* and endogenous genes are linear from 15-500 ng total RNA used per cDNA reaction, with 2 µl of each reaction used per 20 µl PCR reaction. In addition, the ratio of endogenous gene to *CerS* genes is not changed over this range of total RNA. c-d) Another step to validate real time PCR assays is to determine the amount of cDNA that can be used within each reaction. cDNA was synthesized with 100 ng total RNA from whole mouse brain. Various amounts of cDNA was used in each reaction. Taqman assays for the *CerS* and endogenous genes are linear from 0.5-4 µl per 20 µl PCR reaction. At 6 µl per 20 µl PCR reaction the assays are no longer linear nor does the ratio of *CerS* to endogenous gene remain constant. Data is a representative experiment performed in duplicate.

3.2.4 Cell Culture and Transfection

Human embryonic kidney cells (Hek 293) were grown in Dulbecco's modified Eagle's medium supplemented with 10% fetal calf serum, 100 IU/ml penicillin, and 100 μg/ml streptomycin. Hek 293 cells were transfected with human *CerS* genes using the calcium phosphate method (0.25 μg of plasmid per cm^2 of culture dish), which gave ~ 90% transfection efficiency. Human *CerS* genes (17) in a pCMV vector, with an N terminus FLAG tag, were obtained from Dr. Richard Kolesnick (Sloan Kettering Institute). *CerS2* was subsequently subcloned into a pcDNA3 vector containing an HA tag, which was located at the C terminus (*CerS2*-HA). Site-directed mutagenesis of *CerS2*-HA was performed using 2-Step PCR and Touch-up cycling conditions.

3.2.5 Liquid Chromatography Electrospray Inonization Tandem Mass Spectrometry

SL analyses by LC ESI-MS/MS were conducted using a PE-Sciex API 3000 triple quadrupole mass spectrometer and an ABI 4000 quadrupole-linear ion trap mass spectrometer as described previously (10,11,18,19). Hek 293 cells were transfected with pcDNA, human *CerS2*, or siRNA and after 36 h, harvested by trypsinization, collected by centrifugation, washed twice with ice-cold phosphate-buffered saline, and lyophilized. The samples were spiked with an SL internal standard mixture (Avanti Polar Lipids) then extracted and analyzed by LC ESI-MS/MS (10, 11, 18, 19). For tissue analyses, the tissues were obtained from C57BL/6 mice at 7 weeks of age and different ages of *CerS2*

knockout mice, homogenized as described above, and aliquots were lyophilized. Samples corresponding to 1 mg of lyophilized tissue were spiked with the SL internal standard mixture, extracted, and analyzed by LC ESI-MS/MS. Fatty Acyl-CoA analyses by LC ESI-MS/MS were performed on a 4000 QTrap triple quadrupole linear ion trap mass spectrometer (Applied Biosystems, Foster City, CA) as recently described (37).

3.2.6 *CerS* Assay

CerS activity was assayed as described previously (10, 11, 14) using Hek 293 cell homogenates and 0.25 μCi of [4,5-^{3}H]sphinganine/15 μM sphinganine/20 μM defatted-bovine serum albumin/50 μM fatty acyl-CoA for 20 min at 37 °C (17). Different amounts of protein were used for homogenates obtained from cells transfected with different *CerS* protein in order that the time of the reaction was linear with respect to protein (17), and different acyl-CoAs were used in accordance with the substrate specificity of each *CerS* (10−12, 14, 15) (*CerS1*, 100 μg of protein, C18-CoA; *CerS2*, 150 μg of protein, C22-CoA; *CerS3*, 200 μg of protein, C24-CoA; C*erS4*, 200 μg of protein, C20-CoA; C*erS5* and *CerS6*, 50 μg of protein, C16-CoA).

3.2.7 Immunofluorescence

The intracellular localization of human *CerS2*-HA was performed by confocal laser scanning microscopy as described for *CerS4* and *-5* (11), using Mito-Tracker Deep Red as a mitochondrial marker and protein disulfide isomerase as an endoplasmic reticulum marker.

3.3 Results

3.3.1 *CerS* expression in mouse tissues

An early study examining the tissue distribution of *CerS* mRNA by semi-quantitative RT-PCR suggested that each *CerS* has a somewhat unique tissue distribution, with *CerS2* (*trh3*) mRNA the most ubiquitously expressed (11). To determine which *CerS* were expressed in different tissues, our collaborators established robust reaction conditions for real time quantitative PCR (qPCR), in which the reactions are linear over 8 to 10 orders of magnitude and are >99% efficient (Fig. 3.2). Using these conditions, they analyzed *CerS* mRNA levels in 14 mouse tissues.

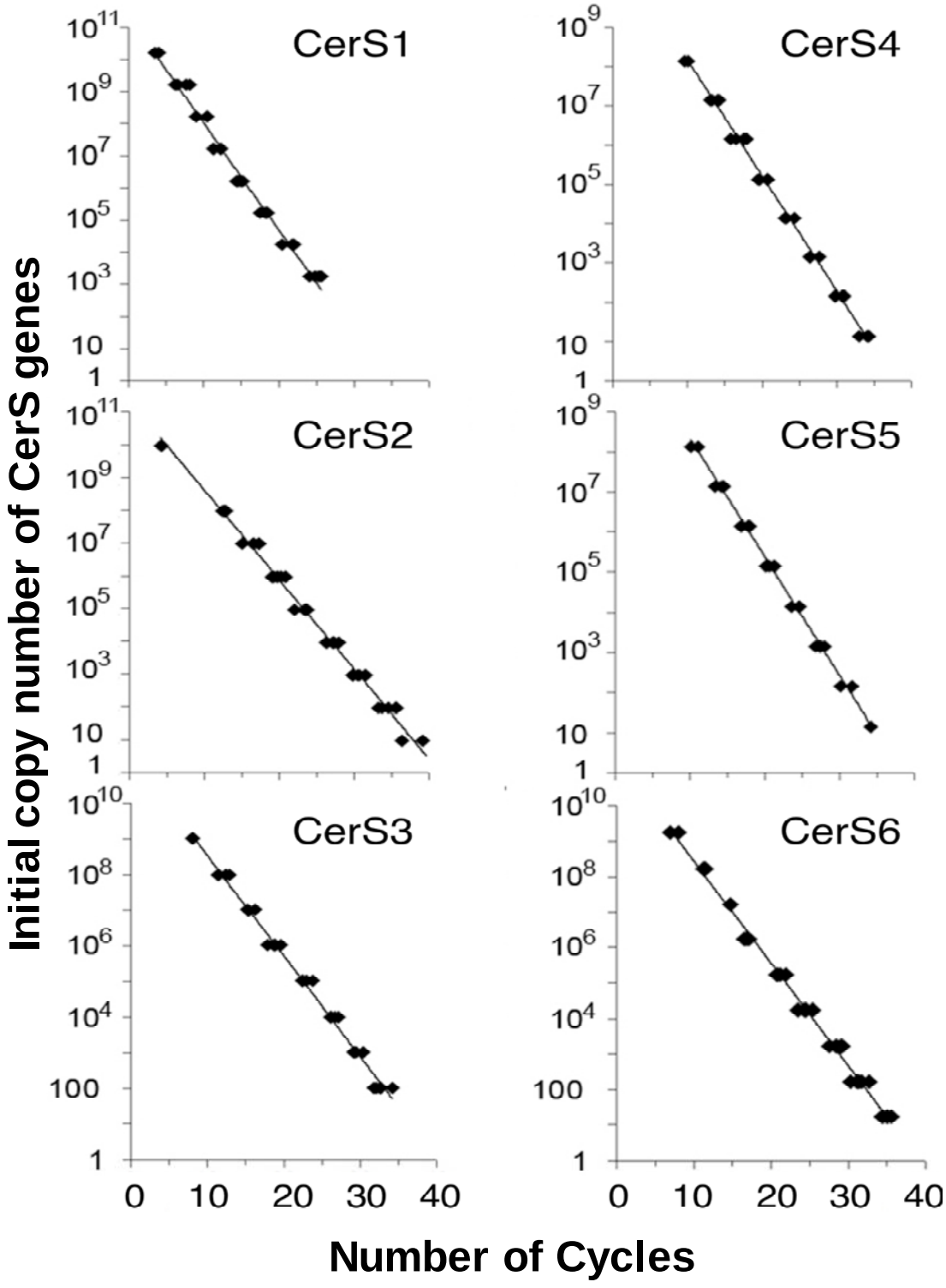

Figure 3.2. qPCR reactions for CerS mRNA are highly sensitivity and linear over 8-10 orders of magnitude.

In agreement with the earlier study (11), *CerS2* is ubiquitously expressed. However, due to the linearity and sensitivity of qPCR, these study demonstrated that *CerS2* mRNA expression levels are significantly higher than those of the other five *CerS* genes, in some cases as much as an order of magnitude higher (Fig. 3.3). Highest *CerS2* expression (30 to 40 molecules RNA/pg total RNA) was detected in liver and kidney (Fig. 3.3), with lower levels (~5 molecules RNA/pg total RNA) in most other tissues. In contrast, *CerS1* and *-3* were expressed mainly in brain and skeletal muscle, and in skin and testis (15), respectively, and were virtually undetectable in other tissues. *CerS4* was expressed at the highest levels in skin, leukocytes, heart and liver, and in the other tissues, was expressed at levels of 1 to 2 molecules/pg total RNA (Fig 3.3). *CerS5* and *-6* were expressed in most tissues, with expression levels of 1 to 3 molecules/pg total RNA (Fig. 3.3). *CerS2* expression tended to be low in tissues expressing highest levels of *CerS1* or *CerS3*.

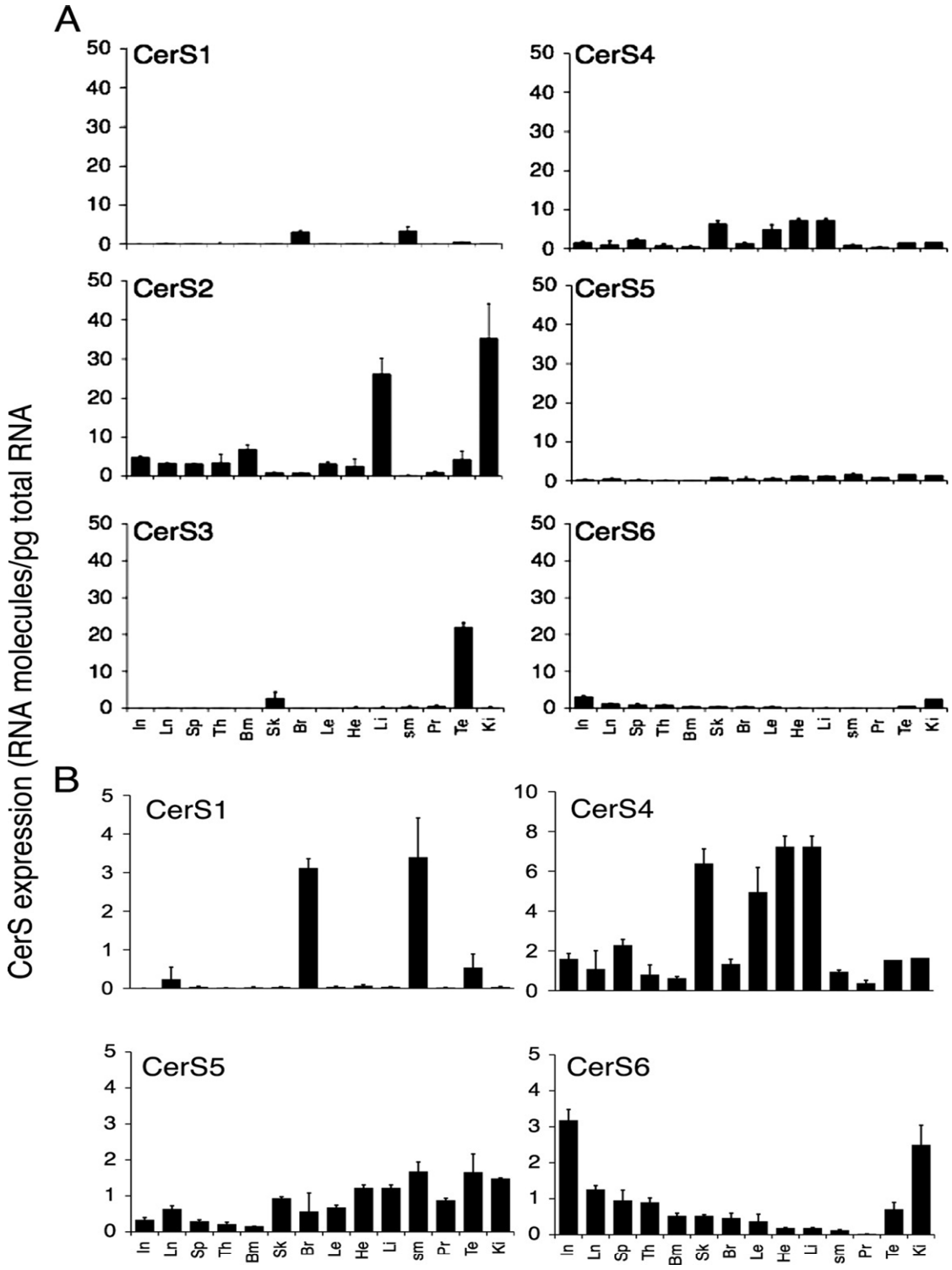

Figure 3.3. *CerS2* is ubiquitously expressed and is highly abundant in mouse tissues.

3.3.2 Acyl-CoA Specificity and Intracellular Localization of *CerS2*

These studies also examined the specificity of *CerS2* toward acyl-CoAs. Phylogenetically, *CerS2* is most closely related to *CerS3* (9), which was suggested to synthesize ceramides containing mainly C16:0 and C24:0 fatty acids (15). LC ESI-MS/MS demonstrated, in contrast, that *CerS2* uses a wider range of acyl-CoAs, synthesizing ceramides containing C20:0, C22:0, C24:1, C24:0, C26:1, and C26:0 fatty acids (Fig. 3.4A), but notably, does not synthesize ceramides containing C16:0 fatty acids and synthesizes only low, and statistically insignificant levels of C18:0-ceramide. *In vitro* analysis of *CerS2* activity using a range of acyl-CoAs (Fig. 3.4B) was entirely consistent with LC ESI-MS/MS analysis.

To confirm the acyl-CoA specificity of *CerS2*, cells were transfected with two different siRNAs in a pSUPER vector, and compared with cells incubated with the pSUPER vector alone. *CerS2* mRNA levels were significantly reduced 24 h after transfection with siCerS2ii and 72 h after transfection with siCerS2i (Fig. 3.5A). *CerS* activity, using C22:0-acyl-CoA as substrate, revealed a more rapid loss of activity after transfection with siCerS2ii compared with siCerS2i. Examination of levels of ceramides by LC ESI-MS/MS after transfection with siCerS2ii (Fig. 3.5C) was consistent with LC ESI-MS/MS data obtained after overexpression of *CerS2* (Fig. 3.4A). Thus, *CerS2* has a completely different profile of use of acyl-CoAs than the other *CerS*, using mainly medium- to long-chain CoAs, but is unable to synthesize C16:0- and C18:0-ceramides.

Similar to other *CerS* for which the intracellular localization has been examined by immunofluorescence after overexpression (10, 11), rather than by biochemical

isolation of mitochondrial fractions (20), *CerS2* is localized to the endoplasmic reticulum (Fig. 3.6), with no co-localization with a mitochondrial marker (21).

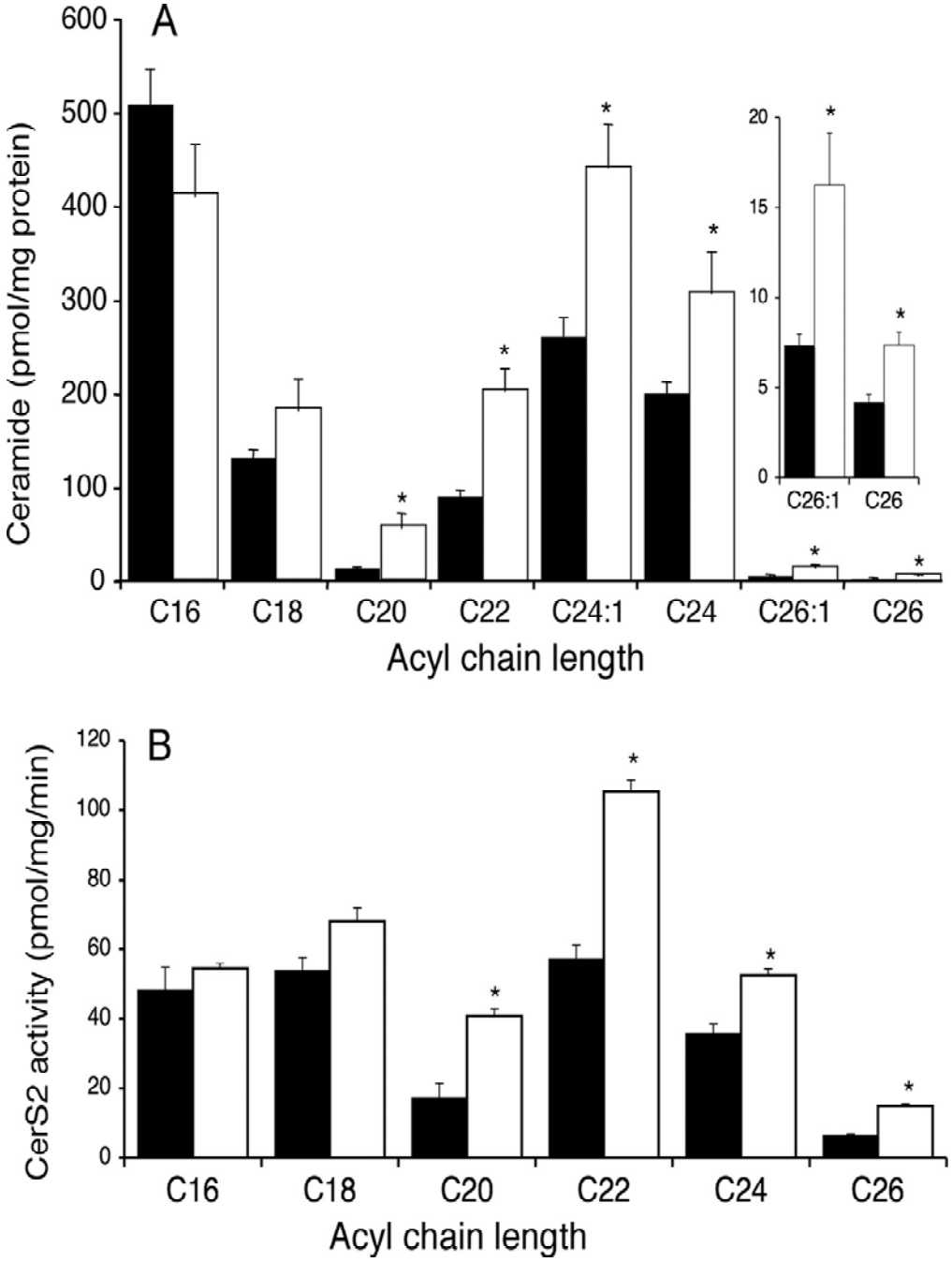

Figure 3.4. Substrate specificity of *CerS2* toward acyl-CoAs. A, the fatty acid composition of ceramide was determined by LC ESI-MS/MS in mock- and *CerS2*-transfected cells. Black columns are mock-transfected cells, and white columns are from *CerS2* transfected cells. Results are means ± S.E. of 4–5 individual experiments. *, $p<0.05$. The inset shows C26:0 and C26:1 levels scaled appropriately. B, *in vitro* analysis of *CerS2* activity. Results are means ± S.D. of a representative experiment performed in triplicate and repeated 3–4 times; *, $p<0.05$.

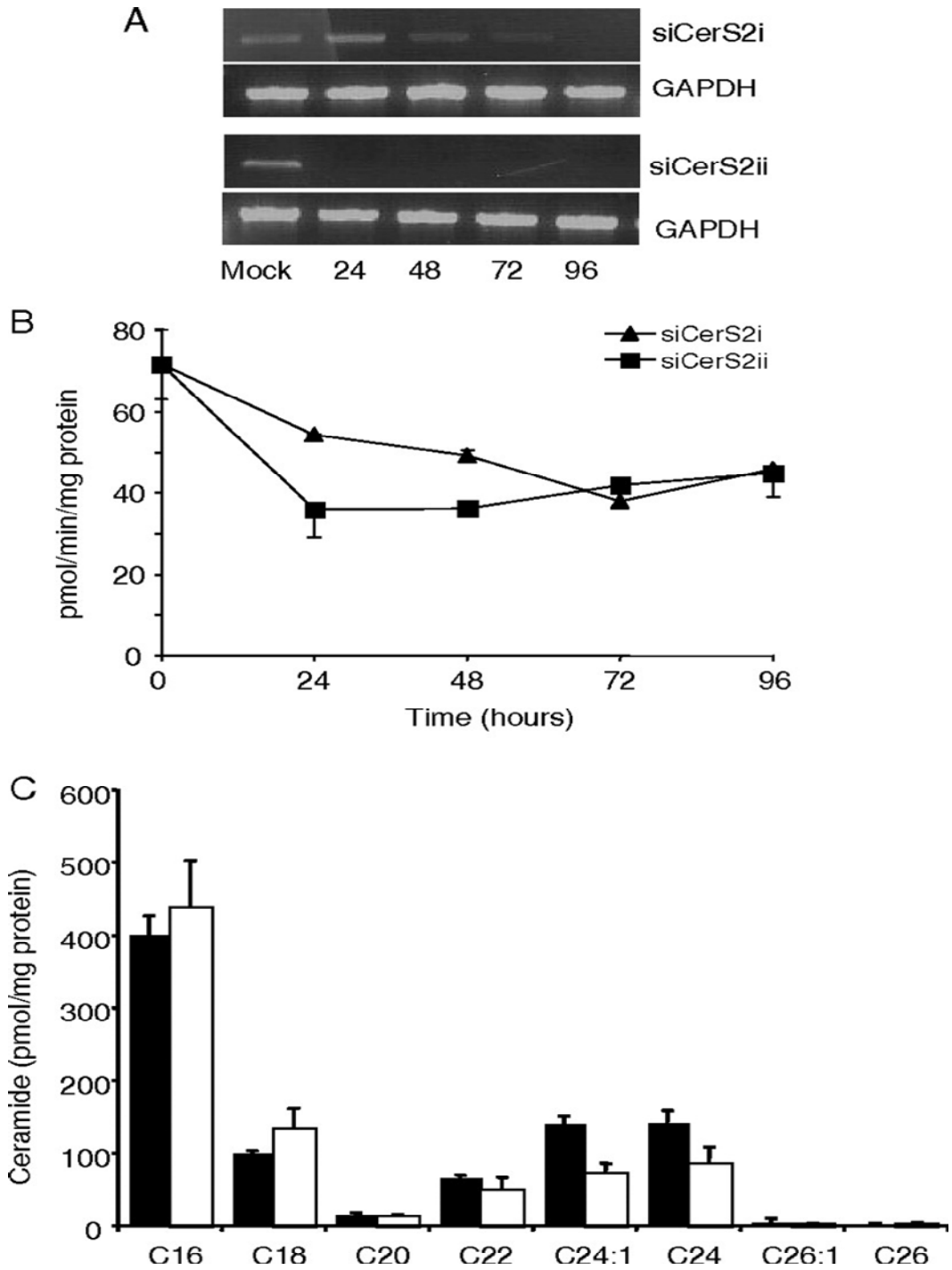

Figure 3.5. Effect of siRNA on mRNA expression, ceramide synthesis, and ceramide levels.

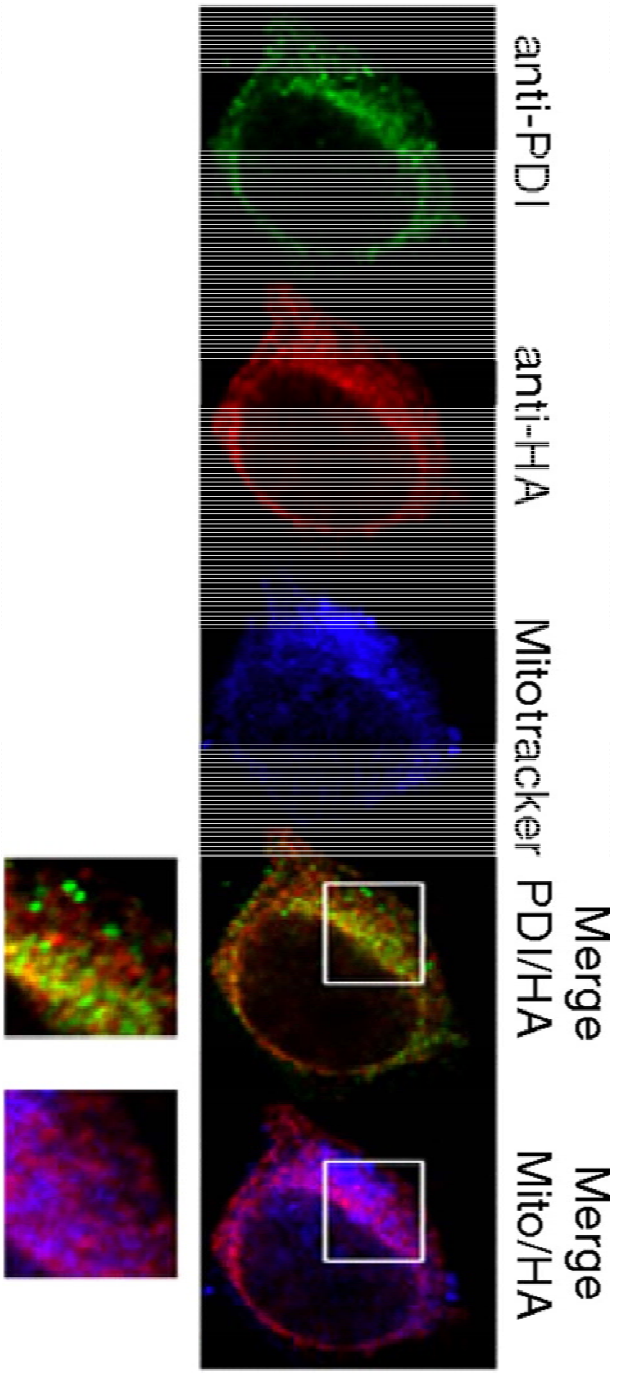

Figure 3.6. *CerS2* is localized to the endoplasmic reticulum. The localization of *CerS2*, HA-tagged at the C terminus (*CerS2*-HA) was compared with the endoplasmic reticulum marker, protein disulfide isomerase, and the mitochondria-specific dye, MitoTracker. The merged views are shown in pseudocolor with co-localization of anti-HA and anti-protein disulfide isomerase in yellow. The insets show enlarged views of the areas indicated by the boxes. Bar, 5 μm.

3.3.3 Relationship between *CerS* mRNA Expression and Ceramide N-Acyl Chain Composition

Although *CerS2* mRNA is widely distributed and found at high levels in various tissues (Fig. 3.3), nothing is known about how this is related to levels of expression of the *CerS2* protein or of the relative proportions of ceramides containing C20:0-C26:0-fatty acids, the subspecies synthesized by *CerS2* (Figs. 3.4 and 3.5). Because there are no antibodies currently available to mouse *CerS2*,[3] we examined the ceramide subspecies distribution by LC ESI-MS/MS to determine if tissues that display high levels of *CerS2* mRNA are enriched in the corresponding ceramide subspecies in ceramides, sphingomyelin (SM), and monohexosylceramide (Hex-Cer) (Fig. 3.7). Comparison of the ceramide N-acyl chain distribution with that of the relative levels of expression of *CerS* mRNA (Fig. 3.7) reveals that the two tissues with highest *CerS2* mRNA levels, kidney and liver, also have the highest proportions of C22- to C24-ceramides. Kidney also has high proportions of C22–C24 acyl chains in SM and HexCer (Fig. 3.7) as does liver, although the N-acyl chain composition of HexCer differs from that of ceramides and SM. For the other three tissues (brain, testis, and skeletal muscle), *CerS2* is less prevalent than the mRNAs of the other *CerS*, and the proportions of C22-, C24-, and C24:1-ceramides and -SMs are correspondingly lower. Interestingly, for two of these tissues (brain and skeletal muscle), HexCer contains surprisingly high proportions of C22–C24-ceramides,

---

[3] A Commercial antibody is available for human *CerS2* but unfortunately shows no cross-reactivity to mouse *CerS2*.

suggesting that there are factors other than the relative amounts of the *CerS* mRNA that affect the subspecies distribution, particularly in downstream complex SLs and glyco-SLs.

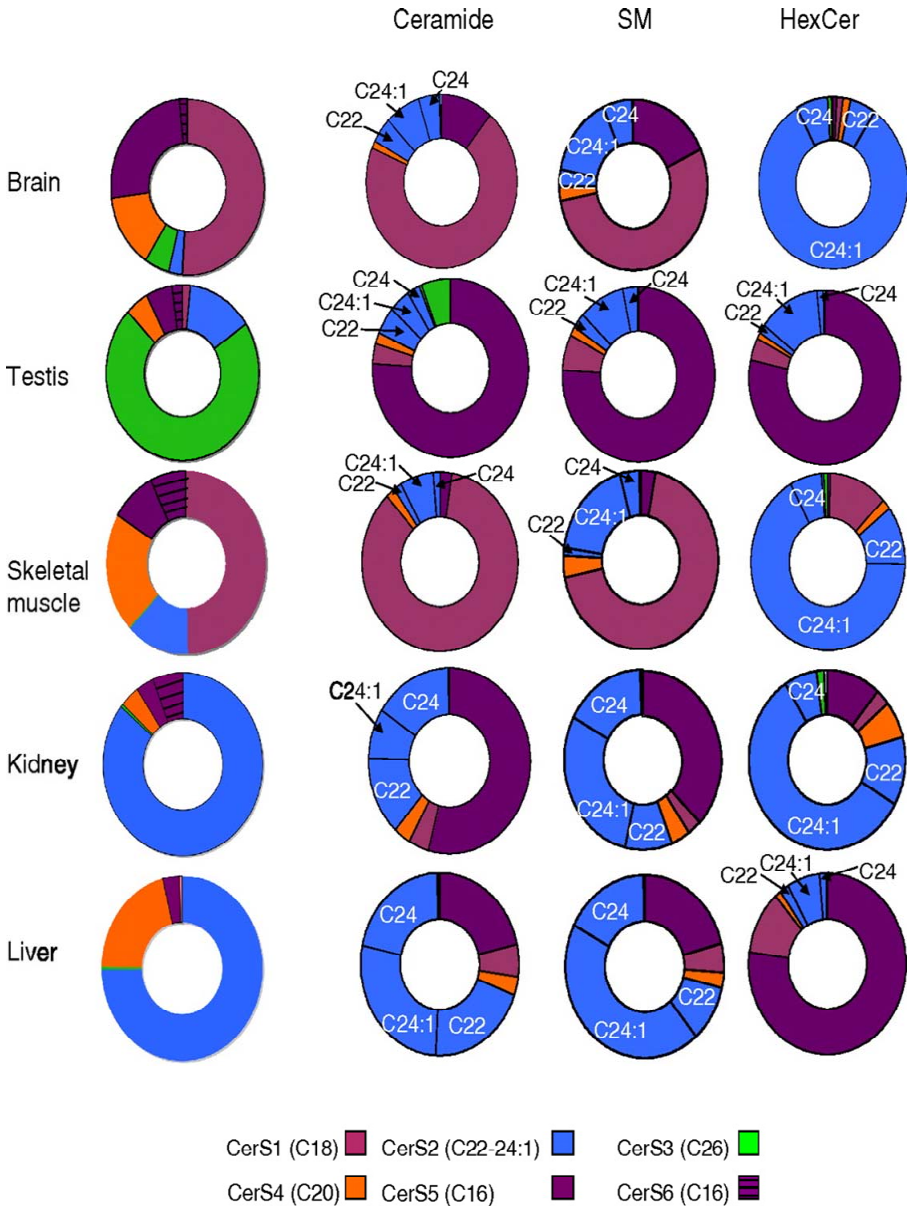

Figure 3.7. mRNA expression levels for *CerS1* to *-6* compared with the N-acyl chain distribution of ceramides, SM, and HexCer in five mouse tissues. The left-hand panel shows the percent distribution of *CerS* mRNA in the five tissues analyzed, taken from the data used in Fig. 3.1. The three right-hand panels show the percent distribution of acyl chains in ceramide, SM, and HexCer for the same tissues. The pie charts are colorcoded according to the specific CerS and the ceramide species that they synthesize, as shown in the legend. For simplicity, only the main ceramide species synthesized by each *CerS* are shown. Thus, C22, C24, and C24:1 are shown for *CerS2* with C20 (which is only a minor species) excluded; the different ceramides made by *CerS2* are indicated in the figure. For *CerS4*, only C20 is shown. Data are from three triplicate analyses from two animals. Levels of ceramides (in pmol/mg of protein) for each tissue are given in Table 3.2.

Table 3.2 Levels of ceramide, HexCer and SM are shown for five different tissues. This data is presented in Fig. 3.7 as a percent distribution, and are from three triplicate analyses from two animals.

Acyl chain length	Kidney	Liver	Brain	Skeletal muscle	Testis
Ceramide (pmol/mg protein)					
C16:0	346 ± 41	108 ± 47	49.3 ± 7.8	24.3 ± 9.9	614 ± 178
C18:0	26.1 ± 2.4	29.8 ± 13.7	1628 ± 477	152 ± 17	30.1 ± 7.1
C20:0	21.6 ± 2.8	16.7 ± 7.5	39.6 ± 12.6	3.2 ± 0.6	15 ± 5
C22:0	88.3 ± 5.3	102 ± 39	31.8 ± 6.8	9.9 ± 2.4	40.9 ± 12.1
C24:0	99.3 ± 11.1	107 ± 34	25± 5	9.8 ± 1.8	20.3 ± 3.5
C24:1	55.6 ± 3.7	139 ± 57	138 ± 11	16.4 ± 3.9	37.2 ± 6.4
C26:0	1.1 ± 0.4	1.5 ± 0.5	0.7 ± 0.3	0.5 ± 0.5	50.2 ± 19.8
C26:1	1.0 ± 0.6	1.4 ± 0.6	1.6 ± 1.1	0.8 ± 1.0	2.9 ±1.0
Hexosylceramide (pmol/mg protein)					
C16:0	3.6 ± 1.3	16.6 ± 3.0	3.9 ± 0.7	1.1 ± 0.8	28.0 ± 5.3
C18:0	1.0 ± 0.5	2.4 ± 0.9	75.1 ± 12.8	2.3 ± 0.4	1.5 ± 0.4
C20:0	2.2 ± 0.3	0.3 ± 0.2	12.0 ± 4.5	2.2 ± 0.6	0.3 ± 0.2
C22:0	4.0 ± 0.9	0.4 ± 0.2	64.3 ± 16.5	8.4 ± 2.8	0.7 ± 0.2
C24:0	2.2 ± 0.9	0.3 ± 0.1	39.4 ±10.7	10.3 ± 2.7	0.5 ± 0.2
C24:1	18.9 ± 4.7	1.4 ± 0.6	409 ± 100	122 ± 28	4.6 ± 1.3
C26:0	0.2 ± 0.2	0	4.8 ± 1.5	0.4 ± 0.3	0.1 ± 0.1
C26:1	0.6 ± 0.3	0.1 ± 0.1	4.3 ± 1.4	1.4 ± 0.6	0.1 ± 0.1
Sphingomyelin (pmol/mg protein)					
C16:0	2510 ± 313	301 ± 17	81 ± 12	122 ± 36	2078 ± 322
C18:0	183 ± 18	76.2 ± 5.5	1801 ± 160	363 ± 49	178 ± 21
C20:0	260 ± 36	40.5 ± 4.2	100 ± 17	16.9 ± 1.7	49.9 ± 7.0
C22:0	655 ±100	146 ± 21	39.1 ± 12.6	23.3 ± 2.5	76.3 ± 10.5
C24:0	1122 ± 180	249 ± 28	112 ± 40	43.3 ± 6.4	83.6 ± 8.2
C24:1	1972 ± 363	628 ± 45	478 ± 158	103 ± 18	265 ± 16
C26:0	14.0 ± 1.7	2.1 ± 0.4	1.1 ± 0.3	0.6 ± 0.1	1.5 ± 0.5
C26:1	14.3 ± 2.3	2.8 ± 0.4	4.2 ± 1.2	1.1 ± 0.2	2.8 ± 1.2

3.3.4. Analysis of sphingolipid profiles in *CerS2* null mice

To further study the role of *CerS2*, we have analyzed tissues from a *CerS2* null mouse that we have received from Dr. Futerman. *CerS2* null mice are born with a normal

Mendelian distribution but are born significantly smaller than their littlemate controls; they live for at least one year.

LC ESI-MS/MS analyses of SLs of livers derived from *CerS2* null mice (-/-) found that very-long chain Cer with chain lengths of C22 and C24 (both C24:0 and C24:1) were *ca*. 80 ~ 99 % lower than in livers from wild type *CerS2* mice (Fig. 3.8, 3.9 and 3.10). The C26:1- and C26-SL in *CerS2* null mice livers also appeared lower than in wild type *CerS2* mice livers, however, the amounts were very low for both and difficult to quantify accurately. The very-long chain Cer backbones were also undetectable or barely detectable in SM and HexCer from the *CerS2* null mice. In contrast, the CerS2 null mice livers had higher C16-Cer and C16-SLs than the wild type mice, with increases of up to 10-fold (Fig. 3.8, 3.9 and 3.10).

Interestingly, livers from wild type mice displayed changes in the amounts of some Cer subspecies over developmental time: decreasing amounts of C16-Cer and increasing amounts of C22-Cer (Fig. 3.8). The latter might imply that *CerS4*, which is selective for C20 $\pm$ 2 carbon atom-Cer synthesis might be involved, which could be of interest to study in the future. In contrast, the amounts of C24:1- and C24-Cer increased after 30 days (Fig. 3.8).

In addition, Sa levels were very low in wild type mice, but started high in null, and then highly increased. Sa levels were ~30-fold higher on day 30 and 95-fold higher on day 120 in *CerS2* null mice (Fig. 3.11). Moreover, there were no differences in acyl CoA levels between livers from wild type mice and *CerS2* null mice (Fig. 3.12). Note that livers from different mice have shown the similar N-acyl chain distributions of SL,

although, in this thesis, we show one set of data analyzed by LC ESI-MS/MS from one animal on developmental time and that results are means ± S.D. of a representative experiment performed in triplicate.

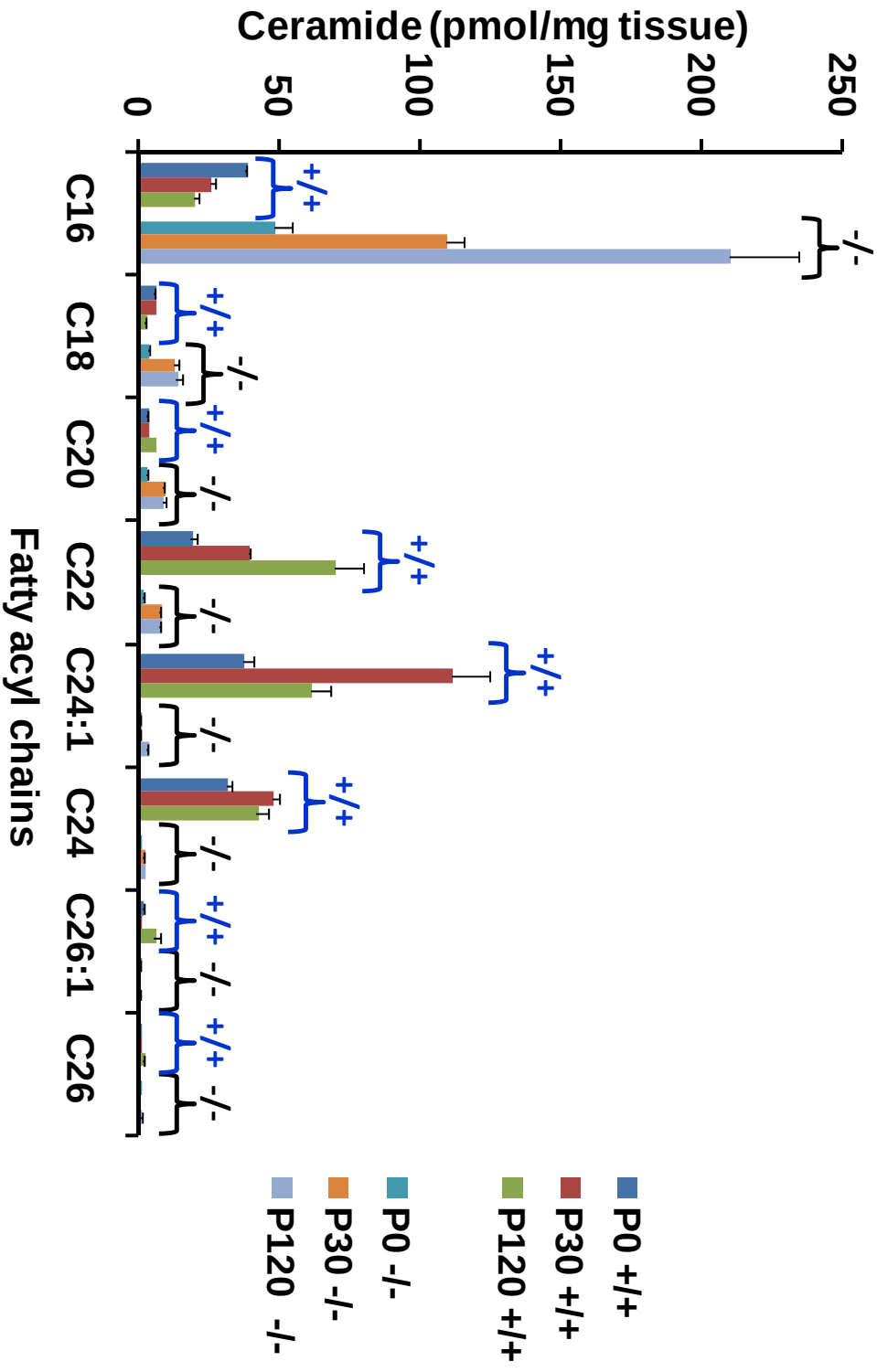

Figure 3.8. Ceramide profiles in livers derived from wild type mice (+/+, *blue*) and *CerS2* null mice (-/-, *black*) at ages (days).

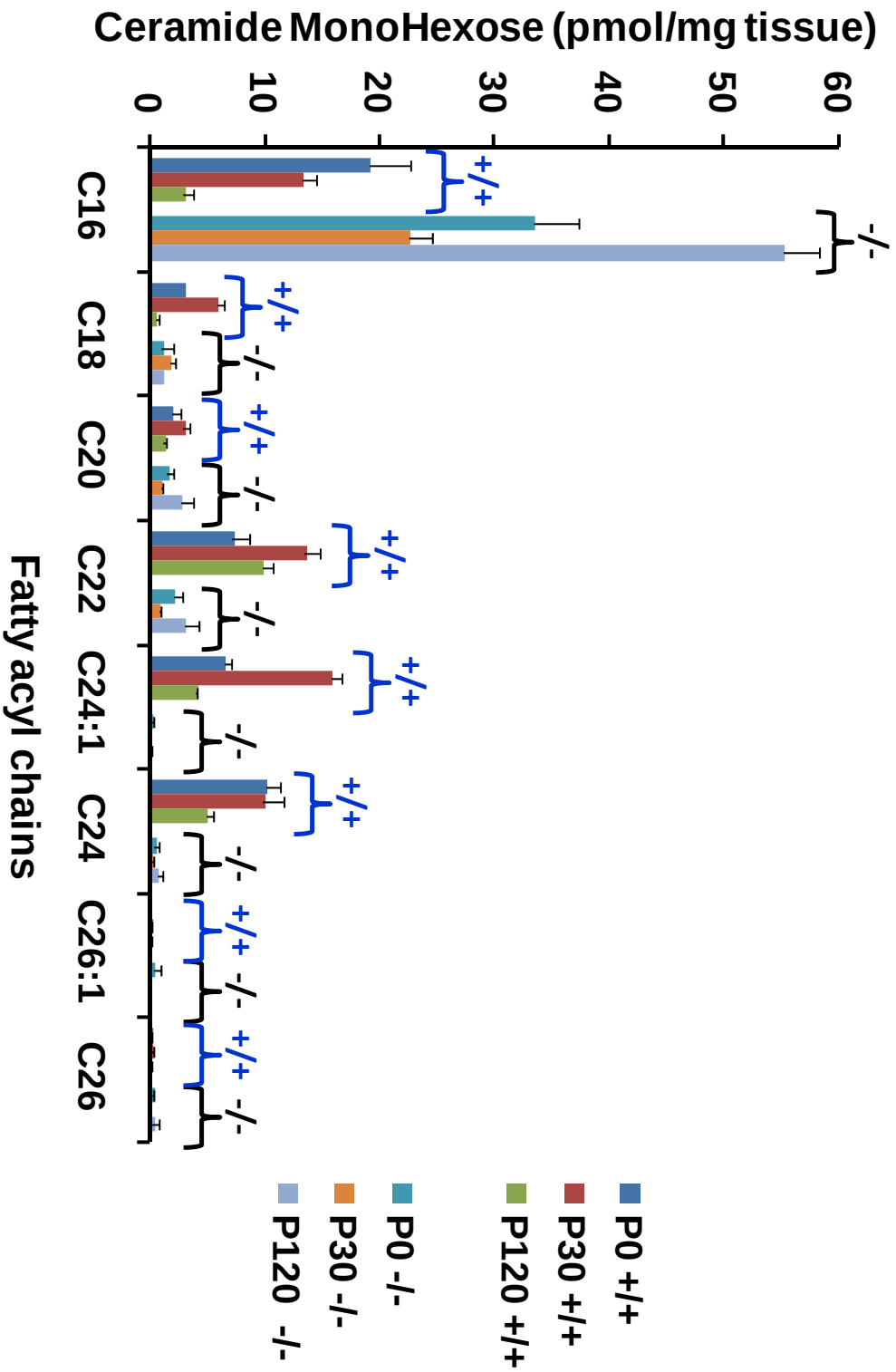

Figure 3.9. Ceramide monohexoses profiles in livers derived from wild type mice (+/+, *blue*) and *CerS2* null mice (-/-, *black*) at ages (days).

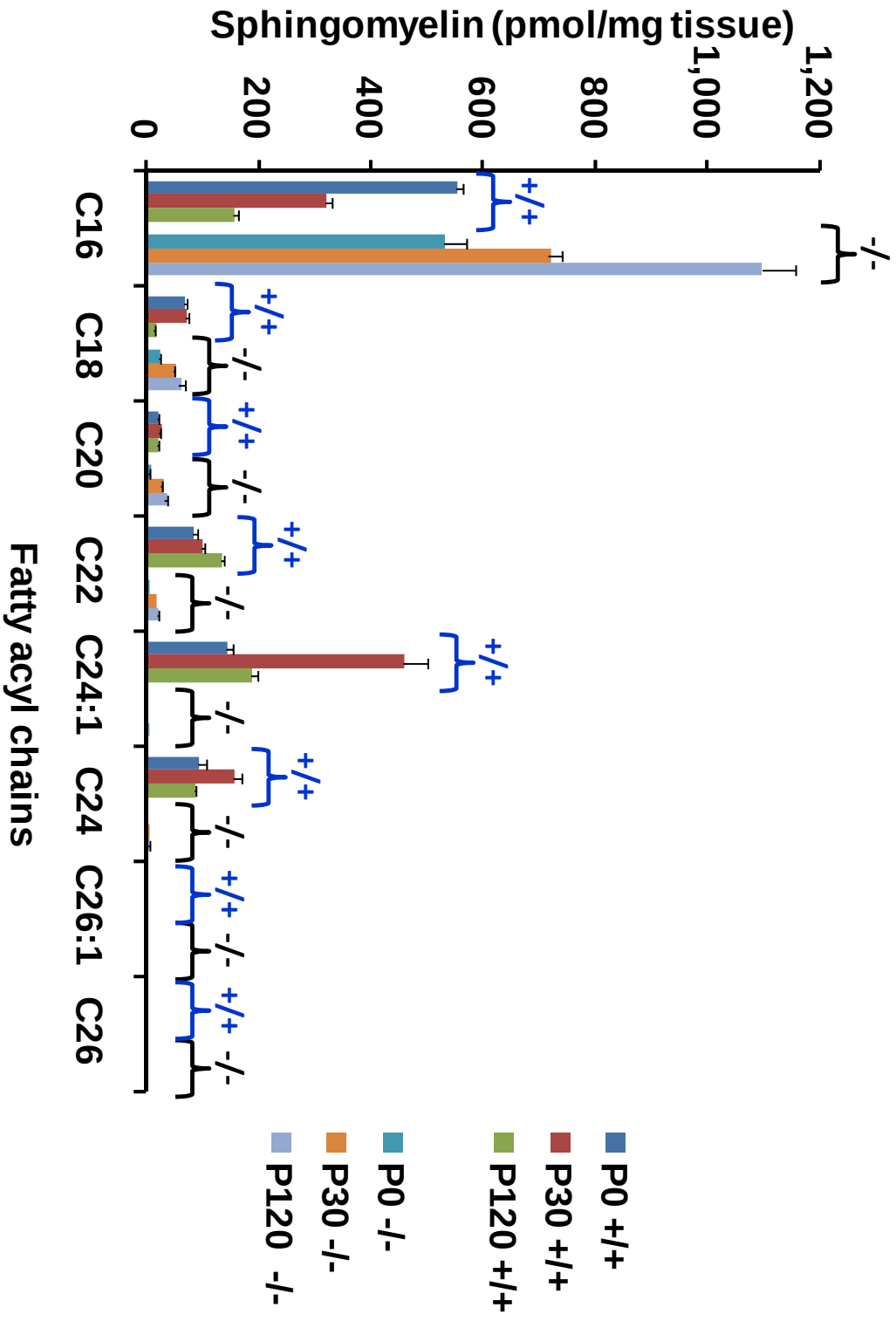

Figure 3.10. Sphingomyelin profiles in livers derived from wild type mice (+/+, *blue*) and *CerS2* null mice (-/-, *black*) at ages (days).

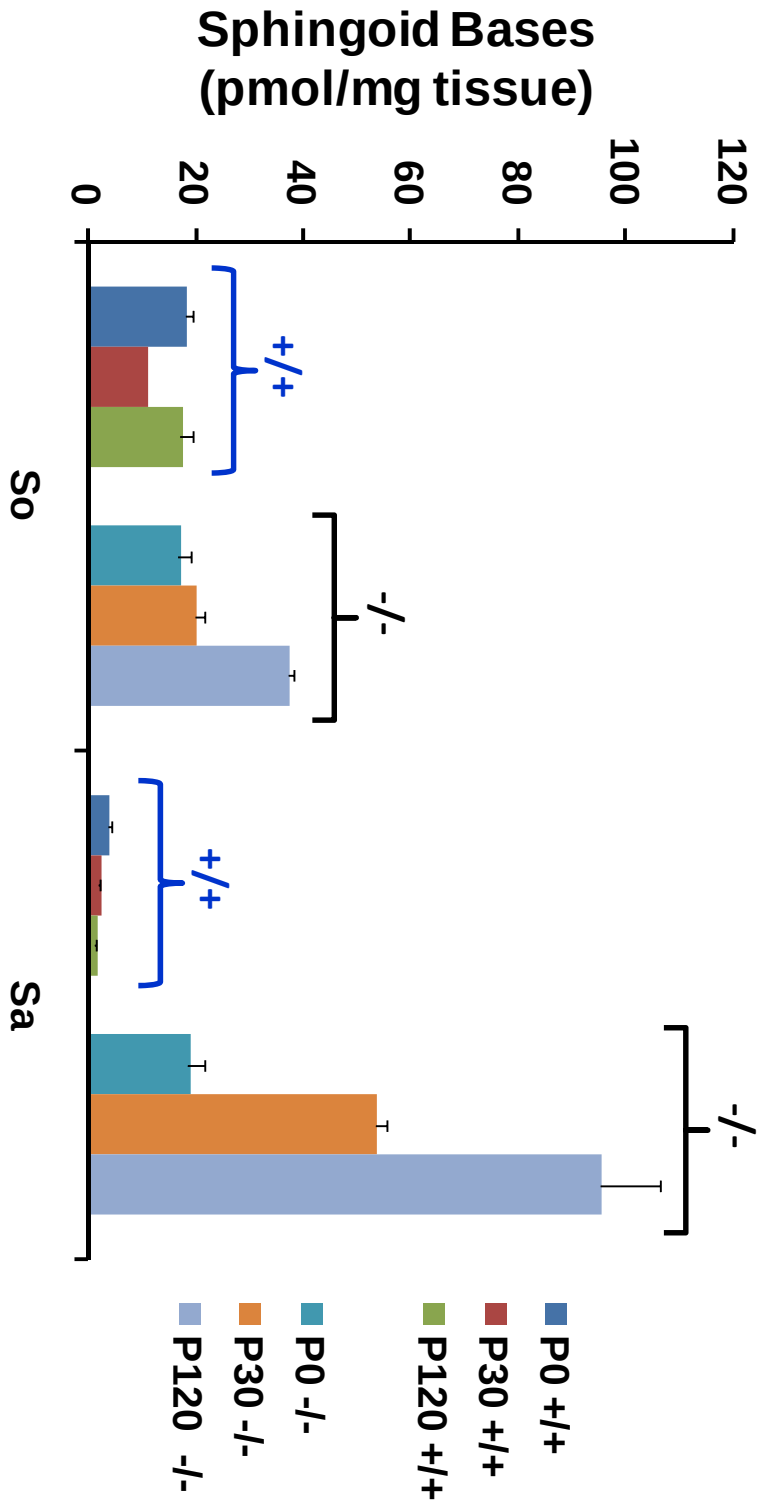

Figure 3.11. Sphingoid bases (sphingosine and sphinganine) profiles in livers derived from wild type mice (+/+, *blue*) and *CerS2* null mice (-/-, *black*) at ages (days).

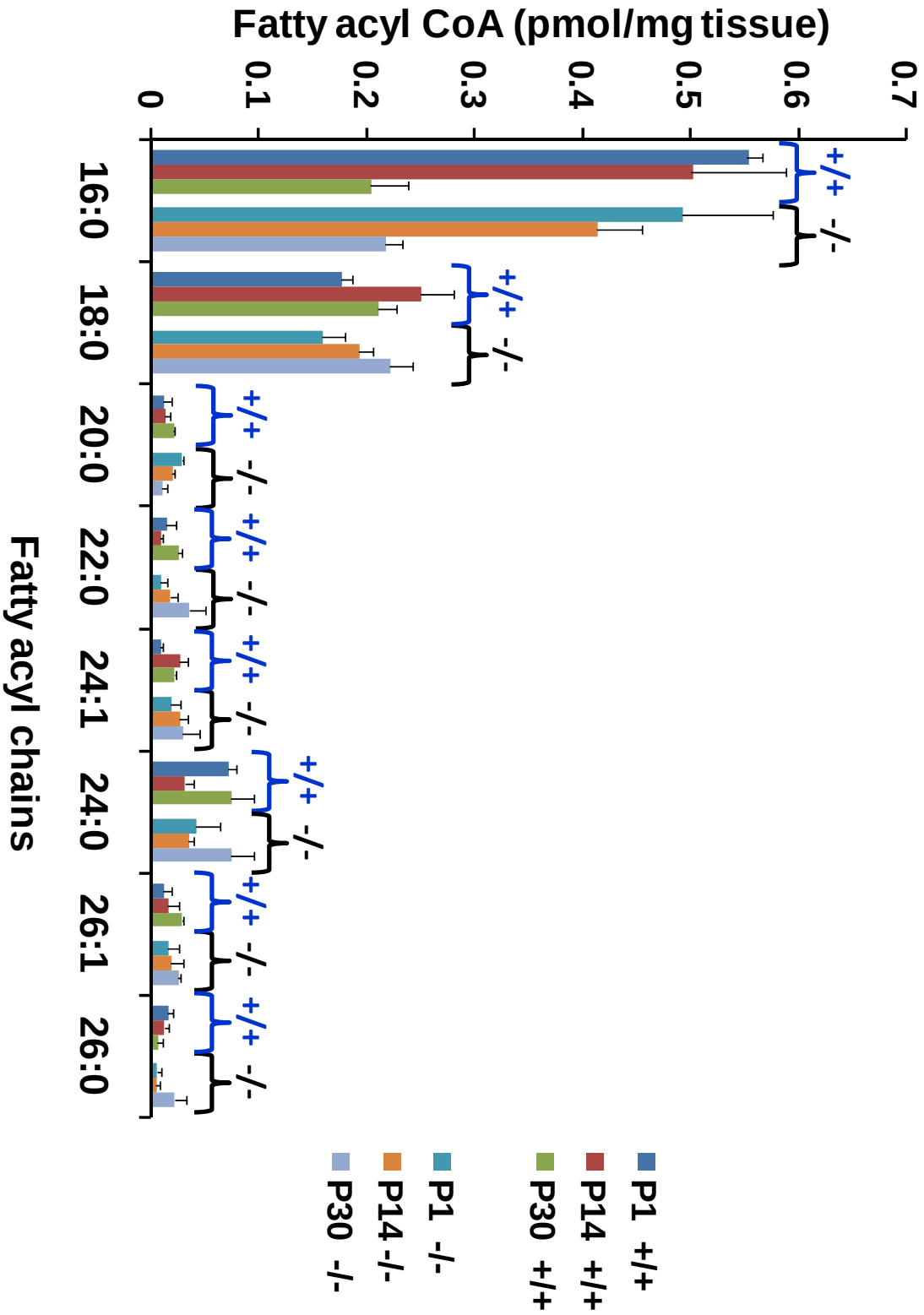

Figure 3.12. Fatty acyl-CoA profiles in livers derived from wild type mice (+/+, *blue*) and *CerS2* null mice (-/-, *black*) at ages (days).

3.4 Discussion

Since the initial molecular identification of *CerS1* (*uog1*) (10) as a ceramide synthase, considerable effort has been invested in characterizing the six members of this mammalian gene family. Most studies to date have focused on the acyl-CoA specificity of the proteins (10–12, 15). However, with the exception of one *in vitro* ceramide synthase assay reported in Mizutani et al. (12), *CerS2* has not been well characterized. We now rectify this situation and report the surprising results that *CerS2* mRNA is highly abundant, that *CerS2* displays a remarkable fatty acyl-CoA specificity, showing essentially no activity with C16-CoA, very low or no activity with C18-CoA, and less selectivity among longer chain fatty acyl-CoAs when assayed in cells in culture, but a C24 $\pm$ 2 specificity in the studies with *CerS2* null mice. Together, these results suggest important differences in both the biology of *CerS*, and in their biochemical modes of regulation.

The distinctiveness of *CerS2* from other *CerS* can also be ascertained from study of its genomic organization (Table 3.3). *CerS2* has a compact gene size, a low number of introns, short 5'- and 3'-UTRs, with a large percentage of surrounding chromosomal sequence containing CpG and Alu elements, and contains a low percentage of retrotransposon LINE-1s. Further, our collaborator has noted that *CerS2* is located within chromosomal regions that are replicated early within the cell cycle (I. Simon, Hebrew University of Jerusalem, Israel, personal communication). These genomic features are characteristic of a "housekeeping" gene; indeed, predictive analysis performed using multiple parameters (27–29) supports the possibility that the *CerS2* gene is a genuine

housekeeping gene (Table 3.3). Interestingly, no other *CerS* genes display these characteristics.

Table 3.3 *CerS2* has genomic features characteristic of a housekeeping gene.
Gene size and length of introns were calculated by examination of each gene using the UCSC genome browser. The presence or absence of Line-1 and Alu elements were analyzed in chromosomal regions 100,000 bp upstream and downstream using the RepeatMasker program that screens DNA for interspersed repeats and low complexity sequences. CpG elements in the same region were analyzed using the CpG report program, which searches for regions of 50 bp or longer with >50% GC content.

Gene	Species	Accession #	Gene	5'-UTR	3'-UTR	Intron	Line-1	Alu	CpG
			Length (bp)				*%*		
CerS1	Mouse	NM_138647	14,084	30	333	12,668	0.41	8.92	5.79
	Human	NM_021267	27,593	72	1,433	25,035	1.78	32.78	13.00
CerS2	Mouse	NM_029789	8,315	95	777	6,300	1.58	11.52	4.52
	Human	NM_181746	9,791	387	974	7,287	5.68	37.29	8.91
CerS3	Mouse[a]	DQ35808	57,667	7	0	56,545	12.91	1.66	2.27
	Human	NM_178842	144,325	424	2,300	140,432	24.39	8.70	4.78
CerS4	Mouse	NM_026058	32,254	88	1,977	29,007	34.07	2.44	1.84
	Human	NM_024552	53,046	280	309	51,272	3.38	50.26	10.83
CerS5	Mouse	NM_028015	36,924	136	629	34,914	0.57	6.99	6.59
	Human	NM_147190	36,774	13	326	35,483	7.32	1.96	6.60
CerS6	Mouse	NM_172856	249,732	79	2,694	245,804	12.89	1.71	1.08
	Human	NM_203463	253,782	69	1,065	249,797	1.43	9.56	1.06

[a] The *CerS3* mouse sequence is currently incomplete and the reported sequence does not include all UTRs.

Classically, a housekeeping gene is defined as a gene with consistent levels of expression from tissue to tissue and that encodes a protein that is generally involved in routine cellular metabolism. However, the advent of qPCR and microarray analysis has indicated that housekeeping genes can display considerable variation in expression levels in tissues and can respond to stimuli (30, 31).

The fact that *CerS2* fulfils many of the genomic criteria of a housekeeping gene does not necessarily mean that it is a housekeeping ceramide synthase. However, some of the intracellular signaling functions of ceramides have been ascribed to C16-ceramide (reviewed in Ref. 9), which, conspicuously, *CerS2* does not synthesize. The broad tissue distribution of *CerS2* might imply that ceramides synthesized by *CerS2* are intermediates in SL metabolism in most cells, whereas other *CerS*, which are found at lower expression levels and which synthesize a more restricted subset of ceramide acyl chains (i.e. *CerS5*, which synthesizes C16-ceramide (11), and *CerS1*, which synthesis in specific tissues under specific physiological conditions, or after certain stimuli, such as in apoptosis or cell proliferation (13, 32).

Indeed, our data imply that there are multiple ways to regulate *CerS* activity and expression, and to regulate levels of ceramides containing specific acyl chains. Thus, although there is a relatively good correlation between *CerS2* mRNA expression and levels of C20–26-ceramides, C20–26-SM and C20–26-HexCer in kidney, there is a remarkable difference between the acyl chain composition of SM and HexCer in liver, even though both tissues contain high levels C20–26-ceramide, and high levels of *CerS2* expression. Likewise, levels of C16-ceramide, C16-HexCer, and C16-SM are high in testis, even though expression of *CerS3* mRNA is highest in this tissue; *CerS3*

synthesizes mainly long chain ceramides, but perhaps also C16-ceramide (15). C18-ceramide and C18-SM levels are high in brain and skeletal muscle, which contains correspondingly high levels of *CerS1* mRNA (33), but HexCer contains mainly longer acyl chain ceramides in these tissues. This clearly demonstrates multiple levels of regulation of ceramide biosynthesis, which most likely also includes the availability of the co-substrate, fatty acyl-CoAs, subspecies-selective trafficking (because CERT, a protein involved in ceramide transport from the endoplasmic reticulum for SM synthesis in the Golgi apparatus (34), has a defined specificity toward different acyl chain ceramides (35)), and factors such as the degree to which ceramide remodeling may occur in at the Golgi apparatus, where ceramidases have been found (36). It is also possible that there is channeling of intermediates into specific ceramides and downstream SLs, in analogy to findings with *CerS1* (10), in which C18-ceramide was channeled into neutral glyco-SLs compared with acidic glyco-SLs (gangliosides) and SM.

The fatty acid chain specificity of *CerS2* was generally confirmed by analysis of the livers from *CerS2* null mice, but was somewhat narrower (i.e., only showing changes in C24 $\pm$ 2 carbons in chain length). This might be due to changes in other *CerS* in the cell culture experiments where *CerS2* was elevated by overexpression or decreased with siRNA. Indeed, in the *CerS2* null mice, C16-Cer and Sa levels were increased in *CerS2* null mice, and in other experiments if this laboratory (Ying Liu, personal communication), changing other aspects of sphingolipid biosynthesis has been found to induce *CerS1*. The differences might also be due to the types of fatty acyl-CoAs that are available, however, the analysis of the fatty acyl-CoAs in livers from *CerS2* null mice did not show that they lack C20-fatty acyl-CoA's (Fig. 3.12).

What are some of the additional issues that should be kept in mind when thinking about what might cause these changes in the backbone composition of sphingolipids (i.e., increases in C16- and decreases in C24 $\pm$ 2-Cer) when CerS2 is eliminated? There are a number of possibilities, for examples: (i) it has been noted that all CerS have similar Km values toward Sa (17), therefore, when one is eliminated, Sa will probably be utilized by the others until all are saturated with substrate (which may explain why Sa is elevated, too); (ii) there might be changes in fatty acid metabolism so that the amounts of the co-substrates change (for example, for palmitoyl-CoA to increase), however, this is unlikely since we did not observe differences in fatty acyl-CoA (Fig.3.12), (iii) it is possible that downstream enzymes that utilize C24-Cer are not able to accommodate alternative substrates (i.e., C16-Cer), so the latter pile up—this is unlikely because all of the sphingolipids that we have examined contain both long-chain and very-long-chain Cer, albeit often in varying ratios; (iv) it is possible that the knockout of *CerS2* and changing the types of sphingolipids leads to cell stress, which has been noted to induce C16-Cer production (38); and (v) it is possible that the change in sphingolipid composition affects the production of stress mediators such as interleukins and TNF-α by inflammatory cells, which have been found to induce C16-Cer production from SM by activation of ASMase (39, 40, 41). Indeed, liver cells have been one of the models where TNF-α increased C16-ceramide content. These should be explored in future studies of these *CerS2* null mice.

3.5 References

1. Merrill, A. H., Jr., Wang, M. D., Park, M., and Sullards, M. C. (2007) Trends *Biochem. Sci.* **32,** 457–468
2. Lahiri, S., and Futerman, A. H. (2007) *Cell Mol. Life Sci.* **64,** 2270–2284
3. Hannun, Y. A., and Obeid, L. M. (2002) *J. Biol. Chem.* **277,** 25847–25850
4. Futerman, A. H., and Hannun, Y. A. (2004) *EMBO Reps.* **5,** 777–782
5. Spiegel, S., and Milstien, S. (2003) *Nat. Rev. Mol. Cell. Biol.* **4,** 397–407
6. Hait, N. C., Oskeritzian, C. A., Paugh, S. W., Milstien, S., and Spiegel, S. (2006) *Biochim. Biophys. Acta* **1758,** 2016–2026
7. Schenck, M., Carpinteiro, A., Grassme, H., Lang, F., and Gulbins, E. (2007) *Arch. Biochem. Biophys.* **462,** 171–175
8. Ogretmen, B., and Hannun, Y. A. (2004) *Nat. Rev. Cancer* **4,** 604–616
9. Pewzner-Jung, Y., Ben-Dor, S., and Futerman, A. H. (2006) *J. Biol. Chem.***281,** 25001–25005
10. Venkataraman, K., Riebeling, C., Bodennec, J., Riezman, H., Allegood, J. C., Sullards, M. C., Merrill, A. H., Jr., and Futerman, A. H. (2002) *J. Biol. Chem.* **277,** 35642–35649
11. Riebeling, C., Allegood, J. C., Wang, E., Merrill, A. H., Jr., and Futerman, A. H. (2003) *J. Biol. Chem.* **278,** 43452–43459
12. Mizutani, Y., Kihara, A., and Igarashi, Y. (2005) *Biochem. J.* **390,** 263–271
13. Koybasi, S., Senkal, C. E., Sundararaj, K., Spassieva, S., Bielawski, J., Osta, W., Day, T. A., Jiang, J. C., Jazwinski, S. M., Hannun, Y. A., Obeid, L. M., and Ogretmen, B. (2004) *J. Biol. Chem.* **279,** 44311–44319
14. Lahiri, S., and Futerman, A. H. (2005) *J. Biol. Chem.* **280,** 33735–33738
15. Mizutani, Y., Kihara, A., and Igarashi, Y. (2006) *Biochem. J.* **398,** 531–538
16. Hirschberg, K., Rodger, J., and Futerman, A. H. (1993) *Biochem. J.* **290,** 751–757
17. Lahiri, S., Lee, H., Mesicek, J., Fuks, Z., Haimovitz-Friedman, A., Kolesnick, R. N., and Futerman, A. H. (2007) *FEBS Lett.* **581,** 5289–5294
18. Sullards, M. C., and Merrill, A. H., Jr. (2001) *Science's STKE* http://stke.sciencemag.org/cgi/content/full/OC_sigtrans;2001/67/pl1
19. Merrill, A. H., Jr., Sullards, M. C., Allegood, J. C., Kelly, S., and Wang, E. (2005) *Methods* **36,** 207–224
20. Yu, J., Novgorodov, S. A., Chudakova, D., Zhu, H., Bielawska, A., Bielawski, J., Obeid, L. M., Kindy, M. S., and Gudz, T. I. (2007) *J. Biol. Chem.* **282,** 25940–25949
21. Futerman, A. H. (2006) *Biochim. Biophys. Acta* **1758,** 1885–1892
22. Maceyka, M., Sankala, H., Hait, N. C., Le Stunff, H., Liu, H., Toman, R., Collier, C., Zhang, M., Satin, L. S., Merrill, A. H., Jr., Milstien, S., and Spiegel, S. (2005) *J. Biol. Chem.* **280,** 37118–37129
23. Mandala, S. M., Thornton, R., Galve-Roperh, I., Poulton, S., Peterson, C., Olivera, A., Bergstrom, J., Kurtz, M. B., and Spiegel, S. (2000) *Proc. Natl. Acad. Sci. U. S. A.* **97,** 7859–7864
24. Johnson, K. R., Johnson, K. Y., Becker, K. P., Bielawski, J., Mao, C., and Obeid, L. M. (2003) *J. Biol. Chem.* **278,** 34541–34547
25. Zondag, G. C., Postma, F. R., Etten, I. V., Verlaan, I., and Moolenaar, W. H. (1998) *Biochem. J.* **330,** 605–609

26. Parrill, A. L., Wang, D., Bautista, D. L., Van Brocklyn, J. R., Lorincz, Z., Fischer, D. J., Baker, D. L., Liliom, K., Spiegel, S., and Tigyi, G. (2000) *J. Biol. Chem.* **275,** 39379–39384
27. Eisenberg, E., and Levanon, E. Y. (2003) *Trends Genet.* **19,** 362–365
28. Ganapathi, M., Srivastava, P., Das Sutar, S. K., Kumar, K., Dasgupta, D., Pal Singh, G., Brahmachari, V., and Brahmachari, S. K. (2005) *BMC Bioinformatics* **6,** 126
29. Eller, C. D., Regelson, M., Merriman, B., Nelson, S., Horvath, S., and Marahrens, Y. (2007) *Gene (Amst.)* **390,** 153–165
30. Kouadjo, K. E., Nishida, Y., Cadrin-Girard, J. F., Yoshioka, M., and St-Amand, J. (2007) *BMC Genomics* **8,** 127–143
31. Lee, S., Jo, M., Lee, J., Koh, S. S., and Kim, S. (2007) *J. Biochem. Mol. Biol.* **40,** 226–231
32. Osawa, Y., Uchinami, H., Bielawski, J., Schwabe, R. F., Hannun, Y. A., and Brenner, D. A. (2005) *J. Biol. Chem.* **280,** 27879–27887
33. Becker, I., Wang-Eckhardt, L., Yaghootfam, A., Gieselmann, V., and Eckhardt, M. (2008) *Histochem. Cell Biol.* **129,** 233-241
34. Hanada, K., Kumagai, K., Yasuda, S., Miura, Y., Kawano, M., Fukasawa, M., and Nishijima, M. (2003) *Nature* **426,** 803–809
35. Kumagai, K., Yasuda, S., Okemoto, K., Nishijima, M., Kobayashi, S., and Hanada, K. (2005) *J. Biol. Chem.* **280,** 64488–64495
36. Xu, R., Jin, J., Hu, W., Sun, W., Bielawski, J., Szulc, Z., Taha, T., Obeid, L. M., and Mao, C. (2006) *FASEB J.* **20,** 1813–1825
37. Haynes, C. A., Allegood, J. C., Sims, K., Wang, E. W., Sullards, M. C., and Merrill, A. H., Jr. (2008) *J Lipid Res* **49**, 1113-1125
38. Eto, M., Bennouna, J., Hunter, O. C., Lotze, M. T., Amoscato, A. A. (2006) *Int J Urol.* **13,** 148-156
39. Schwandner, R., Wiegmann, K., Bernardo, K., Kreder, D., and Kronke, M. (1998) *J. Biol. Chem.* **273,** 5916–5922
40. Osawa, Y., Uchinami, H., Bielawski, J., Schwabe, R. F., Hannun, Y. A., and Brenner, D.A. (2005) *J. Biol. Chem.* **280,** 27879–27887
41. Gupta, S., Natarajan, R., Payne, S. G., Studer, E. J., Spiegel, S., Dent, P., and Hylemon, P. B. (2004) *J. Biol. Chem.* 279, 5821–5828
42. Laviad, E. L., Albee, L., Pankova-Kholmyansky, I., Epstein, S., Park, H., Merrill, A. H. Jr, Futerman, A. H. (2008) *J Biol Chem.* **283,** 5677-5684

CHAPTER 4

CERAMIDE SYNTHASE INHIBITION BY FUMONISIN B_1 CAUSES ACCUMULATION OF 1-DEOXYSPHINGANINE: A NOVEL CATEGORY OF BIOACTIVE 1-DEOXYSPHINGOID BASES AND 1-DEOXYDIHYDROCERAMIDES BIOSYNTHESIZED BY MAMMALIAN CELL LINES AND ANIMALS.

4.1 Introduction

Fumonisins (FB) cause diseases of horses, swine, and other farm animals and are regarded to be potential risk factors for human esophageal cancer (1) and, more recently, birth defects (2). Studies of this family of mycotoxins, and particularly of the highly prevalent subspecies fumonisin B_1 (FB_1) (reviewed in Refs. 1 and 2), have established that FB_1, is both toxic and carcinogenic for laboratory animals, with the liver and kidney being the most sensitive target organs (3, 4). Other FB are also toxic, but their carcinogenicity is unknown.

FB are potent inhibitors of ceramide synthase(s) (*CerS*) (5), the enzymes responsible for acylation of sphingoid bases using fatty acyl-CoA for *de novo* *s*phingolipid biosynthesis and recycling pathways (6). As a consequence of this inhibition, the substrates sphinganine (Sa) and, usually to a lesser extent, sphingosine (So), accumulate and are often diverted to sphinganine 1-phosphate (Sa1P) and sphingosine 1-phosphate (S1P), respectively (7), while the product N-acyl sphinganines (dihydroceramides), N-acyl sphingosines (ceramides, Cer), and more complex

sphingolipids decrease (5, 7). This disruption of sphingolipid metabolism has been proposed to be responsible for the toxicity, and possibly carcinogenicity, of FB_1, based on mechanistic studies with cells in culture (5, 7–9). This has been borne out by a number of animal feeding studies that have correlated the elevation of Sa in blood, urine, liver, and kidney with liver and kidney toxicity (4, 7, 10, 11).

Most of the mechanistic studies have focused on the accumulation of free Sa and other sphingoid bases, because these compounds are highly cytotoxic, although the large number of bioactive metabolites in this pathway make it likely that multiple mediators may participate (7, 9). Nonetheless, inhibition of serine palmitoyltransferase (SPT), the initial enzyme of *de novo* sphingolipid biosynthesis, reverses the increased apoptosis and altered cell growth induced by FB_1 treatment (12–19). Therefore, it is likely that these effects of FB_1 are due to the accumulation of cytotoxic intermediate(s) rather than depletion of downstream metabolites, because the latter also occurs when SPT is inhibited.

In studies of the effects of FB_1 on the renal cell line LLC-PK_1 (20) (R. Riley, unpublished observations), we have noted that in addition to the elevation of Sa and So, there is a large increase in an unidentified species that appears to be a sphingoid base. The evidence for this is because it is extracted by organic solvents, derivatized with ortho-phthalaldehyde (OPA), and eluted from reverse-phase liquid chromatography (LC) in the sphingoid base region. Herein we report: (i) the isolation and characterization of this novel sphingoid base as 1-deoxysphinganine (1-deoxySa); (ii) that its origin is the utilization of alanine instead of serine by SPT as well as that the N-acyl-derivatives of 1-deoxySa (1-deoxydihydroceramides (1-deoxyDHCer)) are normally found in mammalian

cells; (iii) that 1-deoxySa has cytotoxicity comparable to other sphingoid bases elevated by FB_1; (iv) that 1-deoxySa is not only elevated in cells in culture but also in tissues of animals exposed to dietary FB_1 and, therefore, might contribute to diseases caused by these mycotoxins; and (v) that the type of sphingoid base is affected dramatically by amino acid supplementation.

4.2 Experimental Procedures

4.2.1 Materials

Pig kidney epithelial cells (LLC-PK_1; CL 101), African green monkey kidney cells (Vero cells; CCL 81), and the human prostate cancer cell line (DU-145, HTB-81TM) were from the American Type Culture Collection (ATCC, Manassas, VA). The LY-B and LY-B-LCB1 cells were a generous gift from Ken Hanada (21). P53N5-W mice, 5–7-week-old, were purchased from Taconic Farms, Inc. (The P53N5 strain was derived originally from the C57BL/6 mouse strain).

FB_1 used in the in vitro studies was prepared and purified (>95% purity) as described in Meredith et al. (22) (establishing that the impurities were primarily other FBs and FB dimers) or for the experiments specified were purchased from Biomol (Philadelphia, PA). FB_1 used in the mouse feeding study was supplied by Dr. Marc Savard (Agriculture and Agri-Food Canada, Ottawa, ON, Canada). Myriocin was prepared as described in Riley and Plattner (23). Free sphingoid bases, sphingoid base 1-phosphates, and the internal standard mixture for sphingolipids (Sphingolipid Mixture II,

LM-6005) were purchased from Avanti Polar Lipids (Alabaster, AL) except for D-rythro-C16-sphingosine, which was from Matreya (Pleasant Gap, PA). 1-DeoxySa was initially synthesized by minor modifications of a recently developed method for the synthesis of So (24) and has subsequently become available commercially from Avanti Polar Lipids.

Dulbecco's phosphate-buffered saline (PBS), Hanks' balanced salt solution, and Minimal Essential Medium (MEM, Invitrogen catalogue no. 61100-061) were obtained from GIBCO Invitrogen. Eagles Minimal Essential Medium, Dulbecco's modified Eagle's medium (DMEM), Ham's F12, fetal calf serum (FCS), and trypsin/EDTA were obtained from ATCC. L-[U-^{13}C]Alanine, L-[U-^{13}C]serine, and [U-^{13}C]palmitic acid (all ≥98% purity) were purchased from Cambridge Isotope Laboratories, Inc. Preparative C18 bulk packing material (55–105 μm) was purchased from Waters (Waters Corp., Part No. WAT010001). Acetonitrile (Burdick&Jackson) and water (J. T. Baker) were high performance LC (HPLC) grade and formic acid (>95%; Sigma-Aldrich) and all other reagents and chemicals were of analytical grade or better and were from various commercial suppliers.

4.2.2 Cell Culture

LLC-PK$_1$ cells were grown and maintained in 25-cm^2 culture flasks containing DMEM/Ham's F12 (1:1) with 5% FCS at 37 °C and 5% CO_2. For experiments using confluent cultures of LLC-PK$_1$ cells, the cells were seeded at ~15,000 to 30,000 viable cells/cm^2 in 8-cm^2 dishes and then allowed to attach and grow to at least 90% confluence (3–5 days) prior to addition of test agents added directly to the media without addition of

fresh growth medium. For experiments measuring effects on rapidly proliferating cells, the LLC-PK_1 cells were seeded at ~2,500 viable cells/cm^2 in 8-cm^2 dishes and allowed to attach and grow for 2 to 3 days (until ~30% confluent) prior to addition of fresh growth medium containing the various test agents. The seeding density was chosen so that cell number in control cultures increased linearly over the entire experimental time course. Vero cells were grown and maintained in 25-cm^2 culture flasks containing Eagles MEM with 10% FCS at 37 °C and 5% CO_2. All experiments with Vero cells used rapidly proliferating cells that had been subcultured from confluent cultures at a 1:36 split ratio into 8-cm^2 dishes. This split ratio resulted in cultures that were ~30% confluent after 24 h. The DU-145 cells were grown in Eagles MEM and 10% FCS at 37 °C and 5% CO_2 as described in the technical literature from the ATCC. The LY-B and LY-B-LCB1 cells were cultured in medium containing DMEM/Ham's F12 (1:1) with 5% FCS at 37 °C and 5% CO_2, essentially as described in Ref. 21.

After treatments, cells were washed twice with ice-cold PBS, the dishes placed on ice, and cells removed from the surface of the dishes using a rubber scraper. The cells detached by scraping were collected in polypropylene tubes and pelleted by centrifuging at 4 °C. The PBS was removed, and the cells frozen at ~20 °C. Except where noted, cell extracts were normalized by protein amounts, which were determined by the Lowry method (25) and a commercially available kit (Pierce® BCA Protein Assay Kit, Thermo Scientific Pierce) using bovine serum albumin (BSA) as the standard.

4.2.3 Sphingolipid Extraction and Analysis

A number of independent methods were used to characterize the sphingolipids to provide confirmation of the findings, and the specific method is indicated in the text and figure legends: 1) Free sphingoid bases were extracted from the cells and quantified by high performance LC (HPLC) and fluorescent detection of the OPA derivatives using C20-sphinganine (C20 Sa) as an internal standard according to Riley et al. (26). 2) Free sphingoid bases and sphingoid base 1-phosphates were also analyzed (in experiments with proliferating and confluent cultures of LLC-PK_1 cells, Vero cells, and homogenates of mouse liver and kidney) by LC tandem linear-ion trap electrospray ionization mass spectrometry (LC ESI-MS/MS) using the method of Zitomer *et al*. (27) except that instead of extracting pulverized freeze-dried tissues, either fresh liver or kidney homogenates (10–20 mg/100 µl phosphate buffer) or cultured cells (50–100 µg protein) were extracted with C16-So and C17-S1P as internal standards. 3) Free sphingoid bases and N-acyl-derivatives were analyzed by minor modifications of published methods (28) to detect compounds with and without the 1-hydroxyl group based on their resolution by LC. For 1-deoxySa, the precursor ion *m/z* 286.4 and product ion *m/z* 268.4 (-H_2O) in positive ionization mode were followed. (Note: these overlap with ions from other sphingoid bases, such as d17:1; however, these compounds are resolved by LC as described below.) For N-acyl-1-deoxySa, the cell and tissue extracts were first scanned for precursors for *m/z* 268.4 to identify which N-acyl-derivatives were present. Then they were analyzed by LC ESI-MS/MS using multiple reaction monitoring with Q1 and Q3 set to pass the following precursor and product ions for the designated N-acyl-1-deoxySa. The abbreviations connote the sphingoid base, m18:0, and fatty acid chain length and

number of double bonds using standard nomenclature (28): 524.7/268.4 (m18:0/C16:0), 552.7/268.4 (m18:0/C18:0), 580.7/268.4 (m18:0/C20:0), 608.8/268.4 (m18:0/C22:0), 634.9/268.4 (m18:0/C24:1), 636.9/268.4 (m18:0/C24:0), 662.9/268.4 (m18:0/C26:1), and 664.9/268.4 (m18:0/C26:0). The LC ESI-MS/MS of the free sphingoid bases was conducted using reverse phase LC (Supelco 2.1 X 50 mm Discovery C18 column, Sigma) and a binary solvent system at a flow rate of 0.6 ml/min delivered by a Shimadzu LC-10 AD VP binary pump system coupled to an ABI 4000 QTrap (Applied Biosystems, Foster City, CA). The binary system began with equilibration of the column with a solvent mixture of 60% mobile phase A ($CH_3OH/H_2O/HCOOH$, 58/41/1, v/v/v, with 5mM ammonium formate) and 40% mobile phase B ($CH_3OH/HCOOH$, 99/1, v/v, with 5 mM ammonium formate), sample injection (typically in 50 µl of the same mixture), elution with this mixture for 1.3 min followed by a linear gradient to 100% B over 2.8 min, and then a column wash with 100% B for 0.5 min followed by a wash and re-equilibration with the original A/B mixture before the next run. The elution times were 2.1 min for C17 So (internal standard), 2.4 min for C18 So, 2.6 min for C18 Sa, and 2.8 min for C18-1-deoxySa, with all having baseline resolution.

The N-acyl-derivatives were analyzed by normal phase LC (Supelco 2.1 X 50 mm LC-NH_2 column) at a flow rate of 0.75 ml/min and an isocratic solvent system ($CH_3CN/CH_3OH/CH_3COOH/CH_3(CH_2)_3OH/H_2O$, 95/3/1/0.4/0.3, v/v with 5 mM ammonium acetate) delivered by a Perkin Elmer Series 200 MicroPump system coupled to a PE Sciex API 3000 triple quadrupole mass spectrometer (Applied Biosystems, Foster City, CA). Using these LC conditions, the 1-deoxydihydroceramides (1-deoxyDHCer) elute together at 0.3 min and are resolved from ceramides (Cer), which elute at 0.37 min.

The settings for the mass spectrometry were optimized for each category of compounds as described previously (28). Quantitation was based on spiking the original extract with the sphingolipid internal standard mixture from Avanti Polar Lipids and comparison of the areas for m18:0 with d17:0 (which were approximately the same based on comparison of d17:0 with synthetic m17:0) and for N-acyl-1-deoxySa, the C12-Cer internal standard . Therefore, although these are close approximations, absolute quantitation will require the availability of MS internal standards for these specific compounds. 4) High resolution accurate mass MS was conducted on an ABI Q-Star (Applied Biosystems, Foster City, CA) using samples in methanol infused via a TriVersa nanomate (Advion Biosciences, Ithaca, NY) using a D-chip at 1.5 kV and a gas pressure of 0.2 psi. A total of 30 scans were averaged.

To obtain sufficient quantity of the unidentified sphingoid base for chemical characterization, the free sphingoid bases were partially purified from thirty 75-cm^2 flasks of confluent cultures of LLC-PK_1 cells that had been treated with 35 μM FB_1 for 120 h. The cells were scraped and pooled in a single glass tube, and the free sphingoid bases were extracted and treated with 0.1 M KOH in methanol to decrease interference from glycerolipids as described by Riley et al. (26). The extracted sphingoid bases were dissolved in a small volume of CH_3CN:H_2O:HCOOH (49.5:49.5:1, v/v/v) and loaded on a minicolumn of preparative C18 packing material (5 mm X 60 mm) equilibrated with the same mobile phase. Free sphingoid bases were eluted by increasing the percentage of acetonitrile, and the fractions that were enriched in the unidentified sphingoid base were identified by LC linear ion trap-ESI-MS/MS, pooled, dried under nitrogen, and stored at ~80 °C for later analysis.

4.2.4 Analysis of Stable Isotope-labeled Sphingoid Bases using L-[U-^{13}C]Alanine and L-[U-^{13}C]Serine

Vero cells at ~30% confluence in 8-cm^2 culture plates were incubated in MEM (Invitrogen 61100-061 without serine or alanine) with 2% FCS and 7 amino acid supplements (with 16 dishes per supplement): (i) 100 μM L-serine (natural abundance ^{13}C) + 100 μM L-alanine (natural abundance ^{13}C), (ii) 100 μM L-serine + 100 μM L-[U-^{13}C]alanine, (iii) 100 μM L-serine + 300 μM L-[U-^{13}C]alanine, (iv) 100 μM L-serine + 500 μM L-[U-^{13}C]alanine, (v) 100 μM L-[U-^{13}C]serine + 100 μM L-alanine, (vi) 300 μM L-[U-^{13}C]serine + 100 μM L-alanine, and (vii) 500 μM L-[U-^{13}C]serine + 100μM L-alanine. After 24 h in culture, half of the dishes in each group were administered sterile FB_1 for a final concentration of 35μM. After 48 h of additional incubation, half of the dishes in each group were used for sphingolipid analysis and half for protein assays. This experiment was repeated twice. Analysis of the sphingolipids in the extracts included *m/z* for the ^{12}C-labeled products and the [^{13}C] masses of relevant compounds (mass of [^{12}C] parent ion + 2 mass units resulting from incorporation of 2 carbons from the L-[U-^{13}C]amino acid with the third ^{13}C-labeled carbon lost as $^{13}CO_2$).

4.2.5 Analysis of 1-DeoxySa and Metabolites in LY-B and LY-B-LCB1 Cells

These cell lines were plated in 100-mm culture dishes to ~50% confluence, and then new medium (a 1:1 mixture of DMEM and Ham's F12 media with 10% FCS) containing 0.1 mM [U-^{13}C]palmitic acid bound to fatty acid-free BSA (as a 1:1 molar complex) was added. After 24 h, the lipids were extracted as described previously (28)

and analyzed for the ^{12}C and ^{13}C-labeled sphingolipids (with the latter having a M + 16 or M + 32 *m/z* offset from the ^{12}C-species) using LC ESI-MS/MS as described above.

4.2.6 Effect of Sa and 1-DeoxySa on Cell Growth, Accumulation of Sphingoid Bases, Sphingoid Base 1-Phosphates, Cer, and 1-DeoxyDHCer

As described previously (8, 13), LLC-PK_1 cells were grown in 8-cm^2 dishes to ~30% confluence. Then Sa or 1-deoxySa was added as the 1:1 (mol/mol) complex with fatty acid-free BSA with or without addition of FB_1 (dissolved in water) at the concentrations described in the text. After 48 h, cell protein was measured (25) for the attached cells, which we have determined to be linearly related to cell number [μg protein = 1.63 + 3.29 X (viable cells X 10^{-4}), $r^2 = 0.96$, n = 53] (8). All experiments were conducted with DMEM/Ham's F12 plus 5% FCS. The effect of treatments on the detachment of cells was determined by collecting the medium and pelleting the detached cells for a separate analysis of the protein amounts. In earlier studies, we have shown that both FB_1 and free Sa inhibit cell growth and increase the number of detached cells, which are dead, based on uptake of trypan blue and lactate dehydrogenase release (8, 13, 15). A duplicate set of dishes (n = 3/treatment) was collected for determining changes in endogenous sphingoid bases, sphingoid base 1-phosphates, Cer, and 1-deoxyDHCer by LC-ESI-MS/MS as described previously.

The effects of 1-deoxySa and Sa on DU-145 cells were examined by culturing the cells to ~25–50% confluence in 24-well dishes, addition of the sphingoid base as a 1:1 (mol:mol) complex with fatty acid-depleted BSA (sterilized by filtration), incubation for

24 h, and then assessment of cell viability using the WST-1 Cell Proliferation Reagent (Roche Applied Science) following the manufacturer's instructions.

4.2.7 Analysis of 1-DeoxySa in Mice Fed FB_1

Upon receipt, mice were housed individually under conditions meeting the requirements of the Canadian Council for Animal Care. Similar to the FB feeding protocols described by Gelderblom *et al.* (29), male mice (n−10) received a modified AIN 76A diet supplemented with 0 –50 mg FB_1/kg for 26 weeks, and then were killed under isoflurane anesthesia by cardiac puncture. Liver and kidney tissues were removed as quickly as possible, flash-frozen in liquid N_2, and stored at ~80 °C until used for sphingolipid analysis.

4.2.8 Synthesis of N-Acyl-1-Deoxysphinganine

Two internal standards were synthesized for mass spectrometric characterization and evaluation of LC mobility: N-palmitoyl- and N-lignoceroyl-1-deoxysphinganine. Both were made by the coupling of the fatty acid using the N-hydroxysuccinimide ester. N-palmitoyl-succinimide was available commercially but it was necessary to synthesize the N-hydroxysuccinimide ester of lignoceric acid following the method described in ref. 41 and 42. Briefly, 0.4 mmol of lignoceric acid was added to a solution of N-hydroxysuccinimide (0.4 mmol) in 1.73 mL of dry ethyl acetate followed by the addition of 0.4 mL of 1 M dicyclohexylcarbodiimide in dichloromethane. The reaction mixture was left overnight at room temperature, then centrifuged and the supernatant was

transferred to a new tube. The pellet was washed using 1.7 mL of ethyl acetate and 0.4 mL of dichloromethane, centrifuged, and the supernatant was added to the first. After the solvent was removed by evaporation, the desired product was purified by recrystallization from ethanol. The purity of the crystallized product was verified by TLC as described in the cited references, and by mass spectrometry.

For the synthesis of N-lignoceroyl-1-deoxysphinganine, 34.8 μmol of 1-deoxySa (Avanti, AL) and 36 μmol of N-hydroxysuccinimide ester of lignoceric acid were dissolved in 4 mL of anhydrous tetrahydrofuran at room temperature for 18 hr. After drying by N_2, the sample was recrystallized from methanol. The purity was checked by TLC and mass spectrometry. The same procedure was used to make the N-palmitoyl-derivative.

4.2.9 Analysis of 1-DeoxySa in SPT1/2 cells with Amino Acid Supplementation

SPT1/2 cells were plated in 100-mm culture dishes to ~50% confluence, and then new medium (a 1:1 mixture of DMEM and Ham's F12 media with 10% FCS) containing 0.1 mM [U-^{13}C]palmitic acid bound to fatty acid-free BSA (as a 1:1 molar complex) was added. These cells were also treated with PBS (as a control), 10 mM L-serine or 10 mM L-alanine, and after 36 h, the lipids were extracted as described previously (28) and analyzed for the ^{12}C and ^{13}C-labeled sphingolipids (with the latter having a M + 16 or M + 32 *m/z* offset from the ^{12}C-species) using LC ESI-MS/MS as described above.

4.2.10 Analysis of 1-DeoxySa in SPT1/2 cells with 3-Phosphoglycerate dehydrogenase (PHGDH) and 3-Phosphoserine phosphatase (PSPH) siRNAs

SPT1/2 cells were grown in DMEM / F12 medium (1:1) (Gibco BRL, MD**)** supplemented with 10% fetal bovine serum (FBS), penicillin (100 U / ml) and streptomycin (100 μg /ml) at 37 °C in a humidified 5 % CO_2 atmosphere. For downregulation of PHGDH and PSPH, cells were plated in six-well plates at a density of 1.5 x 10^5 per well and were transfected with ON-TARGETplus SMARTpool siRNA targeting human PHGDH and PSPH and appropriate control siRNA (Dharmacon, Lafayette, CO)., using Oligofectamine (Invitrogen) according to the manufacturer's instructions. After 72 h, medium were changed to fresh costumed medium (DMEM/F12 medium and DMEM/F12 medium without Serine/Glycine) containing 5 μM FB_1 and 0.1 mM [U-^{13}C]palmitic acid bound to fatty acid-free BSA (as a 1:1 molar complex). After 24 hr incubation, the lipids were extracted as described previously (28) and analyzed for the ^{12}C and ^{13}C-labeled sphingolipids (with the latter having a M + 16 or M + 32 *m/z* offset from the ^{12}C-species) using LC ESI-MS/MS as described above.

4.3 Results

4.3.1 FB_1 Elevates Sa and a Mystery Peak in Cells

Shown in Fig. 4.1 are representative reverse phase HPLC profiles of the amounts of free sphingoid bases detected as the OPA derivatives from LLC-PK_1 cells that have or have not been exposed to 50 μM FB_1. As has been seen before (20), FB_1 treatment increased the amount of Sa by several fold within 6 h, and by orders of magnitude after

48 h. In addition, a new and unidentified peak with an elution time of 12.4 min is noticeable after 6 h of FB_1 treatment, and by 48 h, the area under the curve for this "mystery peak" is nearly half of that for Sa. Several additional peaks can be seen in the extracts from the cells treated with FB_1, but these were much smaller and were not examined further. This phenomenon was not limited to LLC-PK_1 cells because we have seen this mystery peak in almost every cell line that we have treated with FB_1 (which have included Vero cells, J774 cells, HT29 cells, HEK293 cells, *inter alia*) (data not shown).

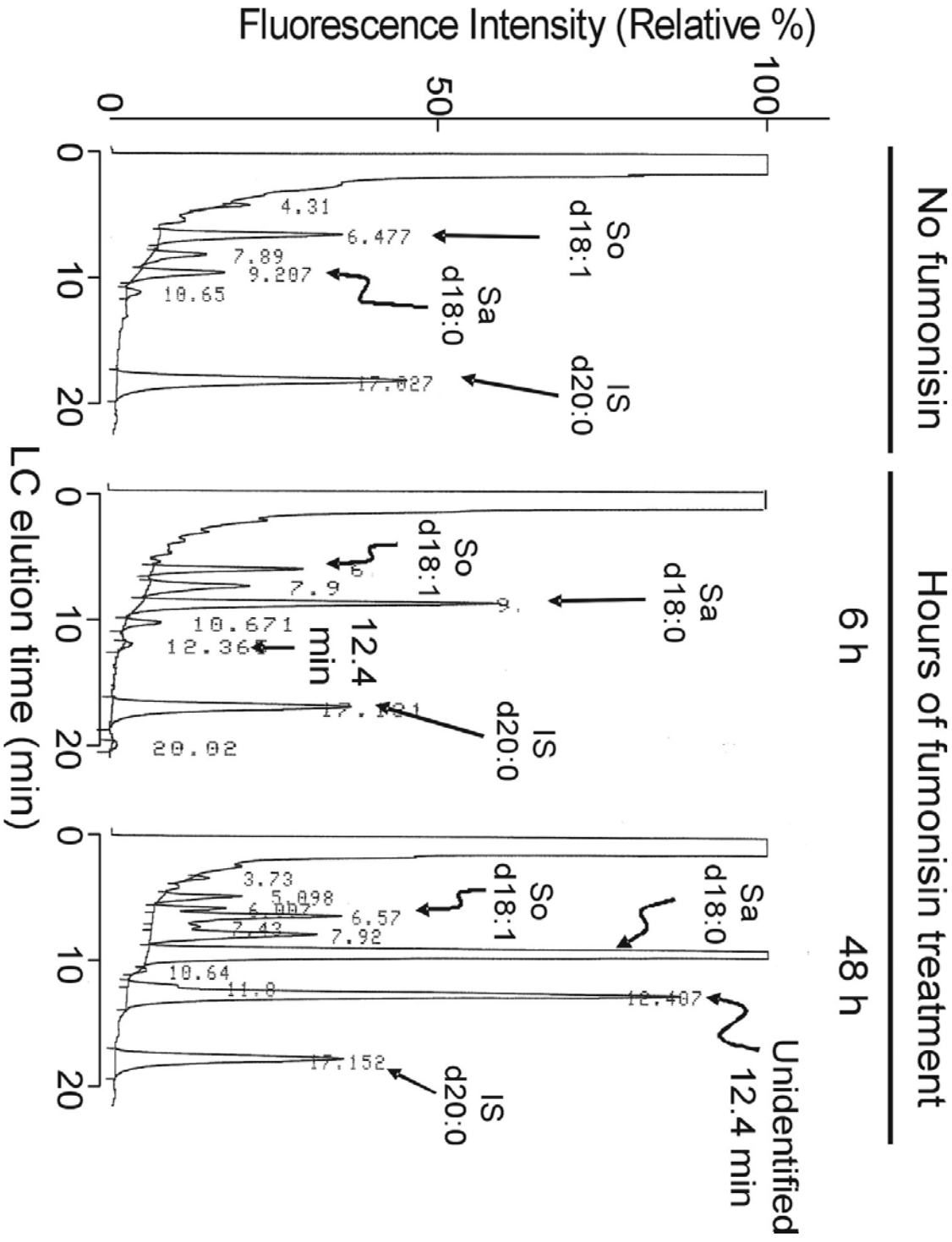

Figure 4.1. Representative chromatograms of lipid extracts from confluent cultures of LLC-PK_1 cells treated with FB_1 and analyzed by HPLC with fluorescence detection of the free sphingoid bases as the OPA derivatives using C20-Sa as an internal standard (26).

4.3.2 Evidence that the Mystery Peak Is an Unidentified Sphingoid Base

Based on its extraction by organic solvents, derivatization by OPA and LC mobility, it was likely that the mystery peak was a novel sphingoid base. If so, its production should be blocked by myriocin (also called ISP1), which is a potent inhibitor of SPT (30), the initial enzyme of *de novo* sphingolipid biosynthesis. As shown in Fig. 4.2A, treatment of LLC-PK_1 cells concurrently with myriocin blocked the FB_1-induced elevation of Sa and the unidentified sphingoid base. Furthermore, if the cells were first treated with FB_1 for 48 h to elevate Sa and this unidentified species (labeled as time 0 in Fig. 4.2B), followed by changing the cells to new medium minus FB_1 with or without myriocin, the presence of the SPT inhibitor greatly accelerated the decline in both free Sa and the unidentified sphingoid base (Fig. 4.2B). The slow decline in Sa and the unidentified compound in Fig. 4.2B when FB_1 was removed (but myriocin not added, hence, the cells continue to synthesize Sa *de novo*) suggests that partial inhibition of CerS persists for awhile. This is consistent with the results of an earlier study showing that the efflux of [U-^{14}C]FB_1 from LLC-PK_1 cells was rapid (half-life 2–3 min); however, a low but persistent amount of [^{14}C] remained associated with the cells (31).

Figure 4.2. Changes in free Sa (d18:0) and the unidentified sphingoid base (UnID) in confluent cultures of LLC-PK_1 cells treated with FB_1 and/or myriocin.

4.3.3 Identification of the Novel Sphingoid Base as 1-DeoxySa (m18:0)

The mystery peak was initially characterized by examining the partially purified extracts from LLC-PK_1 cells (as described under "Experimental Procedures") using a quadrupole-time of flight mass spectrometer (ABI QStar), which established that the samples contained an $[M+H]^+$ ion of *m/z* 286.3123 (data not shown), for which the only plausible formula within 10 ppm is $C_{18}H_{40}NO$ (286.3104), which is consistent with either a 1 or 3-deoxySa.

Using this information, lipid extracts from LLC-PK_1 cells treated with FB_1 for 25 h (Fig. 4.3A) and 120 h (Fig. 4.3B) were analyzed by reverse-phase LC ESI MS/MS monitoring for the $[M+H]^+$ ions for Sa (*m/z* 302.3, *light gray lines*) and deoxySa (*m/z* 286.3, *dark gray lines*). Consistent with the results in Fig. 4.1, Sa eluted first (identified by both precursor *m/z* 302.3 and the known product ion spectrum for Sa, shown in the inset in panel A) (32) followed by deoxySa (*m/z* 286.3), which was more highly elevated at 120 h (panel B) than at 25 h (panel A), consistent with the results shown in Fig. 4.2. Furthermore, the product ion spectrum for the *m/z* 286.3 peak was consistent with a compound with only one hydroxyl group (i.e. a deoxySa) because it displayed loss of one H_2O (*m/z* 268, inset in Fig. 4.3B), whereas Sa produced both single and double dehydration products (Fig. 4.3A).

It is also noteworthy that the product ion spectrum for the deoxySa lacks the *m/z* 60.1 product ion that is obtained from fragmentation between carbons 2 and 3 of the sphingoid base (see inset for Fig. 4.3A) because this implies that the deoxySa lacks the 1-hydroxyl group. To study this further, the MS^3 spectra were compared for synthetic 1-

deoxySa (Fig. 4.4A) and the compound partially purified from LLC-PK_1 cells (Fig. 4.4B), and both contained the *m/z* 44.0 ion predicted for fragmentation between carbons 2 and 3 of a 1-deoxySa. Therefore, based on these criteria, we tentatively identified the mystery peak produced by cells incubated with FB_1 as 1-deoxySa.

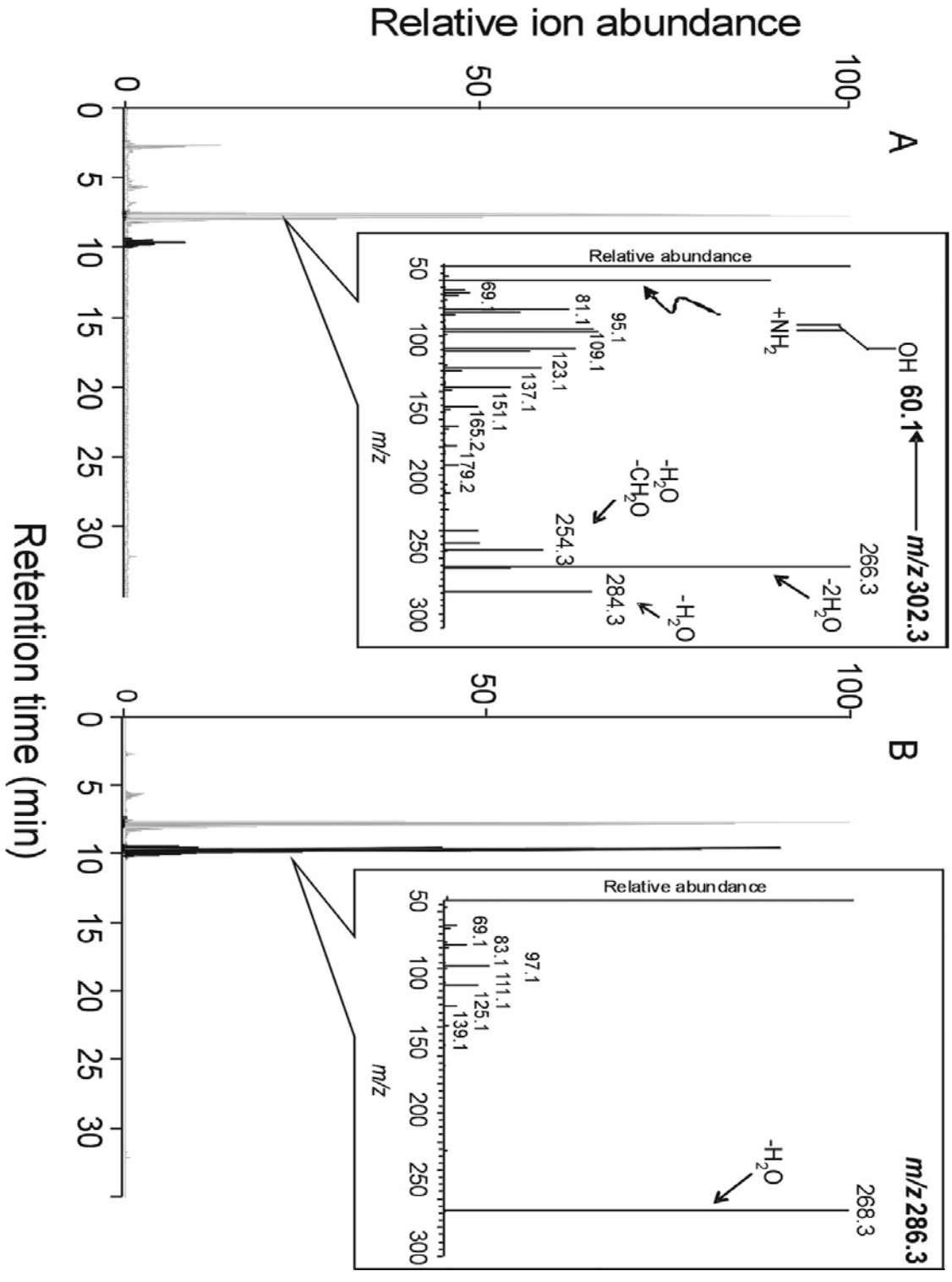

Figure 4.3. Liquid chromatography of LLC-PK_1 cell extracts after 24 h (A) and 120 h (B) of treatment with FB_1 with monitoring for Sa and a novel sphingoid base by electrospray ionization tandem mass spectrometry.

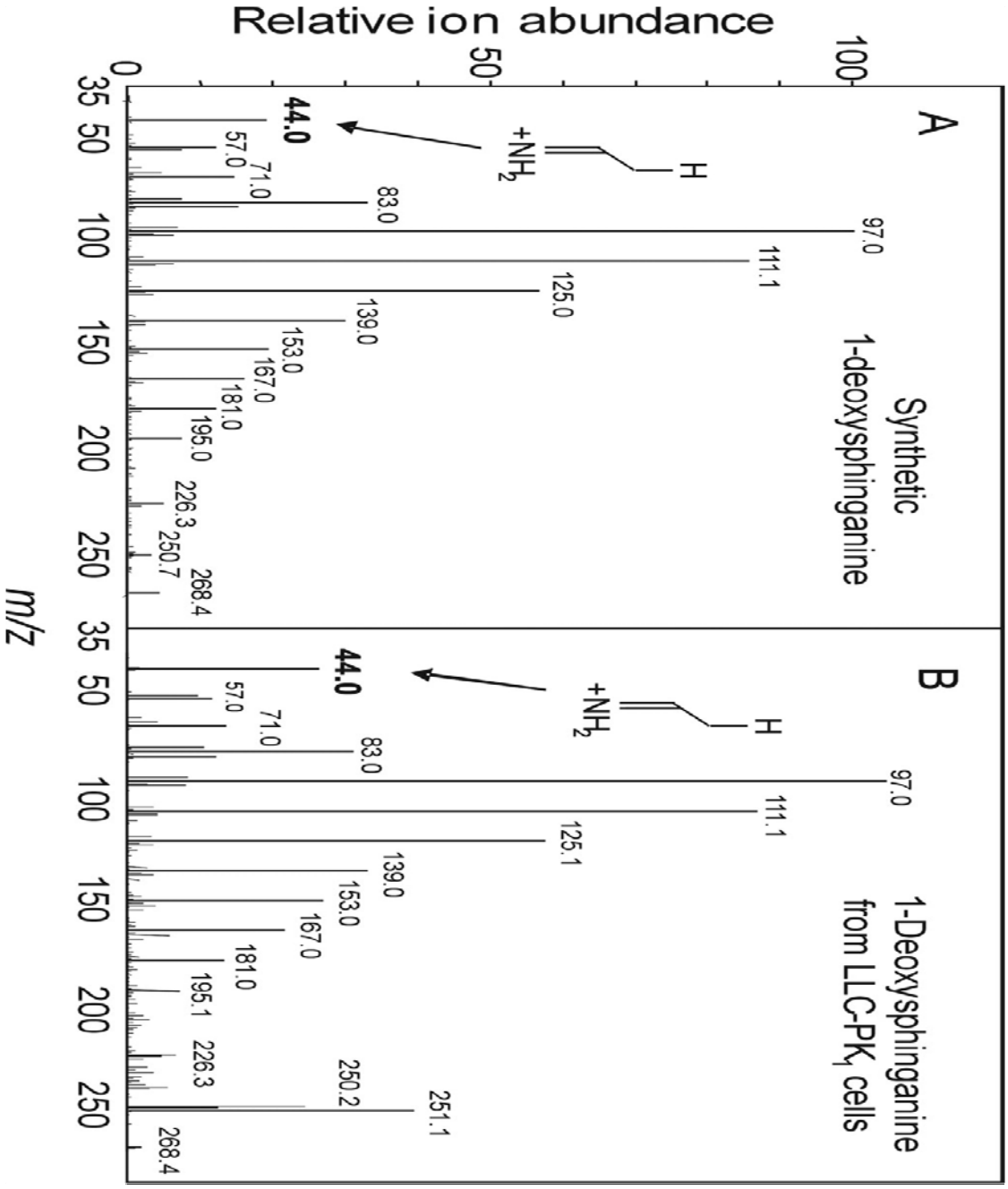

Figure 4.4. Comparison of the MS^3 spectra for synthetic 1-deoxySa (A) and the deoxySa isolated from LLC-PK_1 cell extracts (B) using the method of Riley et al. (26) with subsequent partial purification on a minicolumn of preparative C18 packing material (5 mm X 60 mm); fractions enriched in the deoxySa were pooled for analysis. The samples were introduced into a Thermo Electron Corporation LTQ XL via syringe pump and scanned across the mass range shown for the MS^3 fragments from the single dehydration product (*m/z* 268) of deoxySa. Highlighted is the distinctive fragment for 1-deoxySa at *m/z* 44.

4.3.4 Biosynthesis of 1-DeoxySa from [^{13}C]Alanine by SPT

Because myriocin blocked the formation of 1-deoxySa in FB_1-treated cells (Fig. 4.2), it is possible that this compound arises from the condensation of L-alanine with palmitoyl-CoA by SPT as illustrated in Fig. 4.5. To test this hypothesis, proliferating cultures of Vero cells were grown in medium supplemented with varying ratios of natural abundance and L-[U-^{13}C]alanine and L-[U-^{13}C]serine. Vero cells were chosen for this experiment because they produced easily detectable levels of the deoxySa in control cultures and were somewhat more resistant to the growth inhibitory effects of FB_1 in short term assays compared with the LLC-PK_1 cells (in addition, culture medium without serine or alanine is also available commercially for these cells). The appearance of stable isotope-labeled 1-deoxySa and Sa were monitored by MS analysis of the products that have been produced from these precursors by the M+2 isotope shift (since one ^{13}C of each amino acid is lost as $^{13}CO_2$ in the condensation reaction). The experiment was designed with addition of both precursors because serine and alanine can be metabolically interconverted (albeit, with many intermediate steps) as well as incorporated into the co-substrate palmitoyl-CoA. Therefore, addition of the unlabeled amino acid should diminish the contribution from such ^{13}C-labeled metabolites.

Figure 4.5. Structures of Sa and 1-deoxySa and a scheme for the biosynthesis of 1-deoxySa and its accumulation in cells exposed to FB_1. Also shown are the known sites of inhibition by FB_1 and myriocin.

As shown in Fig. 4.6A, essentially none of the L-[U-^{13}C]serine was incorporated into 1-deoxySa but was preferentially incorporated into [^{13}C]Sa (d18:0) and [^{13}C]Sa1P (d18:0-P) (Fig. 6A). Conversely, L-[U-^{13}C]alanine was preferentially incorporated into ^{13}C-labeled 1-deoxySa (m18:0) (Fig. 4.6B) versus Sa and Sa1P.

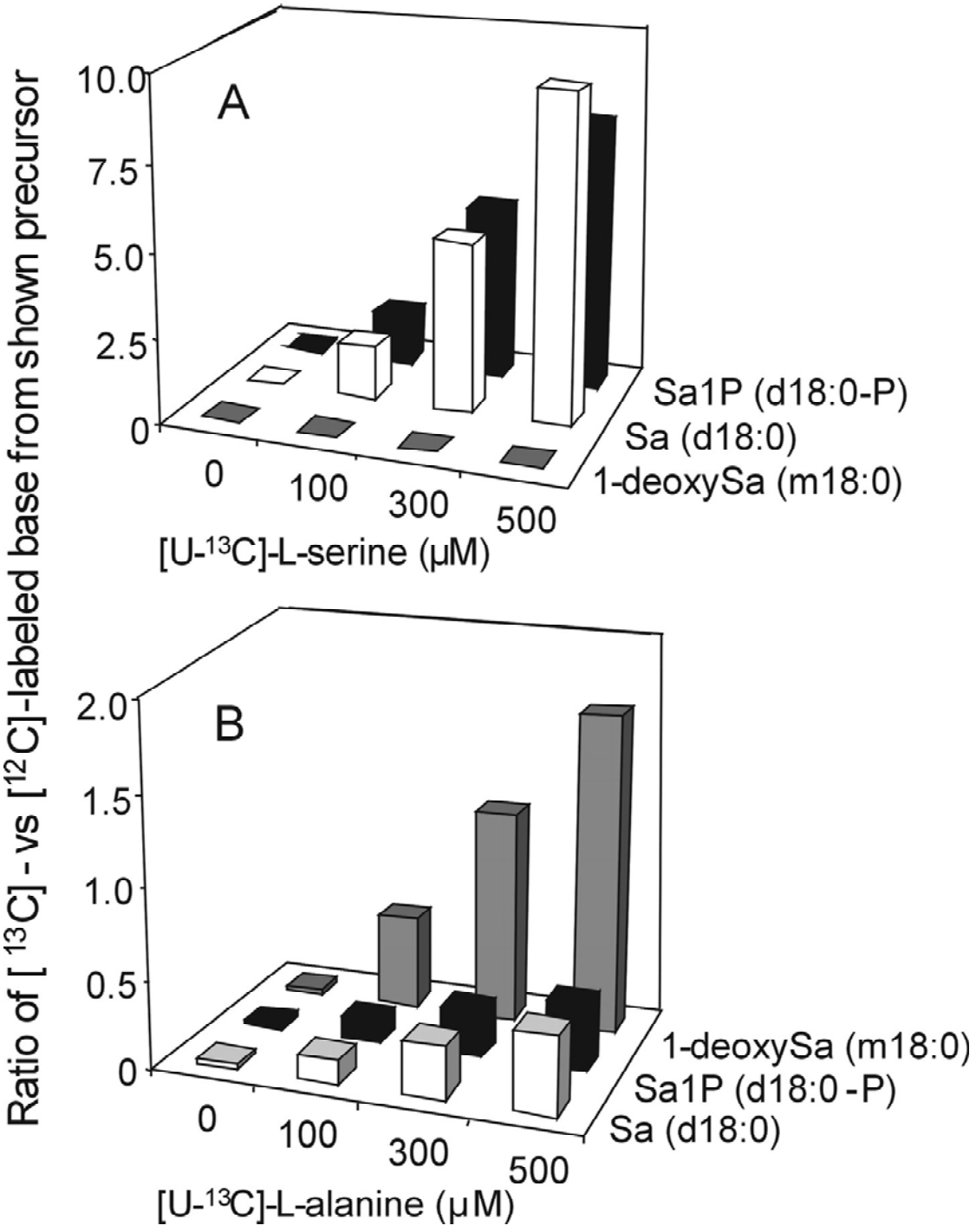

Figure 4.6. Incorporation of L-[U-^{13}C]alanine (A) and L-[U-^{13}C]serine precursors (B) into the 1-deoxySa (m18:0), Sa (d18:0), and Sa1P (d18:0-P) in Vero cells treated with 35 µM FB_1 for 48 h and grown in medium containing increasing concentrations of either L-[U-^{13}C]alanine- or L-[U-^{13}C]serine(100 µM to 500 µM).

The utilization of L-alanine by SPT is surprising, although there has been a recent report of 1-deoxySa in Hek293 cells that express the mutant form of SPTLC1 that is found in human sensory neuropathy type 1 (HSN1) as well as in lymphoblast lines derived from HSN1 patients (33). Therefore, to determine if SPT is responsible for 1-deoxySa biosynthesis in these cells, the incorporation of [U-^{13}C]palmitate into the sphingoid base backbones of sphingolipids and 1-deoxySa was analyzed using LY-B cells, a mutant Chinese hamster ovary (CHO) cell line with undetectable SPT activity due to mutation of the SPT1 subunit (21). As shown in Fig. 4.7, there was no detectable incorporation of ^{13}C-label into 1-deoxySa by LY-B cells with or without addition of FB_1 (panel A), but when LY-B-LCB1 cells were used (which have restoration of SPT activity by stable transfection with the cDNA for SPT1), there is a low but detectable incorporation of [^{13}C]palmitate into 1-deoxySa in these cells and robust biosynthesis and accumulation of 1-[^{13}C]deoxySa when the cells were treated with FB_1 (Fig. 4.7, panel A).

In addition, there was essentially no biosynthesis of Cer or N-acyl-1-deoxySa (1-deoxyDHCer) in LY-B cells (the first two rows of all of the graphs in Fig. 4.7, panel B). In contrast, LY-B-LCB1 cells incorporated [^{13}C]palmitate into the sphingoid base backbone (labeled ^{13}C-base in Fig. 4.7B) and into both the sphingoid base and fatty acid (labeled ^{13}C-base and fatty acid in Fig. 4.7B) of Cer (upper two graphs of Fig. 4.7B) and 1-deoxyDHCer (lower two graphs of Fig. 4.7B). In addition, FB_1 decreased the formation of these compounds, consistent with the accumulation of free 1-deoxySa (Fig. 4.7A). In this experiment, 1-deoxyDHCer was not a minor species because when all of the subspecies are summed, the amount of 1-[^{13}C]deoxyDHCer is about one-third of the amount of [^{13}C]Cer. However, the kinetics of Cer metabolism may be quite different

because 1-deoxyDHCer cannot undergo head group addition. Future studies will need to compare the relative rates of the two arms of the pathway. Nonetheless, all in all, these results establish that the formation of 1-deoxySa requires SPT, and when formed, most appears to be acylated unless FB_1 is present.

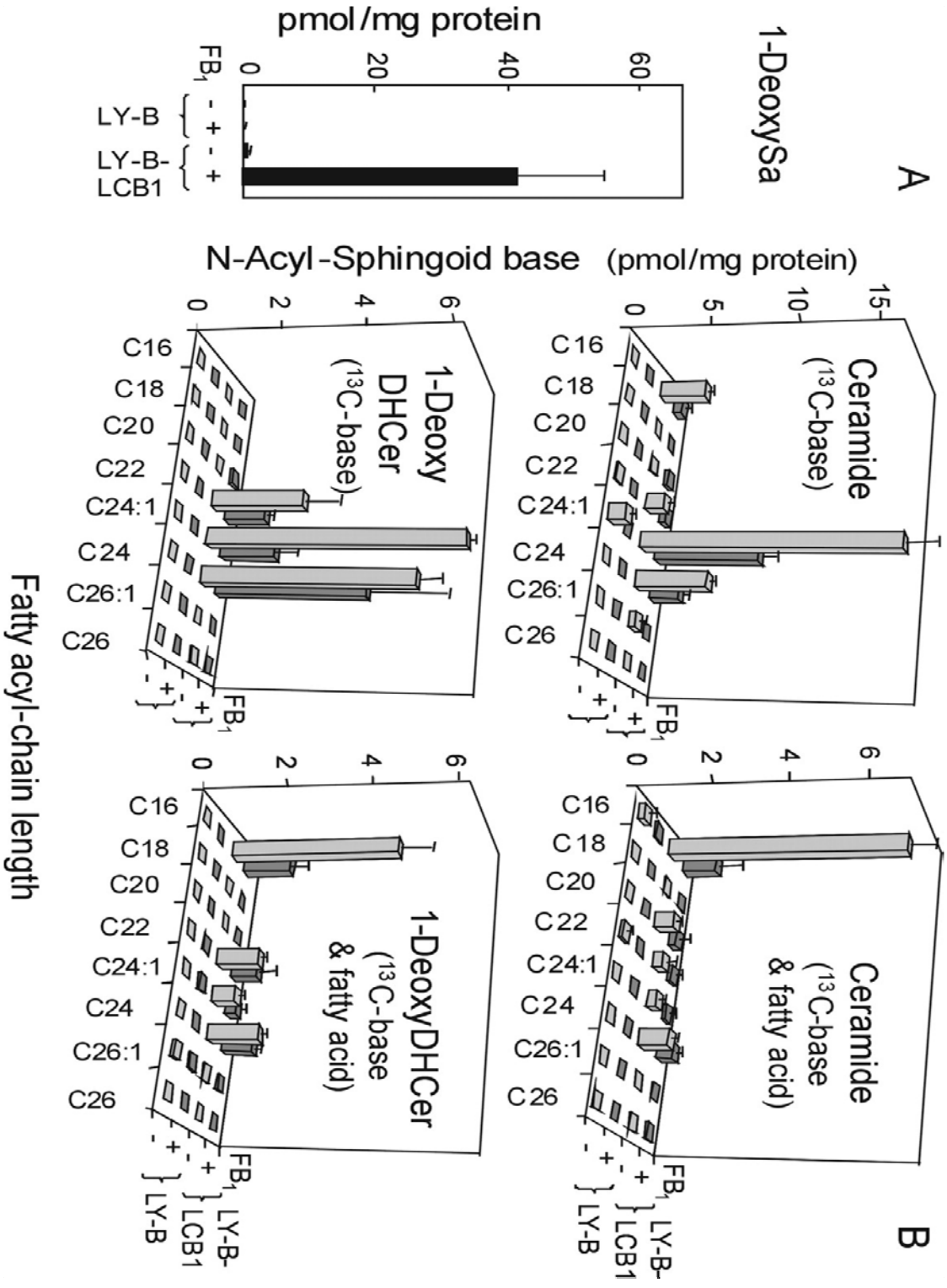

Figure 4.7. Absence of 1-deoxySa biosynthesis by LY-B cells and restoration of its formation in LY-B-LCB1 cells.

4.3.5 Endogenous 1-DeoxyDHCer and Acylation of Exogenously Added 1-DeoxySa in LLC-PK$_1$ Cells

The results with the LY-B and LY-B-LCB1 cells (Fig. 4.7) suggest that the accumulation of 1-deoxySa in LLC-PK$_1$ cells treated with FB$_1$ is due to interruption of the formation of endogenous 1-deoxyDHCer. To test this prediction, the amounts and types of 1-deoxyDHCer and Cer of LLC-PK$_1$ cells were analyzed by LC-ESI-MS/MS. As shown in Fig. 4.8A, control (no addition) LLC-PK1 cells contain on average 32 ± 4 pmol of 1-deoxyDHCer/mg protein that are distributed among a variety of fatty acyl chain lengths that are similar to that of the Cer in the cells (Fig. 4.8B). In addition, when the cells were treated with 10 μM 1-deoxySa and analyzed after 48 h, they contained highly elevated amounts of 1-deoxyDHCer (4,630 ± 396 pmol/mg protein) that were ~90% suppressed if the cells were also treated with 50 μM FB$_1$ (Fig. 4.8A). The addition of 10 μM 1-deoxySa did not appear to have any effect on the amount of ceramide (in contrast the FB$_1$ alone or in combination with 1-deoxySa caused a major suppression of Cer accumulation (Fig. 4.8B). Therefore, the findings with LLC-PK$_1$ cells were similar to what was observed with the LY-B-LCB1 cells, i.e. it appears that cells make a substantial amount of 1-deoxySa that is acylated to 1-deoxyDHCer.

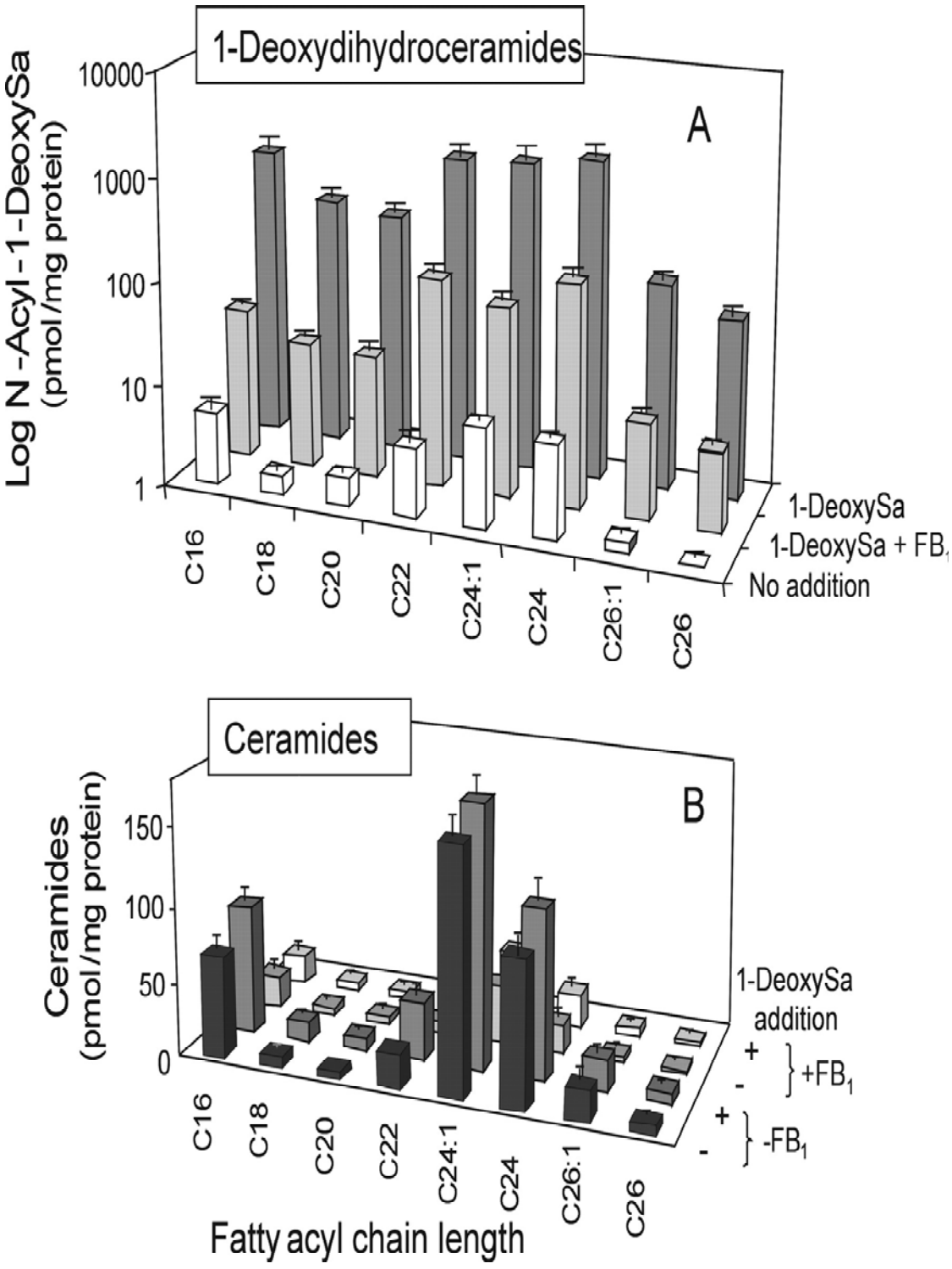

Figure 4.8. Endogenous N-acyl-sphingoid bases in LLC-PK$_1$ cells and after incubation of the cells with exogenously added 1-deoxySa with or without FB$_1$.

4.3.6 Cytotoxicity of 1-DeoxySa

The toxicity of free sphingoid bases (typically added to cells as the complex with BSA) is well known (13, 34), and has been demonstrated previously in LLC-PK_1 cells as a model for FB toxicity (13). The effect of 1-deoxySa on these cells was determined using the chemically synthesized compound as the BSA complex (Fig. 4.9A) versus the effect of a Sa-BSA complex. Both compounds are equally cytotoxic both in terms of decreased cell growth and an increased number of detached-dead cells based on their inability to exclude trypan blue (Fig. 4.9A, inset). Because 1-deoxySa has been reported to be cytotoxic for cancer cell lines (34), we also examined its effect on the human prostate cancer cell line DU-145 using the WST-1 cell proliferation assay. As shown in Fig. 4.9B, 1-deoxySa was several fold more potent (IC_{50} ~ 2 μM) than Sa (IC_{50} ~ 7 μM) for this cancer cell line.

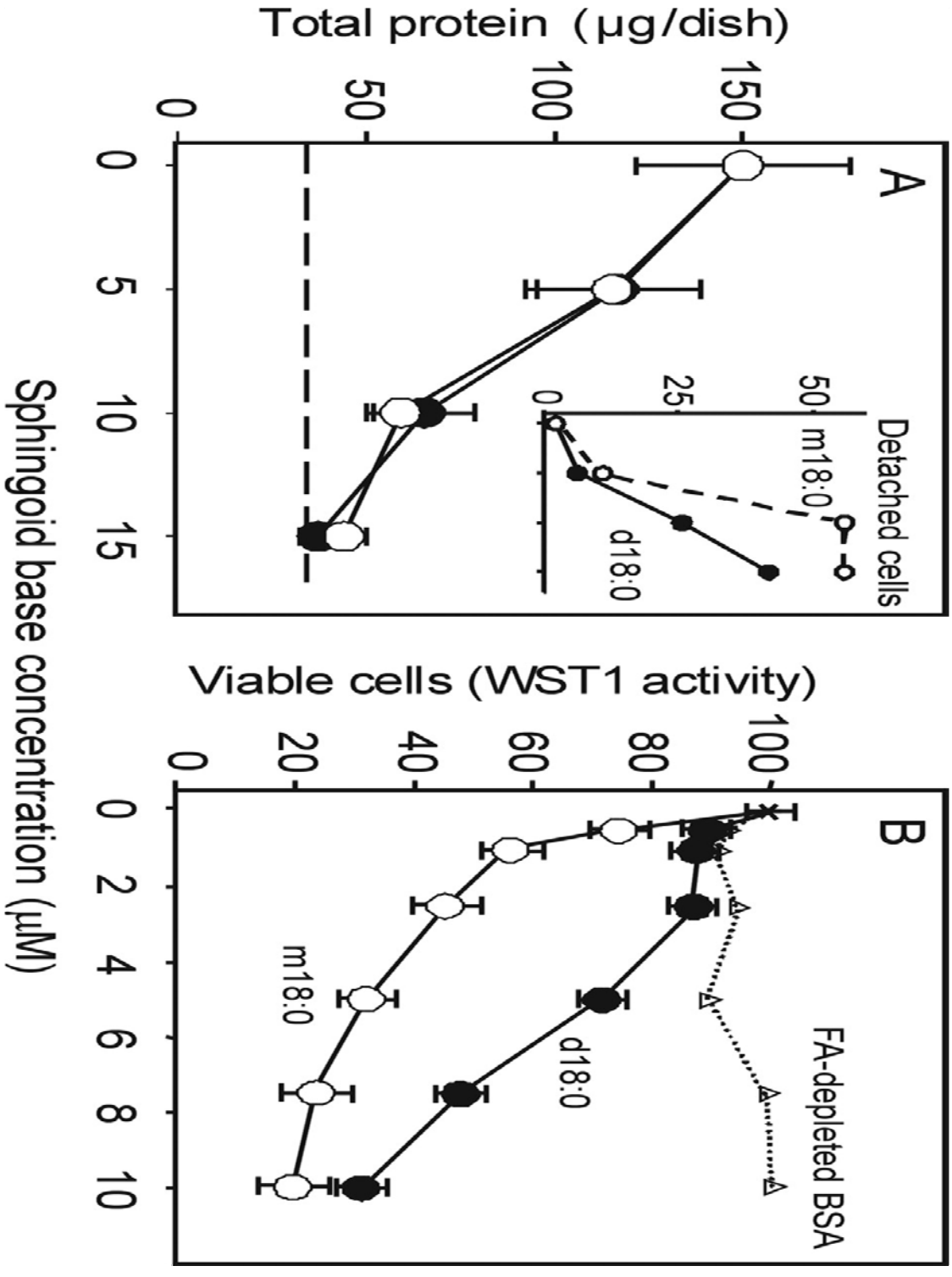

Figure 4.9. Effects of 1-deoxySa on LLC-PK$_1$ and DU-145 cells.

Analysis of the amounts of Sa, Sa1P, and 1-deoxySa in the LLC-PK_1 cells treated with the 10 μM Sa (labeled d18:0 in Fig. 4.10, A–C) revealed that although there was a significant increase in intracellular Sa (Fig. 4.10A) compared with the control, the species that was present in the highest amount (~4 nmol/mg protein, a 27-fold increase) was Sa1P (Fig. 4.10B), indicating that a large fraction of added Sa undergoes phosphorylation. 1-DeoxySa was also easily detected in the cells exposed to 10 μM 1-deoxySa (labeled m18:0 in Fig. 4.10C), and the amount was similar to the Sa in Sa-treated cells (~0.2 nmol/mg protein, Fig. 4.10, A and C). 1-DeoxySa was not detected in the control cells (nor cells treated with Sa), nor was it phosphorylated (data not shown), which is expected since sphingosine kinase adds a phosphate to the hydroxyl group at carbon position 1.

Co-administration of Sa and FB_1 caused large increases in Sa1P versus those obtained with addition of Sa or FB_1 alone (Fig. 4.10, B and E); in contrast, the cellular amounts of Sa, while highly elevated, were not significantly different (Fig. 4.10D). Treatment with FB_1 alone or FB_1 plus 10 μM Sa caused a small but significant elevation in 1-deoxySa compared with the control (labeled none); however, co-administration of 1-deoxySa and FB_1 caused a ~25-fold elevation in 1-deoxySa compared with treatment with only 1-deoxySa or FB_1 alone (Fig. 4.10, F and C). This provides further evidence that cells have a large capacity to acylate exogenous as well as endogenous 1-deoxySa. This was also evident in the large increase in 1-deoxyDHCer when 1-deoxySa was added to the cells (Fig. 4.10H).

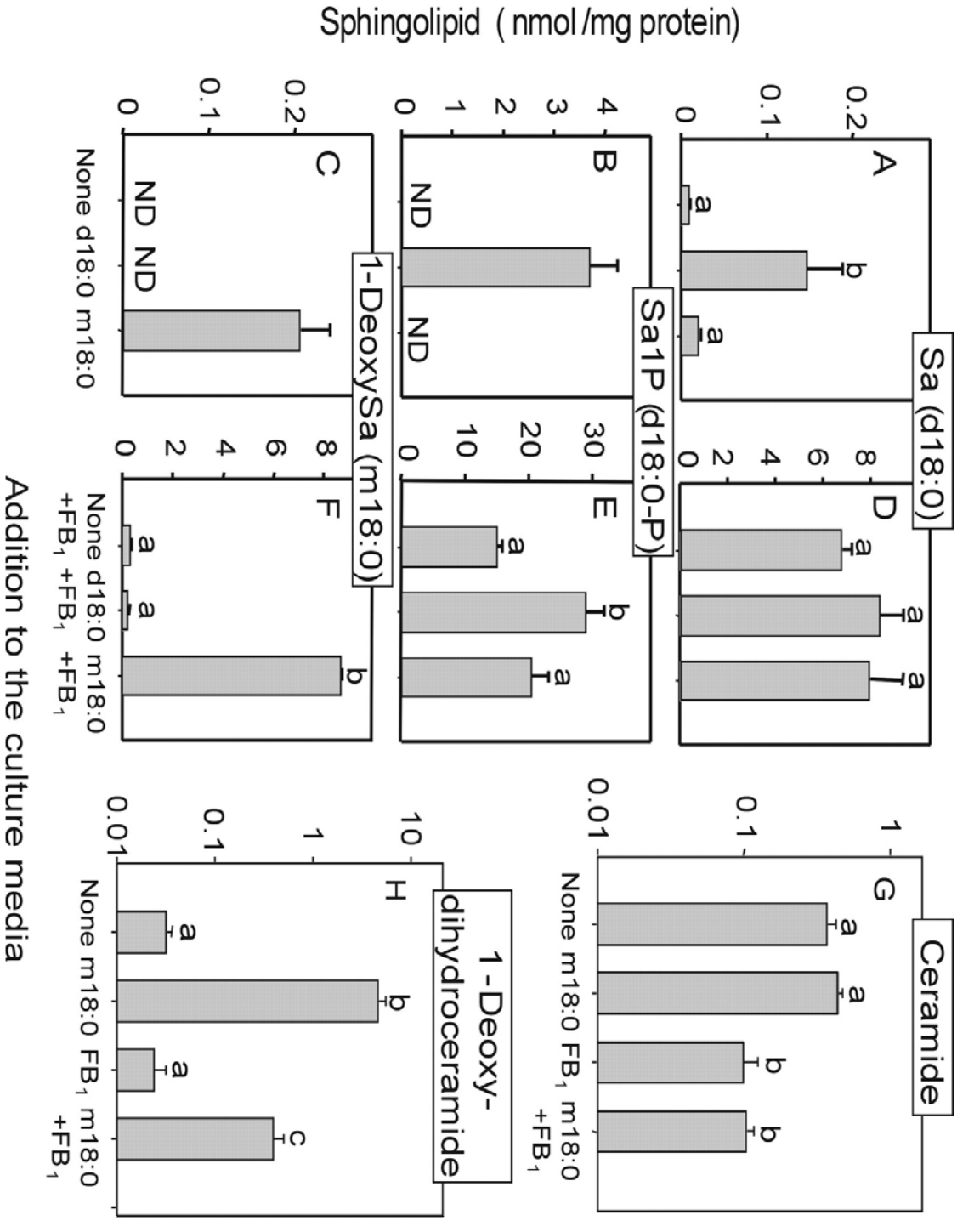

Figure 4.10. Accumulation of Sa (A and D), Sa1P (B and E), 1-deoxySa (C and F), and decrease in ceramide (G) and change in 1-deoxydihydroceramide (H) levels in LLC-PK_1 cells treated as described in Fig. 4. 9 but only at the 10 μM concentration of Sa and 1-deoxySa (A–C) or in combination with 50 μM FB_1 (D–F).

4.3.7 Analysis of 1-DeoxySa in Liver and Kidneys of Mice Fed FB_1

To determine if 1-deoxySa is elevated in the target organs for FB toxicity (liver and kidney for mice) (35), male P53N5-W mice were fed 50 ppm FB_1 in a modified AIN-76A diet for 6 months, and then lipid extracts from the livers and kidneys were analyzed by LC-ESI-MS/MS (Fig. 4.11). These analyses showed the typical elevation of Sa by FB_1 treatment for both organs (34), as well as the presence of substantial amounts of 1-deoxySa in the FB_1-fed mice, with the highest amount in liver. Given the similarity in the amounts of Sa and 1-deoxySa in liver, it is feasible that both compounds contribute to the toxicity of FB for this organ.

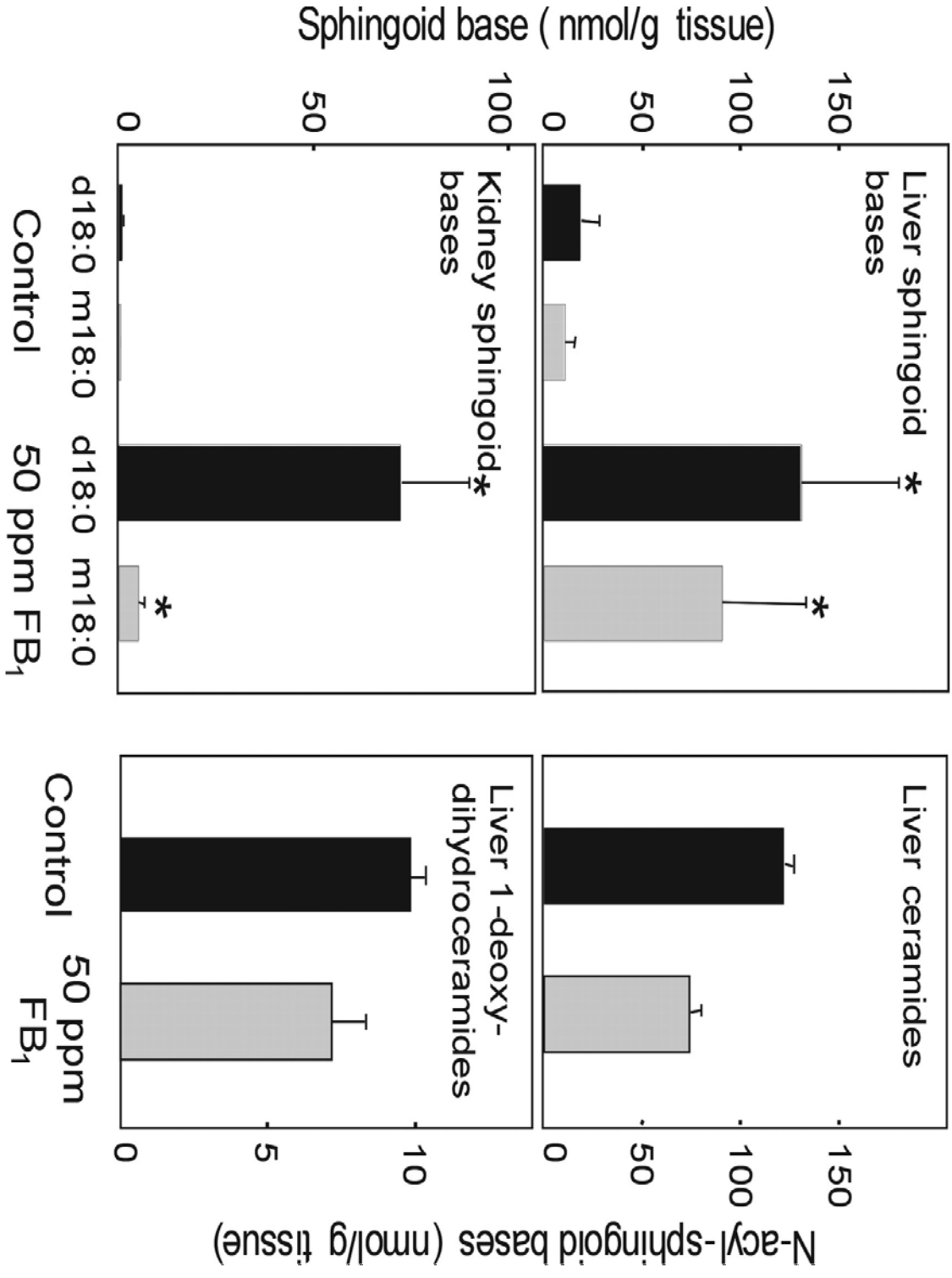

Figure 4.11. Accumulation of Sa (d18:0, *black bars*) and 1-deoxySa (m18:0, *gray bars*) in liver (*upper*) and kidneys (*lower*) of male P53N5-W mice fed a modified AIN-76A diet containing 0 ppm (*Control*) or 50 ppm FB_1 for 6 months.

4.3.8 Validation of LC ESI-MS/MS Conditions for N-Acyl-1-Deoxysphinganine

Up to this point in the studies, we have assumed that the acyl chain-length dependence of the ion yields for N-acyl-1-deoxysphinganines is similar to that for other dihydroceramides; however, this assumption should be validated before further studies are performed. To do so, C16:0- and C24:0-1-deoxyDHCer were synthesized (41.42) and examined by LC ESI-MS/MS to determine how the ionization parameters for the MRM pairs for these N-acyl-1-deoxySa are similar or different than the corresponding Cers. As the alkyl chain length increases, it will usually be increasingly difficult to fragment the compound (i.e., higher eV must be applied, see Tables 4.1), hence, varying the eV as larger N-acyl-sphingoid bases are being analyzed, for this example, the collision energies that produce the same signal for C12:0-Cer and C24:0-Cer are 35 eV and 50 eV, respectively. Because Cer and 1-deoxyDHCer showed a similar ionization efficiencies, the precursor/product ion *m/z*'s and associated parameters for MRM detection of individual molecular species of 1-desoxymethyldihydroceramide (1-desoxyMeDHCer) were applied by Cer and 1-deoxyDHCer parameters. However, the parameters for 1-desoxyMeDHCer should be confirmed or optimized using standards in the future study.

Using these conditions, standard curves for these N-acyl-1-deoxySa were obtained by graphing the integrated ion intensities for these analytes, the corresponding ceramides and C12-Cer, since it is available as an internal standard for sphingolipid quantitation (from Avanti Polar Lipids). Using optimized LC and ionization parameters, all of the subspecies displayed a linear signal response from 0.5 to 500 pmol, with little difference in cps due to the length of the fatty acyl-chain. The similarity in signal

response across all these chain lengths and for both Cer and 1-deoxyDHCer allows the C12:0 internal standard to be used for these species.

Table 4.1. API 3000 Mass Spectrometer Settings for ceramide, 1-deoxydihydrceramide and 1-desoxymethyldihydroceramide

	N-Acyl	Precursor ion *m/z*	Product ion *m/z*	DP (V)	FP(V)	CE (V)
Cer (d18:1)						
	C12:0	486.6	264.4	40	220	35
	C16:0	538.7	264.4	40	220	40
	C18:0	566.7	264.4	40	220	42.5
	C20:0	594.7	264.4	40	220	45
	C22:0	622.8	264.4	40	220	47.5
	C24:1	648.9	264.4	40	220	50
	C24:0	650.9	264.4	40	220	50
	C26:1	676.9	264.4	40	220	50
	C26:0	678.9	264.4	40	220	50
1-DeoxyDHCer (m18:0)						
	C16:0	524.7	268.4	40	220	40
	C18:0	552.7	268.4	40	220	42.5
	C20:0	580.7	268.4	40	220	45
	C22:0	608.8	268.4	40	220	47.5
	C24:1	634.9	268.4	40	220	50
	C24:0	626.9	268.4	40	220	50
	C26:1	662.9	268.4	40	220	50
	C26:0	664.9	268.4	40	220	50
1-DesoxyMeDHCer (m18:0)						
	C16:0	510.7	254.3	40	220	40
	C18:0	538.7	254.3	40	220	42.5
	C20:0	566.7	254.3	40	220	45
	C22:0	594.8	254.3	40	220	47.5
	C24:1	620.9	254.3	40	220	50
	C24:0	622.9	254.3	40	220	50
	C26:1	648.9	254.3	40	220	50
	C26:0	650.9	254.3	40	220	50

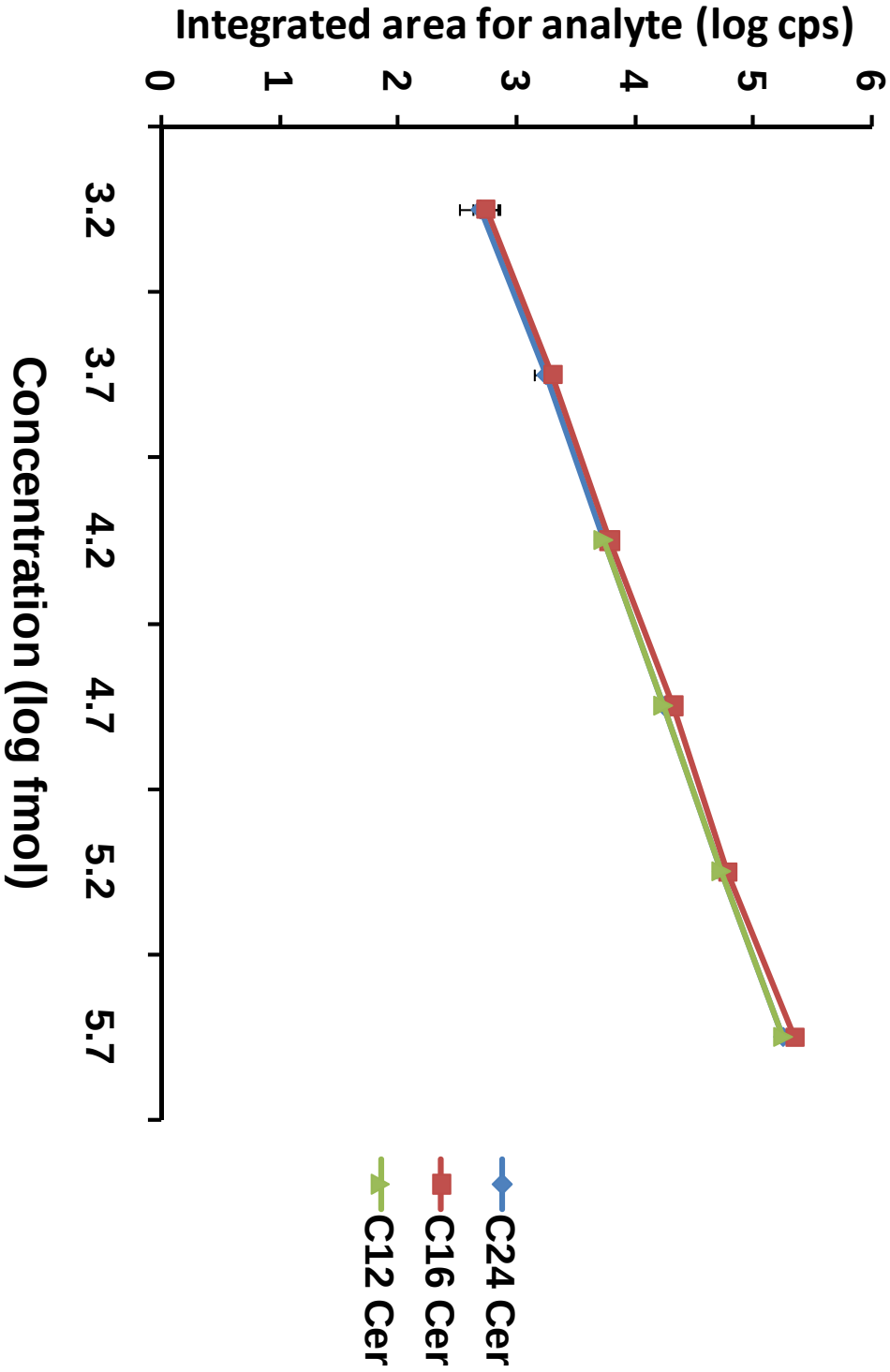

Figure 4.12. Signal response for ceramides using LC ESI-MS/MS.

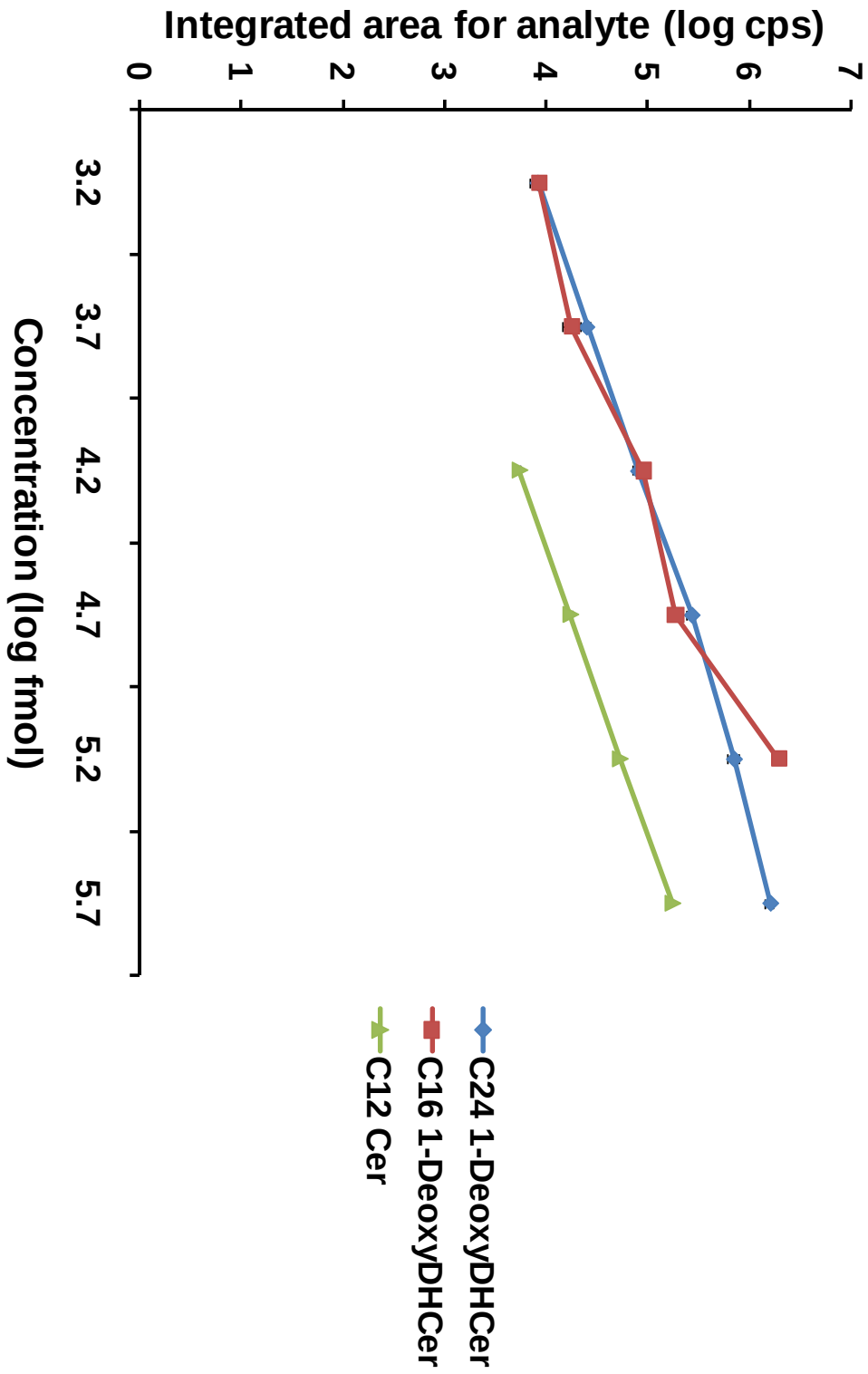

Figure 4.13. Signal response for 1-deoxydihydroceramides using LC ESI-MS/MS.

4.3.9 Re-examination of the Biosynthesis of Novel Sphingoid Bases upon Supplementation of the Culture Medium with Different Amino Acids

Since serine palmitoyltransferase is able to utilize L-alanine in addition to L-serine, it is possible that it can also utilize the smaller amino acid glycine. To investigate this hypothesis, RAW 264.7 cells were incubated with 10 mM of these three amino acids (individually) for 24 hr and the respective sphingoid bases were analyzed by LC ESI-MS/MS; 10 μM FB_1 was included in the incubation to inhibit acylation since that would necessitate the measurement of a large number of downstream metabolites and the goal of this study was to detect the sphingoid bases *per se*. As shown in Fig. 4.14 are elution profiles for the MRM pairs for sphinganine and 1-deoxySa and the predicted MRM pair for 1-desoxymethylsphinganine (1-desoxyMeSa) from a reverse phase column (note that the 1-deoxy sphingoid bases were analyzed as described in "Experimental procedures", but with the additional MRM pair of *m/z* 272.3/254.2 for 1-desoxyMeSa in Fig. 4.14D; the elution times were 2.6 min for Sa, 2.7 min for 1-desoxyMeSa and 2.8 min for 1-deoxySa, with all having baseline resolution.). It is evident from these results that the assignments of the sphingoid bases based on these MRM pairs not only agree with the order of elution from the column (i.e., for sphinganine to be most polar and elute first, followed by 1-desoxyMeSa, then 1-deoxySa) but also by the relative abundance of the fragment ions relative to the amino acids that has been added (e.g., 1-desoxyMeSa is higher with glycine supplementation, etc.). Thus, these LC ESI-MS/MS results further validate our hypothesis that L-serine (Fig. 4.14A), L-alanine (Fig. 4.14A B) and L-glycine (Fig. 4.14A C) are incorporated into the Sa, 1-deoxySa, and 1- 1-desoxyMeSa.

A number of other amino acid were also examined because they might also be envisioned to be utilized by serine palmitoyltransferase if the active site has room to accommodate an additional methylene (threonine and valine) or larger moieties (leucine and isoleucine). Because there are no standards for the predicted condensation products, it was assumed that at least one of the prevalent fragments would be the dehydration product, so the LC ESI-MS/MS analysis used MRM pairs for the intact parent ion and the dehydration product. None of these additions produced an increase in ion abundance at the respective MRM pair, therefore, it appears unlikely that these additional amino acids are utilized to produce additional categories of alternative sphingoid bases.

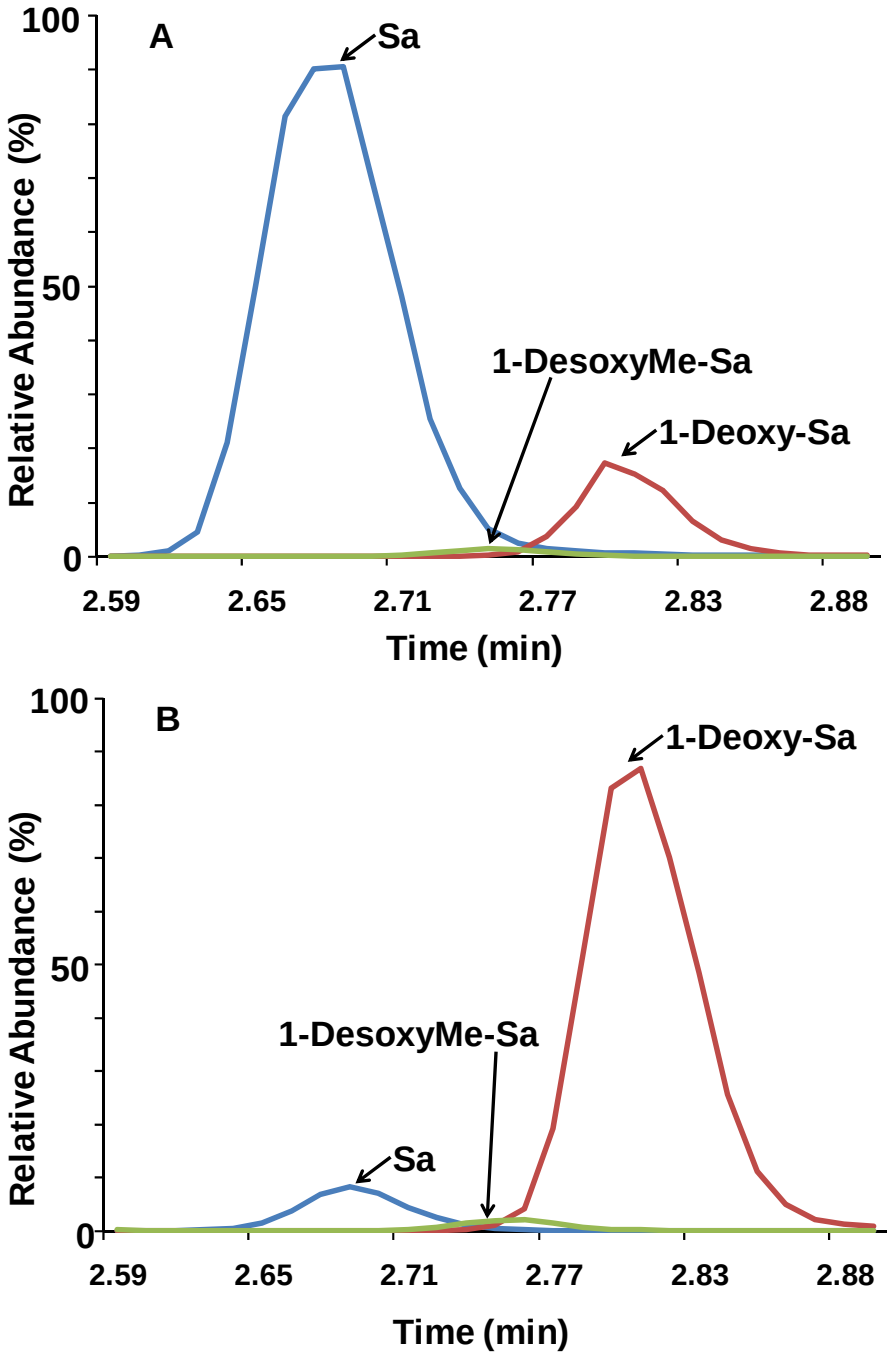

Figure 4.14 Re-examination of the biosynthesis of novel sphingoid bases upon supplementation of the culture medium with different amino acids. This is a plot of the relative ion abundance of the shown selected MRM pairs (D) at different elution times from reverse phase LC (Supelco 2.1 X 50 mm Discovery C18 column, Sigma) column. L-serine (A), L-alanine (B) and L-glycine (C) (each has 10 mM concentration) were supplemented in RAW 264.7 cells. (D) The structures of sphingoid bases and their fragmentations.

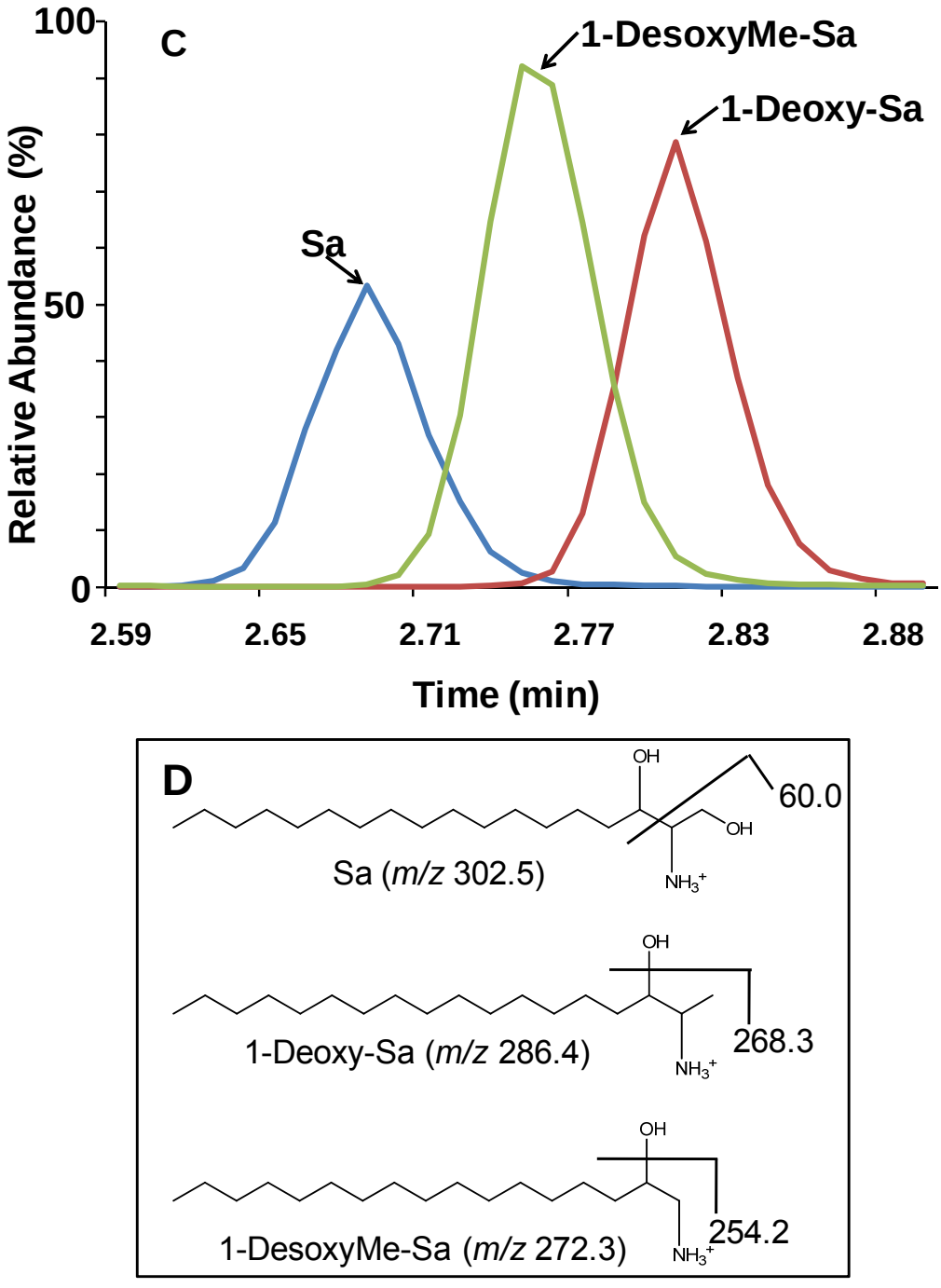

Figure 4.14 Re-examination of the biosynthesis of novel sphingoid bases upon supplementation of the culture medium with different amino acids (Continued). This is a plot of the relative ion abundance of the shown selected MRM pairs (D) at different elution times from reverse phase LC (Supelco 2.1 X 50 mm Discovery C18 column, Sigma) column. L-serine (A), L-alanine (B) and L-glycine (C) (each has 10 mM concentration) were supplemented in RAW 264.7 cells. (D) The structures of sphingoid bases and their fragmentations.

Table 4.2. ABI 4000 Mass Spectrometer Settings for Long Chain Bases and 1-deoxy-sphingoid bases

	Precursor ion *m/z*	Product ion *m/z*	DP (V)	CE(V)	CXP (V)
d17:1 So	286.4	268.3	40	15	15
d17:0 Sa	288.4	60.0	50	45	9
d18:1 So	300.4	282.4	40	19	16
d18:0 Sa	302.4	60.0	50	45	10
m18:0 1-DeoxySa	286.4	268.4	80	30	15
m17:0 1-DesoxyMeSa	272.3	254.2	70	20	15

4.3.10 The Types and Amounts of the Sphingoid Bases that Are Produced by Can Be Affected Substantially by Amino Acid Supplementation

In addition to determining if these three categories of sphingoid bases could be made by mammalian cells, we were interested in knowing if supplementation with one type would both increase the amounts of the respective sphingoid base and decrease the amounts of the alternatives—as would be predicted from them being made by a single enzyme. To conduct these studies, a stable isotope precursor was used to allow the newly made sphingoid bases to be distinguished from ones already in the cells, and [U-^{13}C]palmitate was selected because it is incorporated into all three types of sphingoid bases. As before, the products were analyzed by LC ESI-MS/MS and the cells that were selected for the experiment were a SPT1/2 cell line, which is derived from HEK293 cells that are stably overexpressing both of the subunits of serine palmitoyltransferase (SPT1 and SPT2) (as described in J. Wei *et al.,* in press). These experiments did not include FB_1 to block acylation because we were interested to see how the relative amounts of the downstream metabolites were also affected.

As shown in Fig. 4.15A, under basal conditions the amount of free [^{13}C]-Sa is very low, but detectable. As predicted addition of serine caused a large increase, although the SD was high (perhaps because Sa is also converted to Sa1P, and we did not control carefully for the possibility that this metabolite might turn over during the scraping of the cells before lipid extraction, etc). Interestingly, addition of both alanine and glycine caused increased [^{13}C]Sa—which is not surprising for glycine since it can be converted to serine by serine hydroxymethyltransferase.

In a similar way, a small amount of [^{13}C]1-deoxySa was produced when the cells were in control medium (ca. 4 pmol/mg protein), and the amount increased substantially ca. 10-fold upon alanine supplementation (Fig. 4.15B). It was also interesting that the production of [^{13}C]1-deoxySa was reduced when the cell medium was supplemented with serine or glycine (Fig. 4.15B). The amounts of [^{13}C]1-desoxyMeSa were below detection (estimated to be ~0 pmol/mg protein) in cells in control medium (and medium supplemented with serine or alanine), but increased substantially when glycine was added (Fig 4.15C).

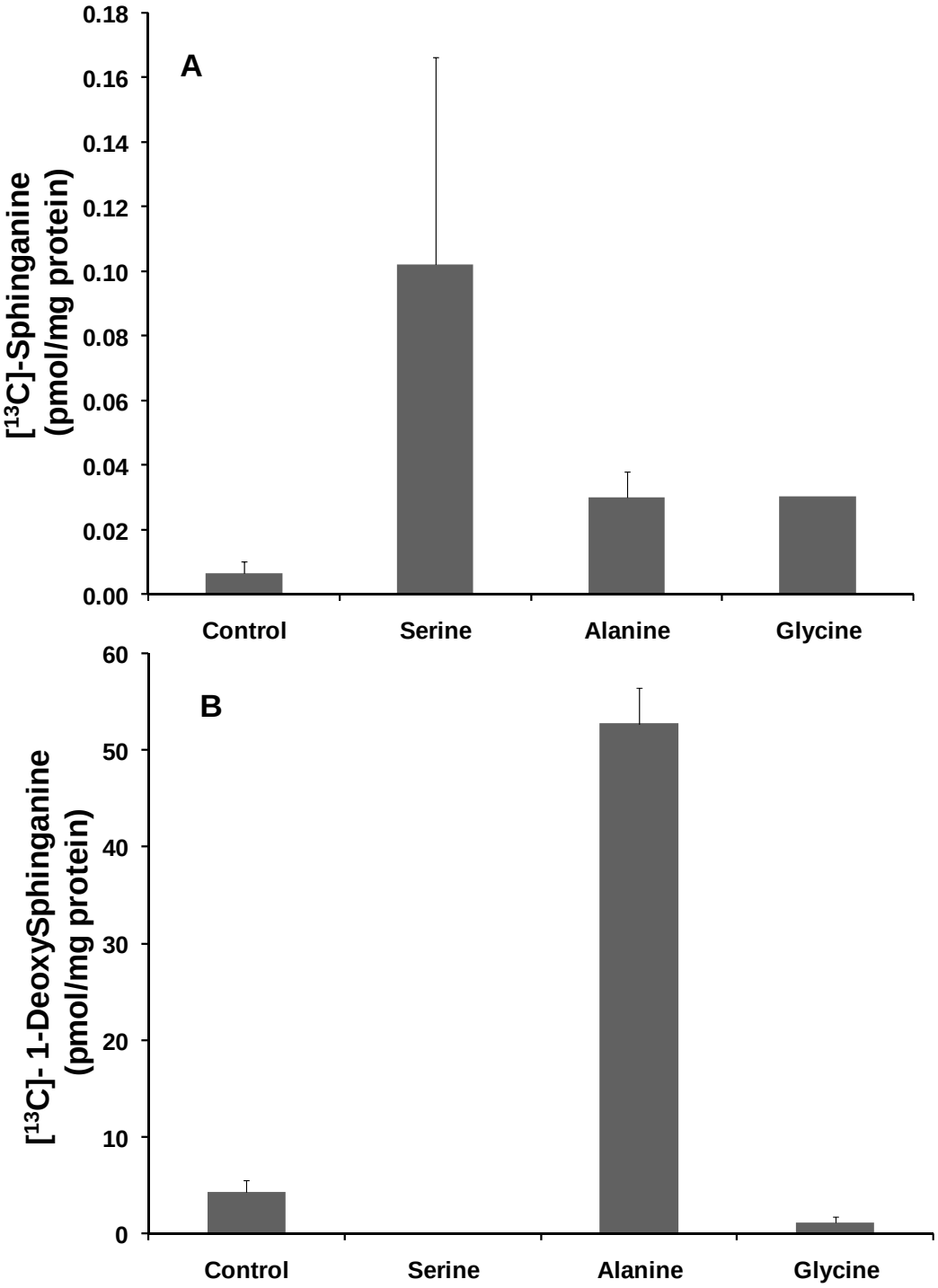

Figure 4.15. Evaluation of the biosynthesis of novel sphingoid bases upon supplementation of the culture medium with different amino acids. L-serine (A), L-alanine (B) and L-glycine (C) (each has 10 mM concentration) were supplemented with [U-^{13}C]palmitate in SPT 1/2 cells.

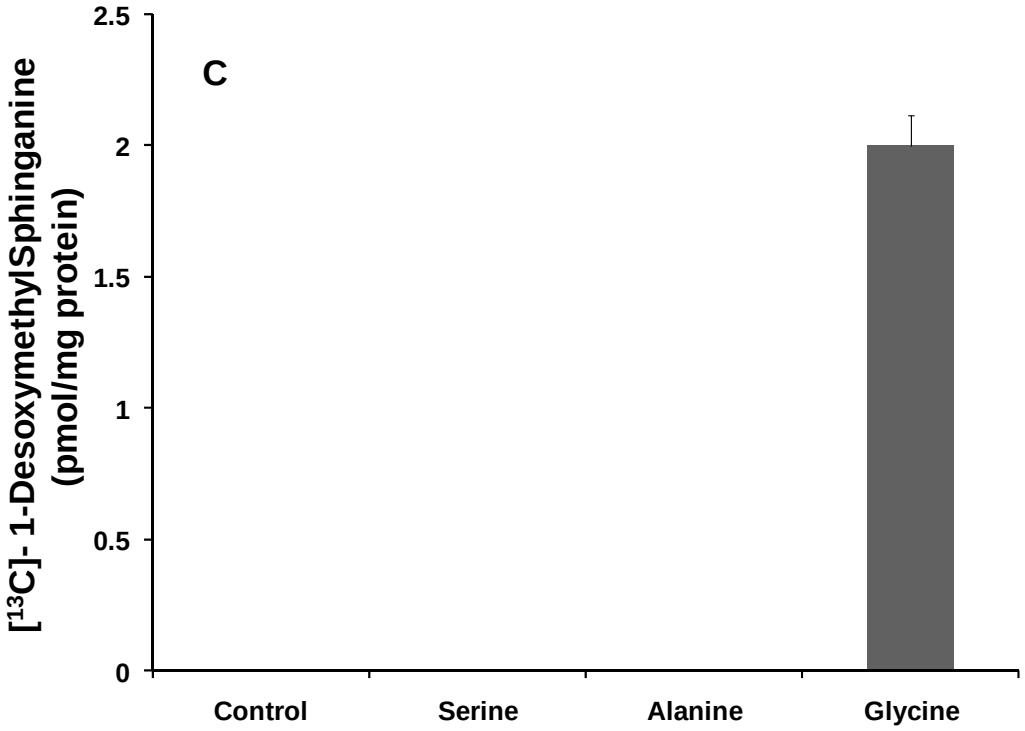

Figure 4.15. Evaluation of the biosynthesis of novel sphingoid bases upon supplementation of the culture medium with different amino acids (Continued). L-serine (A), L-alanine (B) and L-glycine (C) (each has 10 mM concentration) were supplemented with [U-^{13}C]palmitate in SPT 1/2 cells.

The types and amounts of N-acyl-metabolites were affected similarly. In these analyses, there are two categories of compounds that have been made from [^{13}C]palmitate, one group where the stable isotope was incorporated into the sphingoid base backbone but the N-acyl fatty acid did not contain ^{13}C (labeled ^{13}C-base in Fig. 4.16), and the other where both the sphingoid base and fatty acid contain ^{13}C (labeled ^{13}C-base and fatty acid in Fig. 4.17). The species with a sphinganine backbone are shown in the upper two graphs of Fig. 4.16 and 4.17, the ones for 1-deoxySa are in the middle two graphs of Fig. 4.16 and 4.17, and for 1-desoxyMeSa, the lower two graphs of Fig. 4.16 and 4.17. Serine

addition led increased the formation of [^{13}C]Cer compounds; alanine addition elevated [^{13}C]1-deoxyDHCers; and glycine addition elevated [^{13}C]1-desoxymethylDHCers. The apparent elevation of ^{13}C-labeled 1-desoxyMeDHCer upon alanine supplementation is likely to be an artifact because the MRM for the ^{13}C-labeled 1-desoxyMeDHCer shares with [^{13}C]1-deoxyDHCer. Therefore LC ESI-MS/MS conditions for 1-desoxyMeDHCer and its ^{13}C-labeled forms should be improved. One of the additionally interesting observations from this experiment is that the chain length subspecies for 1-deoxyDHCer are predominately C18, C22, C24:1 and C24 subspecies (not C16, as often seen with sphinganine), which might indicate that this compound is better utilized by CerS1 and/or CerS2, which are responsible for forming those categories of ceramides (43-45).

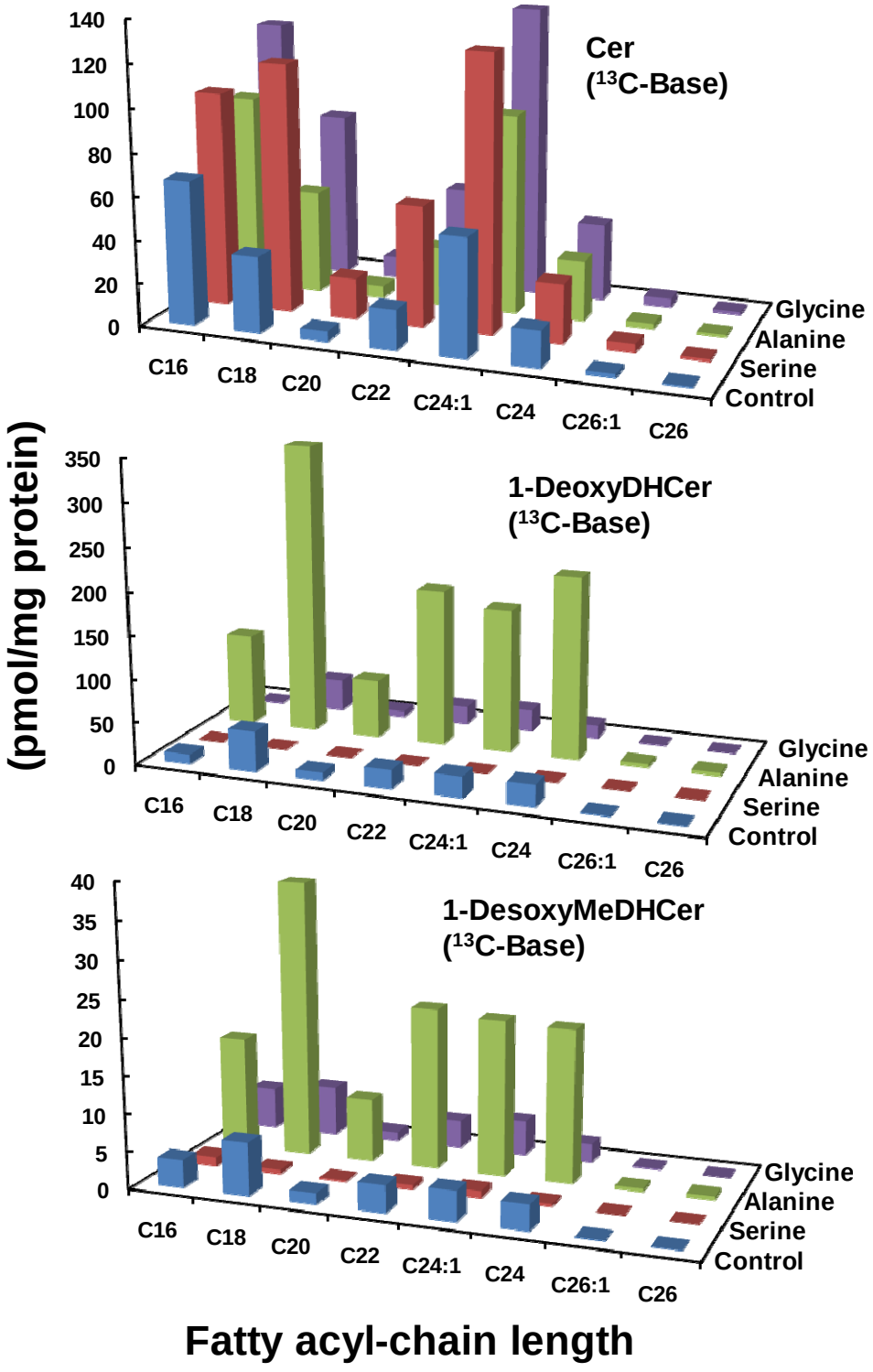

Figure 4.16. N-acyl-sphingoid base biosynthesis by SPT1/2 cells with amino acid supplementations. L-serine, L-alanine and L-glycine (each has 10 mM concentration) were incorporated [^{13}C]palmitate into the sphingoid base backbone (labeled ^{13}C-base).

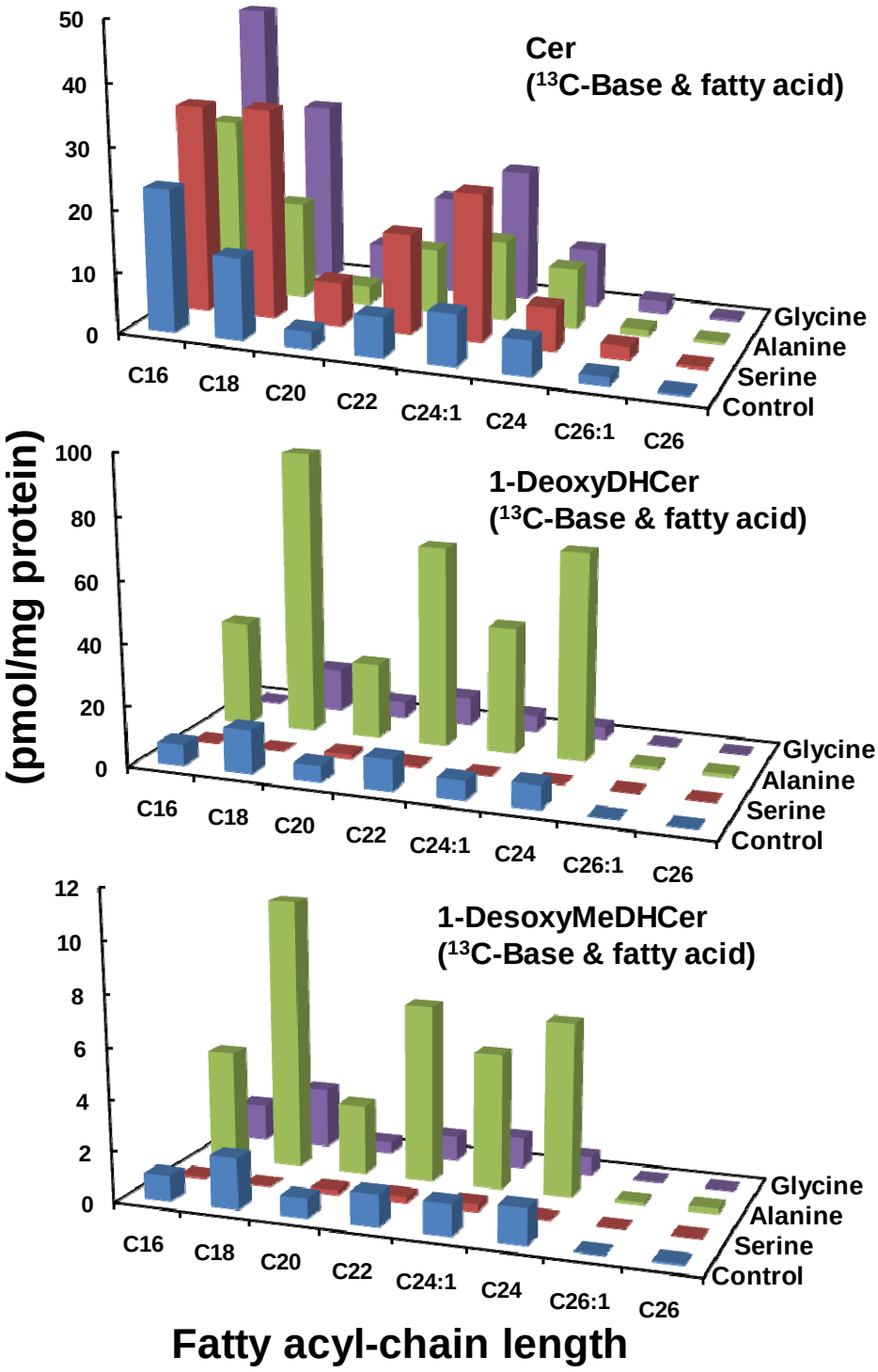

Figure 4.17. N-acyl-sphingoid base biosynthesis by SPT1/2 cells with amino acid supplementations. L-serine, L-alanine and L-glycine (each has 10 mM concentration) were incorporated into both the sphingoid base and fatty acid (labeled ^{13}C-base and fatty acid).

4.3.11 Analysis of 1-DeoxySa in SPT1/2 cells with Knock Down of Serine Metabolism

Serine, a non-essential amino acid, is a necessary precursor for the synthesis of various biomolecules, for examples, proteins, amino acids, phosphatidylserine, sphingolipids, nucleotides, etc., which are important for cellular and tissue functions. Serine is derived from three sources—extracellular uptake, methylation of glycine by serine hydroxymetholtransferase, and de novo biosynthesis. The *de novo* pathway begins with the glycolysis intermediate 3-phosphoglycerate (46) which is oxidized by 3-phosphoglycerate dehydrogenase (PHGDH) to 3-phosphohydroxypyruvate (3-P-hydroxypyruvate) (47) that is converted to 3-phosphoserine (3-P-serine) by phosphoserine aminotransferase, and finally, 3-Phosphoserine phosphatase (PSPH) removes the 3-P-seine to yield seine. All of these sources are physiologically relevant, including the *de novo* pathway, which is known to be defective in a number of genetic diseases (46, 47). Therefore, since we had noted that varying the extracellularly provided amino acid could affect the type of sphingoid bases that were made, we also examined one of the pathways for endogenous modulation—the de novo biosynthesis pathway.

In these preliminary experiments, SPT1/2 cells were treated with siRNA against 3-phosphoglycerate dehydrogenase (PHGDH) and 3-phosphoserine phosphatase (PSPH) (as well as the matched nonspecific siRNA control) for 72 hr followed by labeling of the sphingoid bases by [U-^{13}C]palmitate in medium that contained FB_1 and either no Ser and Gly or these amino acids supplemented to 0.25 mM (Fig.4.18). The prediction of this pilot experiment was that knockdown of serine biosynthesis would elevate biosynthesis of the alternative sphingoid bases because their precursors would still be present, and

indeed, there was an elevation in [^{13}C]1-deoxySa (Fig.4.18). Thus, although this needs to be studied further to confirm knock down of these enzymes of serine metabolism by Western blotting and/or amino acid analysis, this experiment indicates that one of the previously unanticipated consequences of abnormal serine metabolism might be the production of these novel sphingoid bases.

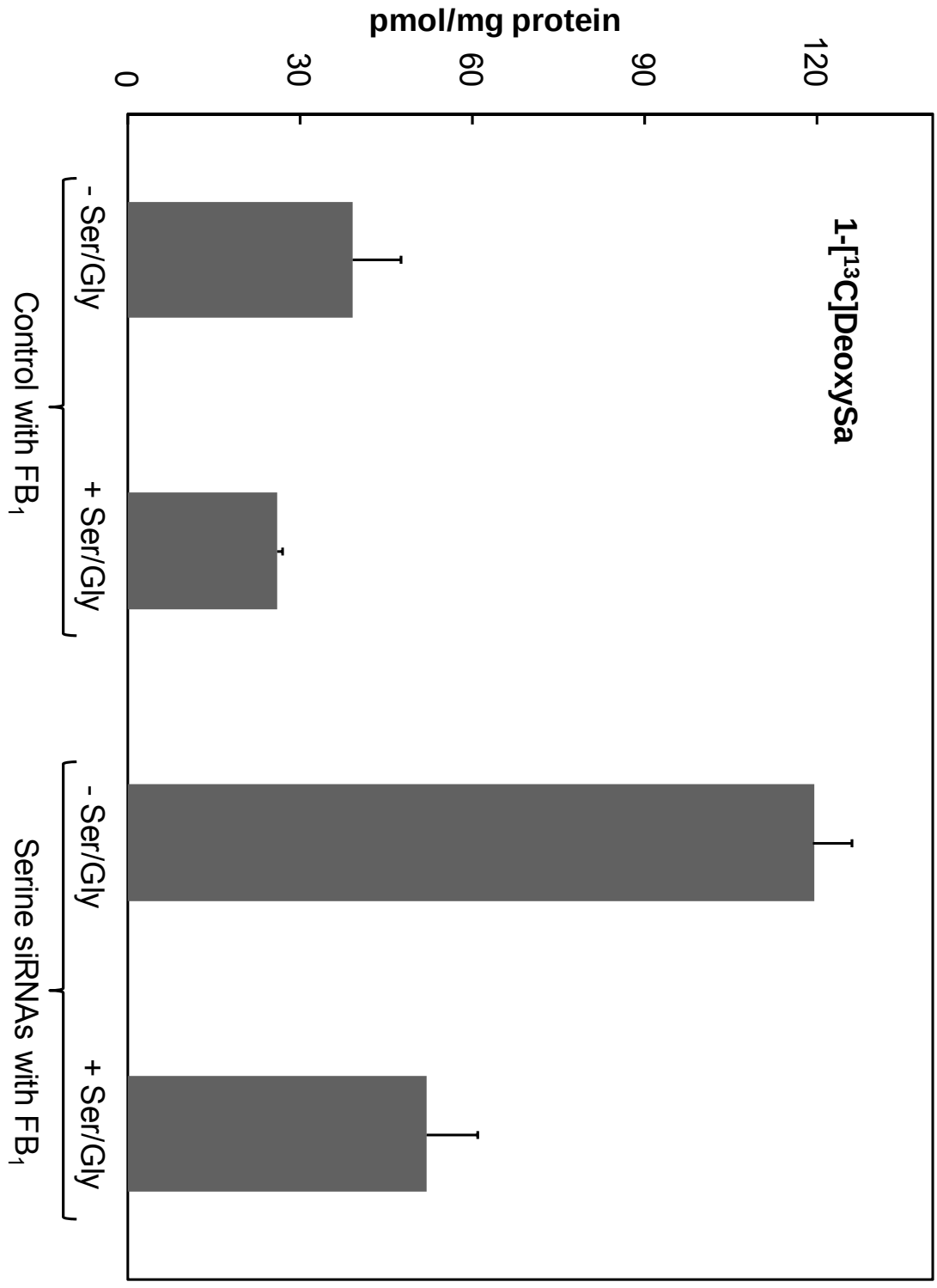

Figure 4.18. Effect of double knockdown by 3-phosphoglycerate dehydrogenase (PHGDH) and 3-Phosphoserine phosphatase (PSPH) siRNAs on 1-deoxySa synthesis. Shown are the amounts of 1-[^{13}C]deoxySa that are produced by SPT1/2 cells.

4.4 Discussion

These studies have established that the mystery peak that we described in FB-treated cells almost a decade ago (20) is 1-deoxySa, a novel sphingoid base that is biosynthesized by SPT via the condensation of palmitoyl-CoA with L-alanine. It is surprising that this compound has not been more widely noted in mammalian cells; however, its presence as mainly the N-acyl derivatives makes it difficult to detect in the much larger pool of cellular Cer and other neutral lipids.

This compound and other 1-deoxysphingoid bases are known to be made by other organisms (36), but have only recently surfaced in mammalian cells in studies of a mutation in the SPTLC1 gene that causes HSN1 (33). However, because our studies have found substantial amounts of these compounds in mammalian cell lines not thought to have a defect in SPT, it is evident that 1-deoxySa and 1-deoxyceramides are normally made by mammals. This does not rule out the possibility that abnormal elevations in 1-deoxySa by a mutant SPTLC1, or due to inhibition of its acylation by FB, could cause cytotoxicity.

The rapid and extensive acylation of 1-deoxySa is not surprising since studies of the structural requirements of sphingoid bases as substrates and inhibitors of CerS had previously shown that this compound was acylated (37). Although very long chain 1-Deoxy-DHCer will be synthesized and optimized for the ionization and fragmentation conditions, we built the methods for the analysis of 1-deoxySa and 1-deoxyDHCer by LC ESI-MS/MS. In LYB-LCB1 cells FB_1 caused a much larger increase in 1-deoxySa (40 pmol/mg protein) than can be accounted for solely by the levels of 1-deoxyDHCer in the

untreated cells. The precise fate of 1-deoxySa is not known and raises interesting questions about the subsequent metabolism and functions of these compounds since 1-deoxyDHCer might be desaturated to 1-deoxyceramides, but none of the usual downstream complex sphingolipids (sphingomyelins, ceramide 1-phosphates or hexosylceramides) can be made. Furthermore, the free sphingoid base cannot undergo phosphorylation, which is a prerequisite step for catabolism of So and Sa via S1P lyase (38). Therefore, there must be alternative mechanisms for elimination of this category of sphingoid bases that are not yet understood.

The cytotoxicity of 1-deoxySa is similar to that previously seen for sphingoid bases (39), although the findings with DU-145 cells indicate that removal of the 1-hydroxyl group has enhanced the potency somewhat. It is possible that some of the biological effects of 1-deoxySa occur after its metabolism to 1-deoxyDHCer, or due to interference with the metabolism of another sphingolipid, such as by inhibition of sphingosine kinase. However, the finding that addition of 1-deoxySa to LLC-PK_1 cells did not decrease the ability of FB_1 to elevate Sa1P (Fig. 4.10E) indicates that it does not eliminate sphingoid base phosphorylation, although its effects might be more pronounced under other circumstances.

The high amounts of 1-deoxysphingolipids in liver versus kidney (Fig. 4.11) is reminiscent of the greater sensitivity of liver to FB_1-induced toxicity in mice (3).We have analyzed a number of tissues from other fumonisin-treated animals, such as liver and kidneys from Sprague-Dawley rats, several strains of mice and pigs (data not shown), and, so far, the highest amounts of 1-deoxySa and 1-deoxyDHCer have been found in P53N5 mice. It would be interesting to know if this species, which was derived originally from

the C57BL/6 mouse, has structural differences in SPT that cause it to produce higher amounts of 1-deoxySa, in analogy to the HSN1 mutation (33).

We have noted also that the appearance of 1-deoxySa in cells in culture increases with the length of time that they have been left in culture (Figs. 4.2 and 4.3). This might be related to whether or not they are growing because we have not noted significant amounts in rapidly proliferating LLC-PK_1 cells (8, 13), whereas, confluent cultures of LLC-PK_1 cells left in medium for several days have amounts of 1-deoxySa that approach the levels of Sa (Figs. 4.2 and 4.3), and 1-deoxyCer that can be higher than Cer (Fig. 4.8). To some extent, this is probably due to the lack of downstream metabolism of these compounds, but another factor might be greater formation of 1-deoxySa after the medium and cells become depleted of serine relative to alanine. Indeed, we were easily able to detect 1-deoxySa in Vero cells even without treatment with FB_1 (data not shown), and Vero cells are known to rapidly deplete serine from culture medium (40). This issue led us to think about the possible participation of amino acid supply in the types of sphingoid bases that are made by cells.

Examination of the composition of the cell culture medium for the HEK293 and SPT1/2 cells (Dulbecco's Modified Eagle Medium: Nutrient Mixture F-12, DMEM/F12), we note that serine and glycine have been added at concentrations that are 5-fold higher than alanine. Thus, it is not surprising that the production of 1-deoxySa has not been noticed previously.

The availability of serine over alanine is not always encountered *in vivo*, however. As shown in Fig. 4.19, serine metabolism in animal cells has been well characterized (46)

and although the biosynthetic enzymes are widely distributed, the amounts are known to vary—for example being significantly upregulated in proliferating cells and neoplastic tissues (48). The phosphorylated pathway is considered to play a chief role in the *de novo* synthesis in various mammalian cells, and its physiological importance has been evidenced in inherited PHGDH deficiency. Patients with this deficiency have reduced enzyme activities and exhibit marked decreases of serine and glycine concentrations in both plasma and cerebrospinal fluid (49, 50). Consequently, they are afflicted with severe neurological disorders.

Thus, since we have shown that 1-DeoxySa and its N-acyl-derivatives are elevated in alanine supplemented medium (Fig. 4.15, 4.16, and 4.17) and—it appears—when biosynthesis was suppressed by siRNAs (Fig. 4.18), this suggests strongly that these compounds will be elevated in some physiologic or pathophysiologic states. Since sphingoid bases are highly bioactive compounds (36), they may be mediators of human diseases.

It is possible that there are additional factors that affect the amino acid selectivity of SPT *in vivo*. Inuzuka *et al.* (51) have reported that Serinc, "named for being a "serine incorporator", facilitates the incorporation of serine into membrane lipids by facilitating the synthesis of phosphatidylserine and sphingolipids. Serinc proteins are found in ER membranes, and it has been proposed that they bind directly to SPT, perhaps linking sphingolipid biosynthesis to a serine synthetic enzyme, such as PHDGH. There are several isoforms, and Serinc1-5 and Serinc2 and Serinc5 were reported to significantly enhance the SPT activity in mammalian cells. Because the membrane topology of Serinc, which contains 11 transmembrane segments similar to amino acid transporters, the

authors have speculated that Serinc may function by carrying a serine molecule into the hydrophobic milieu of membrane lipid bilayers, which is responsible for efficient reactions occurring among serine, hydrocarbon tails, and lipid synthetic enzymes.

Thus, one can envision how SPT might serve as a sensor for changes in the ratios of serine and alanine by producing alternative categories of sphingoid bases with different metabolic fates, effects on membrane structure, cell signaling (52), and (or) interaction with nuclear receptors that bind sphingosine (53).

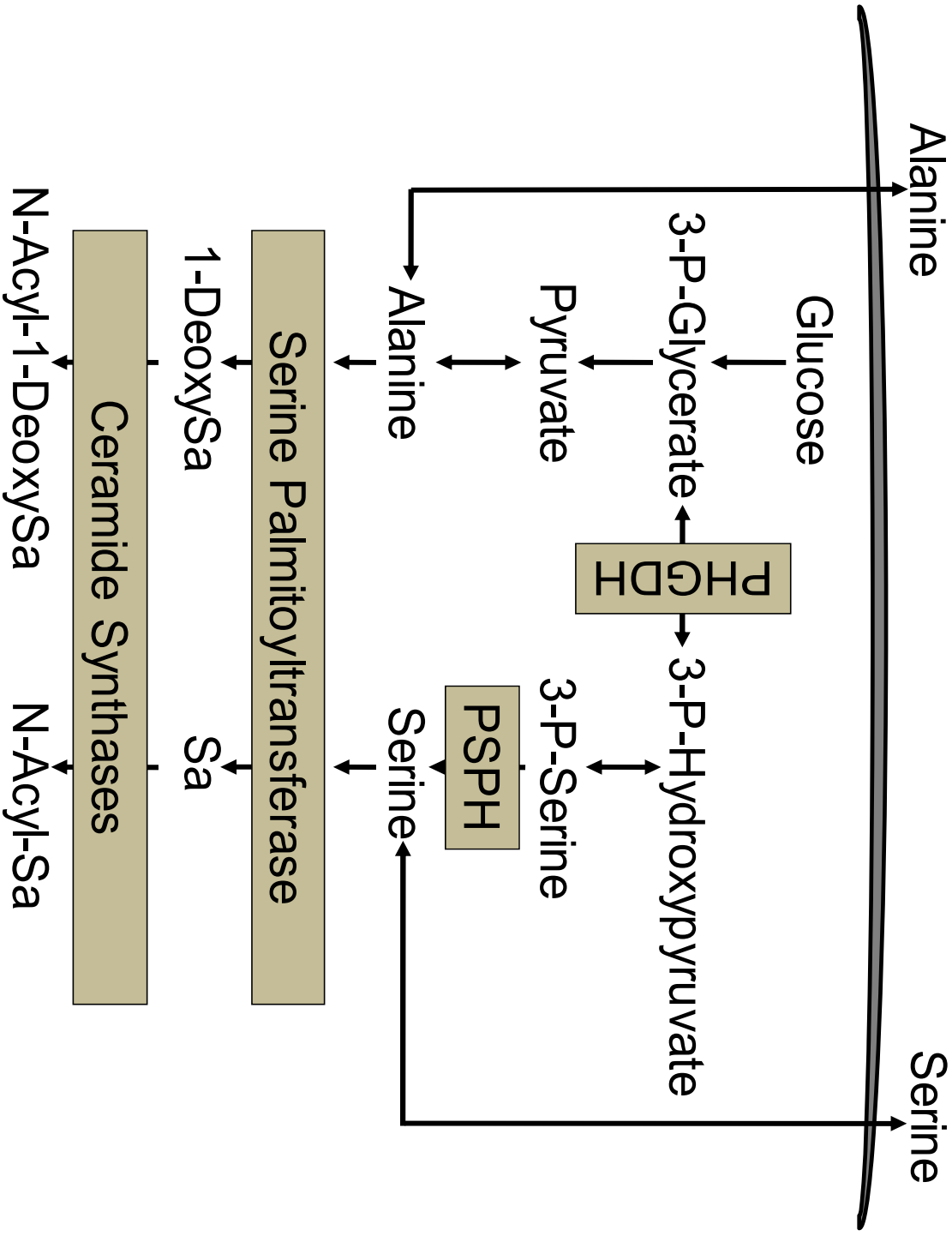

Figure 4.19 The speculation of correlation between amino acid synthesis and sphingolipid biosynthesis. There are two known serine disorder deficiencies, such as 3-phosphoglycerate dehydrogenase (PHGDH) deficiency and 3-phosphoserine phosphatase (PSPH). In Serine deficiency disorder, the increased alanine might cause 1-deoxy SL biosynthesis.

4.5 References

1. Marasas, W. F. O. (2001) *Environ. Health Perspect.* **109,** 239–243
2. Marasas, W. F. O., Riley, R. T., Hendricks, K. A., Stevens, V. L., Sadler, T. W., Gelineau-van Waes, J. B., Missmer, S. A., Cabrera, J., Torres, O., Gelderblom, W. C. A., Allgood, J., Martinez, C., Maddox, J., Miller, J. D., Starr, L., Sullards, M. C., Roman, A. V., Voss, K. A., Wang, E., and Merrill, A. H., Jr. (2004) *J. Nutr.* **134,** 711–716
3. Voss, K. A., Riley, R. T., Norred, W. P., Bacon, C. W., Meredith, F. I., Howard, P. C., Plattner, R. D., Collins, T. F. X., Hansen, D. K., and Porter, J. K. (2001) *Environ. Health Perspect.* **109,** 259–266
4. NTP Technical Report (2002). NIH Publication No. 99-3955
5. Wang, E., Norred, W. P., Bacon, C. W., Riley, R. T., and Merrill, A. H., Jr. (1991) *J. Biol. Chem.* **266,** 14486–14490
6. Pewzner-Jung, Y., Ben-Dor, S., and Futerman, A. H. (2006) *J. Biol. Chem.* **281,** 25001–25005
7. Riley, R. T., Enongene, E., Voss, K. A., Norred, W. P., Meredith, F. I., Sharma, R. P., Williams, L. D., Carlson, D. B., Spitsbergen, J., and Merrill, A. H., Jr. (2001) *Environ. Health Perspect.* **109,** 301–308
8. Yoo, H. S., Norred, W. P., Wang, E., Merrill, A. H., Jr., and Riley, R. T. (1992) *Toxicol. Appl. Pharmacol.* **114,** 9–15
9. Merrill, A. H. Jr., Sullards, M. C., Wang, E., Voss, K. A., and Riley, R. T. (2001) *Environ. Health Perspect.* **109,** 283–289
10. Delongchamp, R. R., and Young, J. F. (2001) *Food Additiv. Contam.* **18,** 255–261
11. Riley, R. T., and Voss, K. A. (2006) *Toxicol. Sci.* **92,** 335–345
12. Schroeder, J. J., Crane, H. M., Xia, J., Liotta, D. C., and Merrill, A. H., Jr. (1994) *J. Biol. Chem.* **269,** 3475–3481
13. Yoo, H. S., Norred, W. P., Showker, J. L., and Riley, R. T. (1996) *Toxicol. Appl. Pharmacol.* **138,** 211–218
14. Schmelz, E. M., Dombrink-Kurtzman, M. A., Roberts, P. C., Kozutsumi, Y., Kawasaki, T., and Merrill, A. H., Jr. (1998) *Toxicol. Appl. Pharmacol.* **148,** 252–260
15. Riley, R. T., Voss, K. A., Norred, W. P., Bacon, C. W., Meredith, F. I., and Sharma, R. P. (1999) *Environ. Toxicol. Pharmacol.* **7,** 109–118
16. Tolleson, W. H., Couch, L. H., Melchior, W. B. Jr., Jenkins, G. R., Muskhelishvili, M., Muskhelishvili, L., McGarrity, L. J., Domon, O. E., Morris, S. M., and Howard, P. C. (1999) *Int. J. Oncol.* **14,** 833–843
17. Kim, M. S., Lee, D. Y., Wang, T., and Schroeder, J. J. (2001) *Toxicol. Appl. Pharmacol.* **176,** 118–126
18. Yu, C. H., Lee, Y. M., Yum, Y. P., and Yoo, H. S. (2001) *Arch. Pharmacal. Res.* **24,** 136–143
19. He, Q., Riley, R. T., and Sharma, R. P. (2002) *Pharmacol. Toxicol.* **90,** 268–277
20. Riley, R. T., Voss, K. A., Norred, W. P., Sharma, R. P., Wang, E., and Merrill, A. H., Jr. (1998) *Rev. Me´d. Ve´t.* **149,** 617–626
21. Hanada, K., Hara, T., Fukasawa, M., Yamaji, A., Umeda, M., and Nishijima, M. (1998) *J. Biol. Chem.* **273,** 33787–33794
22. Meredith, F. I., Bacon, C. W., Plattner, R. D., and Norred, W. P. (1996) *J. Ag. Food Chem.* **44,** 195–198

23. Riley, R. T., and Plattner, R. D. (2000) *Methods Enzymol.* **311,** 348–360
24. Yang, H., and Liebeskind, L. S. (2007) *Org. Lett.* **9,** 2993–2995
25. Lowry, O. H., Rosenbrough, N. J., Farr, A. L., and Randall, R. J. (1951) *J. Biol. Chem.* **193,** 265–275
26. Riley, R. T., Norred, W. P., Wang, E., and Merrill, A. H., Jr. (1999) *Nat. Tox.* **7,** 407–414
27. Zitomer, N. C., Glenn, A. E., Bacon, C. W., and Riley, R. T. (2008) *Anal. Bioanal. Chem.* **391,** 2257–2263
28. Merrill, A. H., Jr., Sullards, M. C., Allegood, J. C., Kelly, S., and Wang, E. (2005) *Methods* **36,** 207–224
29. Gelderblom, W. C. A., Cawood, M. E., Snyman, S. D., and Marasas, W. F. O. (1994) *Carcinogenesis* **15,** 209–214
30. Miyake, Y., Kozutsumi, Y., Nakamura, S., Fujita, T., and Kawasaki, T. (1995) *Biochem. Biophys. Res. Commun.* **211,** 396–403
31. Enongene, E. N., Sharma, R. P., Bhandari, N., Meredith, F. I., Voss, K. A., and Riley, R. T. (2002) *Toxicol. Sci.* **67,** 173–181
32. Sullards, M. C., Allegood, J. C., Kelly, S., Wang, E., Haynes, C. A., Park, H., Chen, Y., and Merrill, A. H., Jr. (2007) *Methods Enzymol.* **432,** 83–115
33. Hornemann, T., Penno, A., and von Eckardstein, A. (2008) *Chem. Phys. Lipids* **154S,** S63, PO 111
34. Sa´nchez, A. M., Malagarie-Cazenave, S., Olea, N., Vara, D., Cuevas, C., and Díaz-Laviada, I. (2008) *Eur. J. Pharmacol.* **584,** 237–245
35. Tsunoda, M., Sharma, R. P., and Riley, R. T. (1998) *J. Biochem. Mol. Toxicol.* **12,** 281–289
36. Pruett, S. T., Bushnev, A., Hagedorn, K., Adiga, M., Haynes, C. A., Sullards, M. C., Liotta, D. C., and Merrill, A. H., Jr. (2008) *J. Lipid Res.* **49,** 1621–1639
37. Humpf, H. U., Schmelz, E. M., Meredith, F. I, Vesper, H., Vales, T. R., Wang, E., Menaldino, D. S., Liotta, D. C., and Merrill, A. H., Jr. (1998) *J. Biol. Chem.* **273,** 19060–19064
38. Fyrst, H., and Saba, J. D. (2008) *Biochim. Biophys. Acta* **1781,** 448–458
39. Stevens, V. L, Nimkar, S., Jamison, W. C., Liotta, D. C., and Merrill, A. H., Jr. (1990) *Biochim. Biophys. Acta* **1051,** 37–45
40. Quesney, S., Marc, A., Gerdil, C., Gimenez, C., Marvel, J., Richard, Y., and Meignier, B. (2003) *Cytotechnology* **42,** 1–11
41. Lapidot, Y., Rappoport, S., Wolman, Y. (1967) *J Lipid Res.* **8,** 142-145
42. Ong, D. E. and Brandy, R. N. (1972) *J. Lipid Res.* **13,** 819–822
43. Venkataraman, K., Riebeling, C., Bodennec, J., Riezman, H., Allegood, J. C., Sullards, M. C., Merrill, A. H., Jr., and Futerman, A. H. (2002) *J. Biol. Chem.* **277,** 35642–35649
44. Riebeling, C., Allegood, J. C., Wang, E., Merrill, A. H., Jr., and Futerman, A. H. (2003) *J. Biol. Chem.* **278,** 43452–43459
45. Mizutani, Y., Kihara, A., and Igarashi, Y. (2005) *Biochem. J.* **390,** 263–271
46. Furuya, S. (2008) *Asia Pac J Clin Nutr.* **17,** Suppl 1:312-315
47. Ichihara, A., Greenberg, D.M. (1955) *Proc Natl Acad Sci* **41,** 605−609
48. Davis, J.L., and Fallon H.J. (1970) *J Biol Chem* **245,** 5838–5846

49. Jaeken, J., Detheux, M., Van Maldergem, L., Foulon, M., Carchon, H., Van Schaftingen, E. (1996) *Arch Dis Child* **74,** 542–545
50. de Koning, T.J., Duran, M., Dorland, L., Gooskens, R., Van Schaftingen, E., Jaeken, J., Blau, N., Berger, R., Poll-The, B.T. (1998) *Ann Neurol* **44,**261–265
51. Inuzuka, M., Hayakawa, M., and Ingi, T. (2005) *J Biol Chem* **280,** 35776-35783
52. Zheng, W., Kollmeyer, J., Symolon, H., Momin, A., Munter, E., Wang, E., Kelly, S., Allegood, J. C., Liu, Y., Peng, Q., Ramaraju, H., Sullards, M. C., Cabot, M., and Merrill, A. H., Jr. (2006) *Biochim. Biophys. Acta* **1758,** 1864–1884
53. Urs, A. N., Dammer, E., Kelly, S., Wang, E., Merrill, A. H. Jr., and Sewer, M. B. (2006) *Mol. Cell. Endocrinol.* **265–266,** 174–178

CHAPTER 5

CONCLUSIONS

This thesis describes Cer biosynthesis by mouse embryonic stem cells and embryoid bodies by transcript profiling and metabolomic analysis (i.e. determining transcript levels for enzymes involved in Cer biosynthesis by qRT-PCR and respective metabolites by liquid chromatography-electrospray ionization tandem mass spectrometry, LC-ESI MS/MS). And, this focused genomic and metabolomic investigation has uncovered changes in expression of Cer synthases, fatty acyl-CoA elongases, fatty acyl-CoA's and Cer subspecies that are in reasonable agreement, and which might reflect important events that occur during embryogenesis.

Mammalian *CerS2* was also characterized and revealed that *CerS2* mRNA is found at the highest level of all *CerS* by qRT-PCR analysis and has the broadest tissue distribution by LC ESI-MS/MS analysis. *CerS2* has a remarkable acyl-CoA specificity, showing no activity using C16:0-CoA and very low activity using C18:0, rather utilizing longer acyl-chain CoAs (C22–C24) for ceramide synthesis. There is a good correlation between *CerS2* mRNA levels and levels of ceramide and sphingomyelin containing long acyl chains, at least in tissues where *CerS2* mRNA is expressed at high levels. These results indicate significant and unexpected biological and biochemical differences between the *CerS* genes and proteins, and imply a unique role for *CerS2*.

Serine palmitoyltransferase (SPT) utilize serine and palmitoyl-CoA as substrates to produce sphinganine (Sa) by sphingolipid *de novo* biosynthesis. Sa is acylated to (dihydro)ceramides containing different fatty acyl chains. In this thesis, I describe that

SPT also exploit alanine instead of serine to generate a novel sphingoid base, 1-deoxysphinganine (1-deoxySa) and its 1-deoxydihydrocermides. 1-DeoxySa was isolated from the North Arctic clam *Spisula polynyma* (1) and disrupts actin stress fibers through the inactivation of Rho (1) and has been suggested to induce cell death in the prostate cancer cell lines via stimulation of the *de novo* synthesis of ceramide and protein kinase C ζ activation (2). This actin depolymerization might lead autophagy in mammalian cell lines. Serine and alanine might compete to be utilized by SPT catalytic site or these amino acids might be brought into play by several factors such as Serinc, serine transporter, etc.

In summary, these findings are as regards the unappreciated category of sphingolipid, gene and their roles in mammalian system. Different amino acids are condensed with fatty acyl-CoA by serine palmitoyltransferase to produce 1-deoxysphinganine and sphinganine. Those sphingoid bases are acylated to form N-acyl derivates by ceramide synthases. In Serine disorder deficiency, the accumulation of alanine might cause 1-deoxy sphingolipids by a deficiency of phosphorylated pathway enzymes and bring about toxicity. Another report from Hornemann (3) is that human sensory neuropathy type 1 patient has the higher amounts of 1-deoxysphinganine. Therefore, this novel category of sphingoid bases and its related genes might play important roles in cell regulation, development, especially in human diseases.

5.1 References

1. Cuadros, R., de Garcini, E. M., Wandosell, F., Faircloth, G., Fernandez-Sousa, J. M., and Avila, J. (2000). *Cancer Lett.* **152,** 23−29
2. Sanchez, A. M., Malagarie-Cazenave, S., Olea, N., Vara, D., Cuevas, C., and Diaz-Laviada, I. (2008) *Eur. J. Pharmacol.* **584,** 237−245
3. Hornemann, T., Penno, A., and von Eckardstein, A. (2008) *Chem. Phys. Lipids* **154S,** S63, PO 111

List of publications

1. Hyejung Park, Anu Koppikar, Meeyoung Park and Alfred H. Merrill, Jr. "Towards characterization of the mouse sphingolipidome. A survey of literature on mouse sphingolipid structure and function", in preparation
2. Hyejung Park and Alfred H. Merrill, Jr. "Ceramide synthase inhibition by fumonisin B1 has allowed the discovery of novel categories of sphingoid bases produced by mammalian cells: 1-deoxysphinganine, 1-desoxymethylsphinganine and their N-acyl-derivatives", in preparation
3. Amin Momin, Hyejung Park, Nathan Bowen, Brent Portz, Elaine Wang, Lilya Matyunina, DeEtte Walker, John F. McDonald and Alfred H. Merrill Jr. "Gene expression pathway analysis, its application in predictive (glycol)sphingolipidomics and marker identification for ovarian carcinoma", in preparation
4. Hyejung Park, Christopher A. Haynes, Alison Narin, Michael Kulik, Stephen Dalton, Kelly Moremen and Alfred H. Merrill, Jr. "Genomic and metabolomic analysis of ceramide biosynthesis in mouse embryonic stem cells and embryoid bodies" *Stem cells,* Submitted, **2009**
5. Amin A. Momin, Hyejung Park, Jeremy C. Allegood, Martina Leipelt, Samuel L. Kelly, Alfred H. Merrill, Jr. and Kentaro Hanada. "Characterization of mutant serine palmitoyltransferase 1 in LY-B cells and its partial stabilization, without detectable enzymatic activity, by chemical chaperons" *FEBS Letters,* Submitted, **2009**
6. Jia Wei, Tokunbo Yerokun, Martina Leipelt, Chris A. Haynes, Harish Radhakrishna, Amin Momin, Samuel Kelly, Hyejung Park, Elaine Wang, Jill M. Carton, David J. Uhlinger and Alfred H. Merrill, Jr. "Serine palmitoyltransferase subunit 1 is present

in the endoplasmic reticulum, nucleus and focal adhesions, and functions in cell morphology", *Biochim Biophys Acta.* in press, **2009**

7. Sujoy Lahiri, Hyejung Park, Elad L. Laviad, Xuequan Lu, Robert Bittman, and Anthony H. Futerman. "Ceramide synthesis is modulated by the sphingosine analog FTY720 via a mixture of uncompetitive and non-competitive inhibition in an acyl CoA chain length-dependent manner" *Journal of Biological Chemistry*, In press, **2009**
8. Meidan Goldfinger, Elad L. Laviad, Rivka Hadar, Miri Shmuel, Arie Dagan, Hyejung park, Alfred H. Merrill, Jr., Israel Ringel, Anthony H. Futerman and Boaz Tirosh. "De novo ceramide synthesis is required for N-linked glycosylation in plasma cells" *Journal of Immunology*, in press, **2009**
9. Nadine Hagen, Paul Van Veldhoven, Richard Proia, Hyejung Park, Alfred H. Merrill, Jr. and Gerhild van Echten-Deckert "Subcellular origin of sphingosine-1-phosphate is essential for its toxic effect in lyase deficient neurons" *Journal of Biological Chemistry*, in press, **2009**
10. Nicholas C. Zitomer, Trevor Mitchell, Kenneth A. Voss, Genevieve S. Bondy, Sarah T. Pruett, Ethel C. Garnier-Amblard, Lanny S. Liebeskind, Hyejung Park, Elaine Wang, M. Cameron Sullards, Alfred H. Merrill, Jr. and Ronald T. Riley. "Ceramide synthase inhibition by fumonisin B_1 causes accumulation of 1-deoxy-sphinganine: A novel category of bioactive 1-deoxy-sphingoid bases and 1-deoxy-dihydroceramides biosynthesis by mammalian cell lines and animals" *Journal of Biological Chemistry*, 284(8):4786-95, **2009**
11. Alfred H. Merrill, Jr., Todd H. Stokes, Amin Momin, Hyejung park, Brent J. Portz, Samuel Kelly, Elaine Wang, M. Cameron Sullards and May Dongmei Wang.

"Sphingolipidomics: A valuable tool for understanding the roles of sphingolipids in biology and disease" *Journal of Lipid Research,* 50: S97-S102, **2009**

12. Ilaria Visigalli, Silvia Ungari, Martina Cesani, Sabata Martino, Margherita Neri, Elaine Wang, Laura Tononi, Hyejung Park, Lucia Sergi, Aldo Orlacchio, Angela Gritti, Luigi Naldini and Alessandra Biffi. "De novo galactocerebrosidase expression affects hematopoietic stem cell survival by altering the intracellular content of bioactive sphingolipids" *Blood*, Submitted, **2008**
13. Christopher A. Haynes, Jeremy C. Allegood, Hyejung Park and M. Cameron Sullards. "Sphingolipidomics: Methods for the comprehensive analysis of sphingolipids" *J Chromatography. B, Analytical Technologies in Biomedical and Life Sciences,* in press, **2008**
14. Rebecca L. Shaner, Jeremy C. Allegood, Hyejung Park, Elaine Wang, Samuel Kelly, Christopher A. Haynes, M. Cameron Sullards and Alfred H. Merrill, Jr. "Quantitative analysis of sphingolipids for lipidomics using triple quadrupole and quadrupole linear ion trap mass spectrometers" *Journal of Lipid Research,* in press, **2008**
15. Elad L. Laviad, Lee Albee, Irene Pankova-Kholmyansky, Sharon Epstein, Hyejung Park, Alfred H. Merrill, Jr. and Anthony H. Futerman. "Characterization of ceramide synthase 2: Tissue distribution, substrate specificity and inhibition by sphingosine-1-phosphate" *Journal of Biological Chemistry*, 283(9):5677-84, **2007**
16. M. Cameron Sullards., Jeremy C. Allegood, Samuel Kelly, Elaine Wang, Christopher A. Haynes, Hyejung Park, Yafang Chen and Alfred H. Merrill, Jr. "Structure-specific, quantitative methods for analysis of sphingolipids by liquid-chromatography tandem

mass spectrometry: "Inside-out" sphingolipidomics". *Meth. in Enzymol*., Academic Press, 432, 83-115, **2007**